REPUBLIC OF TÜRKİYE

AYDIN ADNAN MENDERES UNIVERSITY

GRADUATE SCHOOL OF NATURAL AND APPLIED SCIENCES

DEPARTMENT OF MECHANICAL ENGINEERING

MASTER'S PROGRAMME IN MECHANICAL ENGINEERING

2025-MSc-46

DESIGN OF FIXED WING UNMANNED AERIAL VEHICLES WITH PREDICTIVE MAINTENANCE APPROACH

Saim Taha KARATAŞ

MASTER'S THESIS

SUPERVISOR

Prof. Dr. Ismail BOGREKCI

AYDIN – 2025

ACCEPTANCE AND APPROVAL

The thesis titled "DESIGN OF FIXED WING UNMANNED AERIAL VEHICLES WITH PREDICTIVE MAINTENANCE APPROACH", prepared by Saim Taha KARATAŞ, a student of Department of Mechanical Engineering Program at Republic of Türkiye Aydın Adnan Menderes University, Graduate School of Natural and Applied Science, was accepted as a Master's Thesis by the jury below.

Date of Thesis Defense: 06.08.2025

Jury Member

APPROVAL:

Chair (Supervisor) : Prof. Dr. Ismail BOGREKCI …….
Aydin Adnan Menderes University

Member : Prof. Dr. Pınar Demircioğlu …….
Aydin Adnan Menderes University

Member : Assoc. Prof. Dr Sertan Ozan …….
Yozgat Bozok University

This thesis was approved by the jury above in accordance with the relevant articles of the Aydın Adnan Menderes University Graduate Education and Examination Regulations and was approved on the …… by from the Board of Directors of the Graduate School of Science in the …… numbered decision.

Prof. Dr. Ethem AKTURK

Institute Director

Dedicated to my lovely family.

ACKNOWLEDGEMENTS

I would like to show my sincere thanks to my supervisor, Prof. Dr. İsmail BOGREKCI, for his guidance, patience and trust throughout my master study. Despite the health problems which I experienced and the resulting extension of my study period, his continuous support has been invaluable to me.

I would like to extend my deep and sincere thanks to Prof. Dr. Pınar Demircioğlu, for her invaluable support throughout both my academic journey and thesis process. She guide me lots of my lectures and academic career to find my way and find out my capability for this studies. My best regards to him for all supports.

My sincerely thank to my manager and company advisor, Mr. Ali Emre YAŞAR, for his unwavering support and valuable insights regarding my thesis topic throughout this study. I also extend my gratitude to my company, Turkish Aerospace Industries, for all supports.

I owe my deepest gratitude to my beloved family, who have stood by my side at every stage of my life and supported me unconditionally throughout this journey from my childhood to now.

Finally, I would like to thank my dear wife, Aslı, who never withheld her support through this study, always stood my side, and welcomed me with love and warm smile even after long and exhausting work hours.

Thank you all for all important supports and information's for this study,

Saim Taha KARATAŞ

SCIENTIFIC ETHICS STATEMENT

I hereby declare that I composed all the information in my Master's thesis entitled "DESIGN OF FIXED WING UNMANNED AERIAL VEHICLES WITH PREDICTIVE MAINTENANCE APPROACH " within the framework of ethical behavior and academic rules, and that due references were provided and for all kinds of statements and information that do not belong to me in this study in accordance with the guide for writing the thesis. I declare that I accept all kinds of legal consequences in case of any contrary statement of what I have stated is revealed.

Saim Taha Karataş

… / … / ….

TABLE OF CONTENTS

INDEX OF SYMBOLS

GPa	Gigapascal
MI	Maintenance Interval
E	Young Modulus
α	Coefficient-1
J	Joule
β	Coefficient-2
K	Stiffness Matrix
RPN	Risk Priority Number
u	Displacement Vector
S	Severity
F	Force
O	Occurence
ε	Strain
D	Detection
ω	Angular Displacement
RUL	Remaining Useful Life
M	Mass Matrix
R_0	Initial Refference Life
Re	Reynold Number
Hz	Hertz
P	Pressure
mm	Millimeter
v	Velocity
ΔL	Change in Length
C	Aerodynamic Chord
L_0	Initial Length
μ	Dynamic Viscosity of Air Stress
A	Cross-Sectional Area
P	Pressure

ρ	Density
S	Wing Surface Area
Cl	Lift Coefficient
τ	Shear Stress

LIST OF ABBREVIATIONS

AI: Artificial Intelligence

AOA: Angle of Attack

CAD: Computer Aided Design

CBM: Condition Based Maintenance

CFD: Computational Fluid Dynamics

CFRP: Carbon Fiber Reinforced Polymers

CI: Coefficient of Lift

EDF: Electric Ducted Fan

FBG: Fiber Bragg Grating Sensors

FDM: Fused Deposition Modeling

FEA: Finite Element Analysis

FMEA: Failure Mode and Effects Analysis

LSTM: Long Short-Term Memory

MET: Mean Elapsed Time

MLG: Main Landing Gear

MMH: Mean Man Hour

NLG: Nose Landing Gear

RAMS: Reliability, Availability, Maintainability and Supportability

RMS: Root Mean Square

RUL: Remaining Useful Life

SHM: Structural Health Monitoring

SVM: Support Vector Machines

UAV: Unmanned Aerial Vehicle

LIST OF FIGURES

LIST OF PICTURES

LIST OF TABLES

ÖZET

KESTİRİMCİ BAKIM YAKLAŞIMI İLE SABİT KANAT İNSANSIZ HAVA ARACI TASARIMI

Karataş S.T. Aydın Adnan Menderes Üniversitesi, Fen Bilimleri Enstitüsü, Makine Mühendisliği Anabilim Dalı, Yüksek Lisans Tezi, Danışman: Prof. Dr. İsmail BÖĞREKCİ, Aydın, 2025.

Bu çalışmada sabit kanat insansız hava aracının temel tasarımı ve tasarım doğrultusunda oluşturulup sürdürülmesi planlanılan kestirimci bakım yaklaşımı araştırılmıştır. 3 boyutlu tasarım program kullanılarak insansız hava aracı geometrisi oluşturulmuştur. Tasarlanan geometri üzerinden sonlu hacimler metodu kullanılarak dış akış analizleri yapılmıştır. Analizler neticesinde elde edilen verilere istinaden kabul edilen dış geometriye uygun olacak şekilde yapısal ve yerleşimsel tasarım çalışmaları yapılmıştır. Akabinde uygun analiz yöntemleri ve programı aracılığı ile yapısal parçaların mekanik davranışları incelenip; üretim ve kullanım amacına uygun olacak şekilde bir insansız hava aracı tasarımı yapılmıştır. Elde edilen analiz sonucları neticesinde, hava aracı üzerinde kontrol yüzeylerine ve uçak gövdesine sensörler ve kontrol ekipmanlarının yerleşim çalışması lokasyonel olarak öngörülmüştür. Bu durum neticesinde İnsansız Hava Aracının ömrü süresince etkisi altında kalacağı yüklere istinaden; yapısal ve mekanik davranışları tahmin edilmiş ve gerekli değerlendirmeler yapılmıştır. Bu değerlendirmelere bağlı olarak parçalar üzerinde oluşacak yapısal ve mekanik problemler ön görülüp; uygulanılması gereken bakımlar ve süreleri kestirimci bakım ve idame edilebilirlik bakış açısı ile gözden geçirilmiştir. Yapılan çalışmaya istinaden, elde edilmiş veriler de göz önünde bulundurularak; hava aracının ömrü boyunca maruz kalacağı davranışlara göre bakım süreleri, bakım ve bakımcı ücretlerinin iyileştirilmesi ön görülmüştür.

Anahtar Kelimeler: Kestirimci bakım, Sonlu Elemanlar Metodu, Sonlu hacimler metodu, Hava aracı aerodinamiği, İdame edilebilirlik, Durum izleme ve uçak üzerinde bakım sistemi.

ABSTRACT

DESIGN OF FIXED WING UNMANNED AERIAL VEHICLE WITH PREDICTIVE MAINTENANCE APPROACH

Karatas S.T. Aydın Adnan Menderes University, Graduate School of Natural and Applied Sciences, Department of Mechanical Engineering, Master's Thesis, Supervisor: Ismail BOGREKCI, Aydin,

In this study, the basic design of a fixed-wing unmanned aerial vehicle (UAV) and the predictive maintenance approach planned to be developed and sustained in line with the design were investigated. The geometry of the UAV was created using a 3D design software. External flow analyses were performed on the designed geometry using the finite volume method. Based on the data obtained from the analyses, structural and layout design studies were carried out in accordance with the accepted external geometry. Subsequently, the mechanical behavior of the structural components was examined through appropriate analysis methods then software and a UAV design suitable for production and intended use was developed. Based on the results of the analyses, the placement of sensors and control equipment on the control surfaces and the aircraft body was proposed in terms of location. As a result, the structural and mechanical behaviors of the UAV under the loads expected throughout its service life were predicted then necessary evaluations were made. Depending on these evaluations, potential structural and mechanical problems on the components were predicted and the required maintenance types and intervals were reviewed from a predictive maintenance and maintainability perspective. Based on the conducted study and the obtained data, improvements in maintenance intervals, maintenance procedures, and maintenance personnel costs were projected in accordance with the expected operational behavior of the UAV throughout its service life.

Keywords: Predictive maintenance, Finite element method, Finite volume method, Aircraft aerodynamics, Maintainability, On board maintenance.

1. INTRODUCTION

For most of the aircraft in inventories, defined scheduled and unscheduled maintenance activities, maintenance durations, maintenance costs, and unexpected failures occurring during maintenance cause significant increases in average man-hours, total elapsed time, and costs. Accordingly, many field problems arise from issues caused by traditionally defined scheduled maintenance, and aircraft are kept waiting for long periods at line or depot-level maintenance. This issue becomes one of the primary problems for customers in the aviation industry, and considering the enormous economic and workforce volume of the industry, the importance of the current situation's consequences becomes even more apparent. In order to produce faster and lower-cost solutions in the aviation industry, the subject of predictive maintenance needs to be studied more deeply, and scientific research must be conducted. With such studies, it is foreseen that predictive maintenance practices to be implemented will both increase active flight times and solve cost-related problems. Furthermore, predictive maintenance solutions can help to prevent human-induced maintenance errors and thereby reduce accident and failure rates associated with such errors. The aircraft designed and planned to be used in this study is an electrically powered, fixed-wing unmanned aerial vehicle. In the literature, many studies have been conducted on the importance and applications of predictive maintenance. This study also aims to emphasize the importance of the predictive maintenance perspective for the unmanned aerial vehicle.

2. LITERATURE REVIEW

UAV design has always been an important investigation area for mechanical engineers. There exist so many important studies about mechanical and aerodynamical behaviors for an aircraft. In previous studies, mostly structurally and aerodynamically most efficient design for an aerial vehicle investigated considering different conditions. As specified prior, conceptual design of an aircraft is the first step to design an aerial vehicle. This phase is important to gather all information about requirements of ATA systems and desired capabilities. Critical systems exist for Unmanned Aerial Vehicles, which are Electric System (ATA-24), Communication System (ATA-23), Flight Control System (ATA-27), Landing Gear System, Avionic System (ATA-46), Structure System (ATA 51,52...,57) and Power Plant System (ATA 70). In case of the usage the all systems with true communication substructure and efficient conditions; UAV can be controlled for desired missions.

Although the systems described above are considered theoretically sufficient for sustainability of an UAV, there is a situation called failure and maintainability problems in aviation. Due to specified issue, corrective, preventive and predictive maintenance operation applied to the UAV for scheduled maintenance tasks. Despite of corrective and preventive tasks still linger and performed in lots of Line Level Maintenance operations; predictive maintenance tasks getting importance with developing technology. In this study, aircraft structural integrity and thermal behaviors has been investigated to correspond and develop usage of predictive maintenance operations. Predictive maintenance tasks handle the sensor-based failure behavior of the UAV, and gives the practical results as to estimate structural and system sustainability of aero vehicle after or live every flight operation. Literature survey, focused on the research about structural design and CFD design of UAV, health monitoring and predictive maintenance.

2.1. Structural and Fluid Dynamic Design of Unmanned Aero Vehicle

Structural and aerodynamic design has delicate balance with strength of materials, weight and flight efficiency. Previous studies specify the role of thermoset and thermoplastic material like PLA, ABS, carbon fiber and resin, which reducing weight while keeping mechanical integrity under dynamic loads. Fatigue behavior and

thermal expansion of material, become critical concern for these conditions. This concern shows the importance of selected material's thermal stability and mechanics. In parallel with structural a concern, CFD has become important milestone for aerodynamic design to improve airfoil profiles, wing -fuselage transitions and intake geometry. CFD help to investigate region of flow separation, lift drag ratio and ensure laminar airflow toward Electric Ducted Fan systems. Air-intake design reduces pressure distortion at the fan face, improve propulsion performance and extend lifespan. On the structural side, Finite Element Analysis mostly used to simulate stress distribution, vibrational modes and structural deformation under load. This method especially important in FDM based thermoplastic materials, where localized stress concentrations can show break of Thermoplastic lines. Integration of CFD and FEA enables aero-structural relation, which improve the coherence between aerodynamic and structural durability. Studies have shown that first-stage design studies prevent to redesign at late stage of process and improve MMH and MET for design process.

2.1.1. Material Selection of UAV

Within the Material selection has crucial importance in structure design. Usage of materials in UAV directly related with weight, aerodynamic, thermal behaviors, structural integrity and cost. One of the important purposes of UAV structural design is to provide high strength with low weight of fuselage. Weight of an aircraft is decisive parameter for selection of Electric Ducted Fan Engine. According to previous studies; UAV designed using carbon fiber composite, aluminum alloy or fiberglass materials. Due to their high strength to weigh ratio and fatigue behaviors (Guo et al.,2022). On the other hand; thermoplastic materials such as Polylactic Acid (PLA) or resin materials preferred due to their easy printing and cost. Despite of printability properties, cost and tensile of PLA, material has thermal sensitivity and low impact resistance (Graba and Grycz, 2023). In this study, PLA material used for design of UAV with Fused Deposition Modelling.

2.1.2. Air Intake Design of Aerial Vehicle

Design of air-intake is important situation in the usage of Electric Ducted Fan Motor; it has critical role to optimize the aerodynamic performance of UAV. Despite of other engine system's, electric ducted engine requires to directing air flow correctly. Well optimized air intake geometry design is decisive for the usage of UAV with in high velocity and altitude conditions. Inadequate intake geometry design can cause for

turbulent, unsteady flow and pressure loss; in this situation, engine thrust can be reduced and aircraft can be loss during to flight. Geometry of air intakes designed, according to the usage propulsion systems such as internal combustion and electric ducted fan. Intake geometry demonstrated through CFD simulations that elliptical and blended inlets integrated into the wing or fuselage significantly reduce turbulence in flow for EDF engines (Khanna and Shah et al, 2021). These properties important to prevent fan face distortion and relatively, thrust loss and vibration problems. Small size of UAV's drag characteristic can be hold as minimum when improving efficiency.

Location of air intake has decisive role to keep aerodynamic balance and improve stealth charactestic minimizing cross-section area of radar. Dorsal air intakes provide more accurate and precise behavior from ground debris and allow body shapes with streamline. But it can be effected negatively during to strong maneuvers with high angle of attack. In addition to this, air intakes can be affected from foreign objects during takeoff and landing operations in case of the usage bottom of UAV. But it can optimize asymmetric pressure distribution under cross wing condition better than side-mounted inlets for twin engine aircrafts.

Considering thermal stability and light weight importance, carbon fiber air intake model designed for fixed wing aircraft. Carbon fiber materials can withstand thermal behavior and vibration problems during too long missions. Particularly UAVs which working in high speed and warm air conditions, exposed by thermal loads for fatigue behavior. Due to this low thermal expansion materials should be used to provide structural stability in extreme temperature changes. Carbon fiber Reinforced Polymers (CFRP) preferred in many air intake materials due to their good strength to weight ratio and high fatigue resistance. Specified properties provide for low thickness air intake walls without effecting negatively to structural integrity, thereby reducing weight and improving flight efficiency. Moreover, the stiffness of laminates provides to suppress vibration problems. Otherwise, it can cause acoustic resonance and early failure. Apart from the CFRP investigation, authors have explored the use of aramid composites and hybrid laminates to get local reinforcement on intake mounting interfaces (Lim et al, 2022).

2.1.3. Structural Design of Fuselage and Wings

Structural design is the one of the important phases for UAV design, Design of ANOYA UAV shown in Figure 2.1. Mechanical, modal and dynamic behaviors of

aerial vehicle can be observed via structural design methods. In previous studies, structural design of an aircraft often investigated with different perspectives. Mechanical behavior of the unmanned aerial vehicle, under certain loads, examined with finite element method perspective in one of the previous studies. According to the obtained results; structural optimizations has been applied on UAV fuselage and wing structures. In previous study wing structural model has been studied for validation for finite element analysis (Kanesan et al, 2014).

Figure 2.1 ANOYA Unmanned Aerial Vehicle

2.1.4. Wing Profile Selection

Wing profile selection according to the airfoil design, important for both lift and aerodynamic design of fuselage. Considering importance of lift for an UAV; fuselage design can be affected from airfoil profile selection. Bernoulli Principle will be applicable for wing profiles at non-viscos fluid regimes. Airfoil Profile of aerial vehicle shown in Picture 2.1. According to the principle, high pressure and low velocity air will be intensified in below of lower surface and it can be increased with the growth of distance between camber line and chord line. Due to this theory, structure design for different type of wing profiles studied another study. (Li et al, 2023)

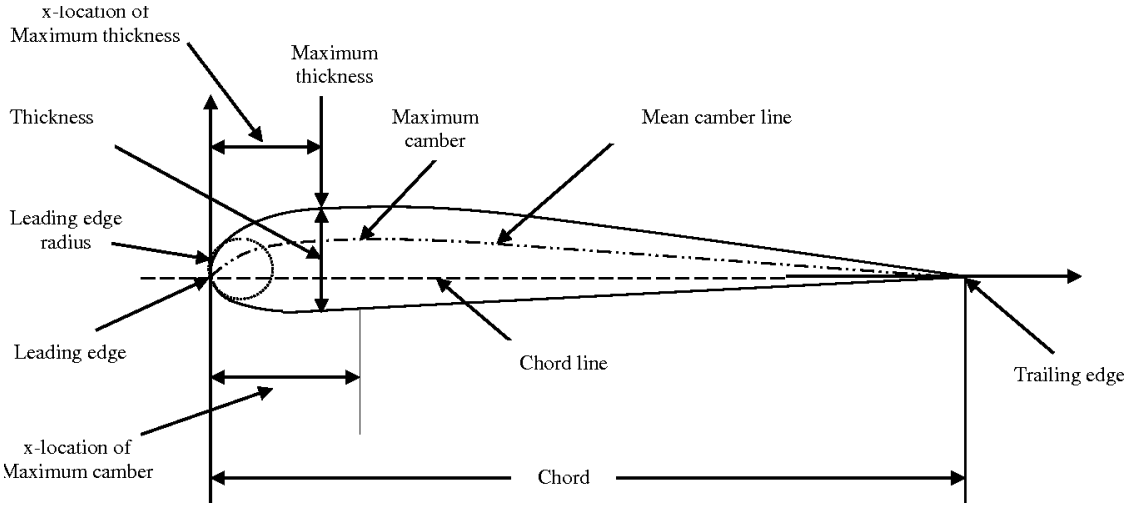

Picture 2.1 Example of Wing Profile

2.2. Health Monitoring

In previous physical system models with sensor data to detect early anomalies studied for UAV's health monitoring for propulsion and actuating. Process starts with signal processing and classification then progressing through fault detection layer. This layered approach used for description of both mechanical faults and behavioral deviations. Mostly, gyroscopes, accelerometer and temperature data help to provide more diagnostic accuracy. Deviation in component performance are detected with live sensor outputs. For instance, vibration behavior can reveal failure in EDF before catastrophic problems. Some studies include fault detection analysis to predict downstream effects of localized issues. (Javadi & Larsson et al., 2014)

Recent advancements in UAV technology have provided machine learning models into health monitoring, enabling a shift from fixed-schedule to condition-based maintenance. These models analyze sensor datas of previous flights to detect early indicators of mechanical failure. According to given datas; Support Vector Machines (SVM) and other classifiers are commonly trained with obtained vibration datas, especially for detecting motor anomalies. Feature extraction methods include RMS, peak-to-peak values, frequency spectra, and Kurtosis. By using these features, the models achieve high fault detection accuracy with minimal false positive datas. Sensor inputs include IMUs, motor current, and thermal data, which provide an important view of system health. Real-time classification allows operators to make informed to take decisions before failures occurred. The use of onboard maintenance computing

enables in-flight analysis without dependence on operation from outside. Adaptive thresholds and continuous model training improve the long-term accuracy of these systems. Predictive maintenance reduces downtime and operational costs by avoiding unnecessary part replacements. Intelligibility in AI systems is also important to gain confidence from engineers. Lightweight algorithms are optimized for embedded hardware in small UAVs. Integrating definition of data into flight control systems enables fail-safe actions during critical operations. Data fusion from different sources enhances reliability and toughness to sensor noise and variability. The system supports line-level monitoring by collecting data from different aircrafts. Maintenance teams take information from automated health monitoring system reports and alerts. These results are adaptable to various UAV types and missions for maintenance operations. The methodology provides early scheduling of component replacements according to system data. Study has been demonstrated in both laboratory and real-flight scenarios. Generally, machine learning optimizes UAV reliability, efficiency, and mission safety. (Altınörs et al., 2021)

Structural health monitoring in UAVs has increasingly important role due to the growing use of composite and thermoplastic materials, which are sensitive to damage such as delamination and fatigue. Piezoelectric sensors offer a lightweight and efficient solution for continuous monitoring of aircraft structural integrity. These sensors are installed to UAV wings or fuselage and can detect changes in vibration behavior in operational conditions and loads. In case of the changes on natural frequency or damping ratio signal, show the onset of structural damage. Distributed sensor arrays on specified region of fuselage and wing structures, show and help to observe localization of damage or deformation. Modal analysis techniques help observe evolving mechanical properties over time. On the other hand, Wireless data acquisition systems reduce the need for weight of onboard wiring in aircraft. Real-time analysis enables flight crews or autonomous systems to react to early-stage damage. The system can be integrated to the design phase UAV, allowing seamless sensor placement in composite layers. Environmental durability, such as resistance to humidity and temperature changes, enhances field applicability. Damage detection thresholds are calibrated using baseline modal data obtained during initial UAV qualification tests. Anomaly detection algorithms compare incoming vibration patterns with these baselines. Data visualization tools assist operators in clarify system health.

Maintenance can be scheduled before critical failure, extending the UAV's service life. The lightweight of piezo sensors means, they can be installed in large numbers without effecting flight dynamics. Fatigue behavior crack detection is possible even in submillimeter ranges. Sensor data can also feed into control logic for adaptive response during flight. Long lifespan UAVs especially benefit from embedded SHM capabilities. Structural health feedback may be logged for historical trend analysis across multiple missions. This technology supports both military and civilian UAV reliability improvements. (Zhang et al., 2023)

SHM in UAVs has developed into the integration of sophisticated sensor technologies, such as fiber optic systems. Fiber Bragg Grating (FBG) sensors with properties of lightweight, high sensitivity, and insensitivity to electromagnetic interference, etc., are particularly suitable for application in aerospace fields. These sensors can be incorporated into composite materials in the production stages of UAVs. Multiplexing functionality enables several FBG sensors to be combined in one optical fiber, simplifying cabling. They can be used for the measurement of thermal expansion and mechanical stress because they can differentiate between strain and temperature. Experimental results on the wing and the fuselage components of REPWIN are indicative of accurate strain mapping under operational conditions for a UAV. The sensors are able to withstand severe temperature cycling and long-term vibration without signal drift. The live status of the system is obtained by ground control or onboard diagnostics in real-time data collection systems. Strain measurements serve to detect damage early in its onset, before visual flaws develop. Optical sensor systems have been found to be compatible with finite element simulation, satisfying stress concentration predictions. Incorporating optical sensing measurements into UAVs for life cycle management can offer a reduction of operator inspection time. The systems can be integrated into a variety of UAV platforms, ranging from tactical drones all the way up to those in the high-altitude long-endurance category. Sensor networks are modularly designed to accommodate important load-bearing parts. Its installation does not noticeably disturb aerodynamics or weight budgets. Fiber sensors are also stable in high humidity or corrosion conditions. With continuous verification of structure integrity, operators can have more assurance of robustness for long-term missions. One area of work focuses on improving the user experience of health data using visual dashboards in real-time.

This sensing approach provides prognostic functionality when combined with damage progression models. Fiber optic systems have thus emerged as a strong contender for next-generation SHM in fixed-wing UAVs in general. (Kinet et al., 2014)

Recent approaches to health-monitoring for UAV systems have afforded significant advances in the development and application of probabilistic reasoning models, especially based on Bayesian networks. They are good at treating the uncertainty in the sensor measurement, system uncertainty, and environmental disturbance. In opposition to absolute fault criteria, Bayesian models describe likelihoods for several signs of failure. With the arrival of new sensor data, the model is incrementally adjusting its belief of component conditions. This active approach allows for detecting faults that might otherwise not be explored by deterministic systems. Those are called hidden faults (or compound faults). Relations between the different subsystems of the UAV are represented by the model structure, which allows for advanced inferential capabilities. Exemplary inputs can include vibration intensities, temperature readings, mission length, and flight cycles. These inputs are combined and processed to produce a complete health score for each item. Confidence intervals with RUL can also be predicted. The Bayesian model responds to mission profile and operational condition variations. Motor overheating or servo lag scenarios can be detected without having to sense all the variables directly. And relatively low computational complexity enables real-time operation on an embedded platform. The system is able to raise alarms or advise the pilot to change flight mode depending on the evaluated risk. Health information at the fleet level could be combined to enhance priors and robustness of the model. One of the strengths of Bayesian methods is the modular nature allowing joint use with other maintenance tools. The operators are able to exercise their own judgement in a manner more precise risk-sensitive decision making. The approach is equally suitable for autonomous mission-critical UAVs. Predictive outputs can be helpful for scheduling inspections or replacement of parts. The system may learn about additional fault modes over time, and thus improve its diagnostic intelligence. Properly implemented, these models help minimize unplanned downtime and increase safe margins. The algorithms are relevant to military surveillance UAVs and civilian delivery platforms. (Kulkarni et al., 2020).

2.3. Predictive Maintenance

Predictive maintenance is a revolutionary concept in the context of unmanned aerial vehicle (UAV) operations that provides facilities to organize maintenance based on data-driven projections rather than fixed schedules or reactive measures. By processing previous performance records and live operation data, predictive maintenance provides early warning if equipment is beginning to fail considering calculated algorithm. Then, Appling corrective action to be taken before system components fail, resulting in extended life cycle, and improved mission availability. predictive maintenance has critical importance to improve in the higher degree of operational availability and safety were mission success and vehicle life critical. The target is to review predictive maintenance methods including degradation model, maintenance scheduling, Failure Mode, and Effect Analysis, economic optimization, and regulation compliance.

Predictive maintenance in UAVs not only increase reliability but also plays a critical role to optimize scheduling of mission. By predicting component degradation behaviors, operators can avoid mission interruptions caused by unscheduled maintenance events. Maintenance operations are better aligned with operational cycles, reducing aircraft downtime with predictive maintenance approach. Predictive models provide quantitative estimates of component lifespans, which in provide mission duration, range, and payload planning. Scheduling for a maintenance becomes more efficient when predictive algorithms, such as neural networks or time-series models, process health monitoring data and forecast potential failures for operation. This approach reduces the uncertainty in mission planning and ensures that high-value UAVs are always available for critical operations. Studies such as those by Rodriguez et al. demonstrate that incorporating predictive analytics into mission planning can improve availability by over 20% for all aircrafts in usage. These improvements are especially relevant for long-endurance UAVs or those operating in long distance environments. In addition, mission planning systems that interact dynamically with maintenance logs can manage routes and durations based on the current health state of the UAV components. Advanced algorithms even allow for real-time rescheduling based on in-flight diagnostics. Predictive scheduling also enables more effective resource allocation, especially in multi-aircraft operations. When paired with cloud-based data systems, scheduling engines can access real-time health indicators and automatically suggest

alternate aircraft for critical missions. This operational agility greatly enhances mission assurance, especially in time-sensitive applications such as emergency response and border surveillance. (Rodriguez et al., 2018)

A key analytical approach used in predictive maintenance is Failure Mode and Effects Analysis (FMEA), which helps identify and emphasize potential failure points within UAV systems. By quantifying failure severity, occurrence probability, and detection difficulty, FMEA provides a structured methodology for risk optimization. In UAV applications, FMEA is especially useful in propulsion systems, structural components, and power electronics. It allows engineers to assign criticality level and focus maintenance efforts where they are most needed. Previous research demonstrated the importance of integrating real-time monitoring data with FMEA models to dynamically provide failure risk during flight. This integration allows UAV systems to adjust their maintenance priorities in real time, ensuring mission continuity. Also, probabilistic FMEA approaches use Monte Carlo simulations to model uncertainty in failure behaviors, enhancing reliability estimations. In composite UAV structures, FMEA can be linked to finite element models to assess crack occurrence under operational stresses. By maintaining updated FMEA profiles, line managers can predict systematic failures and optimize maintenance inventory management. The adaptability of FMEA also supports predictive maintenance systems in assessing the failure risk of newly introduced subsystems or software changes. This creates a feedback loop between operational data and maintenance strategy. (Sun et al, 2022)

UAVs deployed in extreme environments desert heat, maritime humidity, arctic cold present unique challenges for predictive maintenance. In these conditions, material fatigue, corrosion, and sensor dis-location are more pronounced. Predictive approach must be adapted to account for these external influences on degradation. Environmental factors are integrated into models to reflect temperature, humidity, and atmospheric pressure fluctuations. In this condition accuracy can be provided better. Specified research shows that when adaptive models were applied to UAVs operating in arid environments.

These models incorporate real-time weather data and flight telemetry to calibrate degradation rates. Additionally, hybrid models combining physical simulations with machine learning provide strong solutions in these environments. For instance, a UAV operating near saltwater coasts must consider accelerated corrosion models in its

maintenance planning. Predictive maintenance cases must be customized to match environmental operating envelopes. Integration with satellite-based weather data also enables proactive planning before deployment in adverse conditions (Saif et al, 2023).

3. MATERIAL AND METHODS

Note: Some details of this section have been derived from the author's previous publication (Karataş et al., 2025).

Cited article presents the initial findings and some methodological perspective of the study. In this thesis, those data have been investigated through detailed analyses and updated results. The reuse is permitted under the Creative Commons Attribution-ShareAlike 4.0 License, with appropriate citation.

This section outlines the methodology of design, analysis, manufacturing, and evaluation of a UAV with integrated health monitoring and predictive maintenance approach. The methods are explained for both physical and fluid dynamic behavior of UAV development. Firstly, the conceptual design of the UAV is presented, aerodynamic configuration, engine and component selection in this study. Static structural analyses were performed using finite element methods to evaluate mechanical behavior of UAV. Also, CFD analyses were studied to evaluate external and internal fluid behavior, especially around the main structure and air intake geometry. Following the design and analysis, the UAV structure was manufactured using additive manufacturing techniques. Sensors were installed at critical locations to observe vibration, temperature, and structural stress data. The obtained data were processed using signal filtering and logging protocols to feed into a predictive maintenance perspective. In this chapter, the detailed workflow and technical concerns in each step of the UAV's development, are described systematically.

3.1. UAV Conceptual Design

Conceptual Design phase of a fixed-wing UAV, explain key parameters such as mission purpose, propulsion system, aerodynamic and structural configuration of UAV. These steps significantly effect the performance and reliability of the aircraft (Raymer, 2018). In this project, UAV is developed with an emphasis on maintainability concerns. The total weight of UAV is limited as 6 kg, making it usable with electric ducted fan (EDF). The UAV designed to ensure high thrust-to-weight ratio and efficient aerodynamic behavior for investigation of maintainability concerns. Selected layout is a

conventional wing-fuselage-tail configuration with 2 engines. This design provides stability, predictable control behavior, and structural simplicity according to new generation UAVs. The fuselage is designed to include critical systems which are battery units, EDF modules, servo motors, avionics, control units and sensors while keeping aerodynamic structure shape. The wing structure is optimized for low-speed stability, with a moderate aspect ratio. The tail assembly includes two fixed horizontal stabilizer and a vertical stabilizer with a rudder. Control surface sizing and deflection ranges were estimated using standard UAV design references. Concept design of ANOYA UAV shown in Figure 3.1.

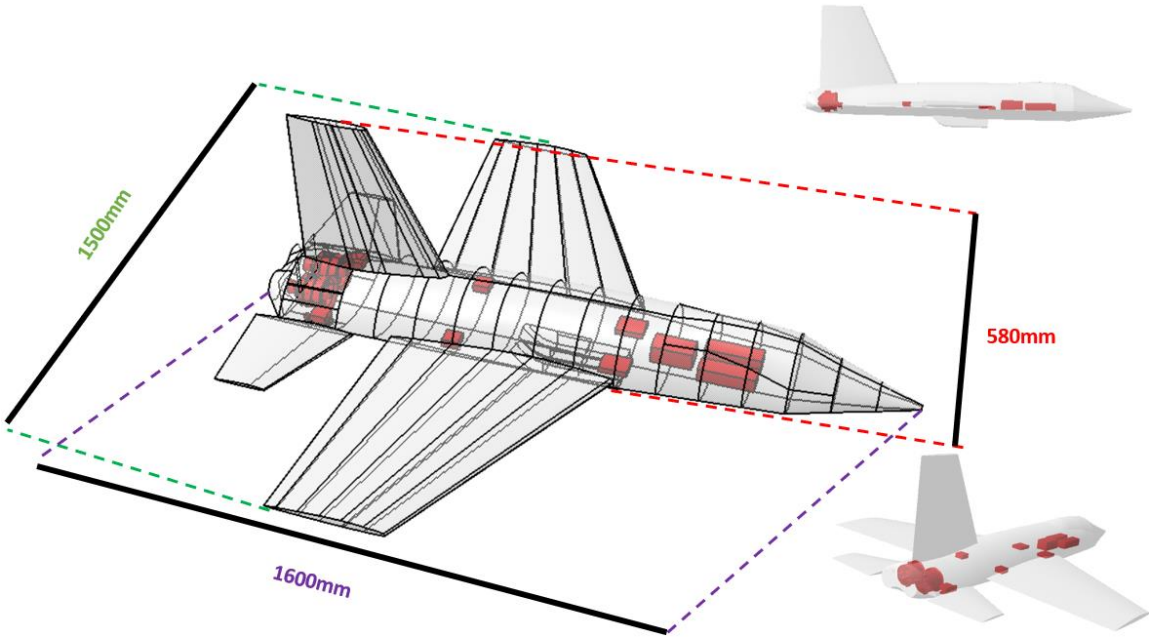

Figure 3.1 ANOYA UAV Conceptual Design

EDF motors is selected due to its compact size, quiet operation and weight. Weight concern depends on selection of material which resist aircraft structure materials against humidity. Two EDF units are integrated into the rear fuselage, increase both propulsion efficiency and internal space usage. This configuration minimizes aerodynamic interference and aligns the thrust vector close to the center of gravity. The UAV is a prototype design and it fabricated using additive manufacturing with PLA material, enabling quick re-manufacturing during the prototype stage. In future studies, stronger composite materials such as carbon fiber-reinforced polymers (CFRPs), Thermoplastic and Thermoset materials are intended to improve structural durability

and reduce weight considering mechanic properties. Intake Geometry and installation shown in Figure 3.2.

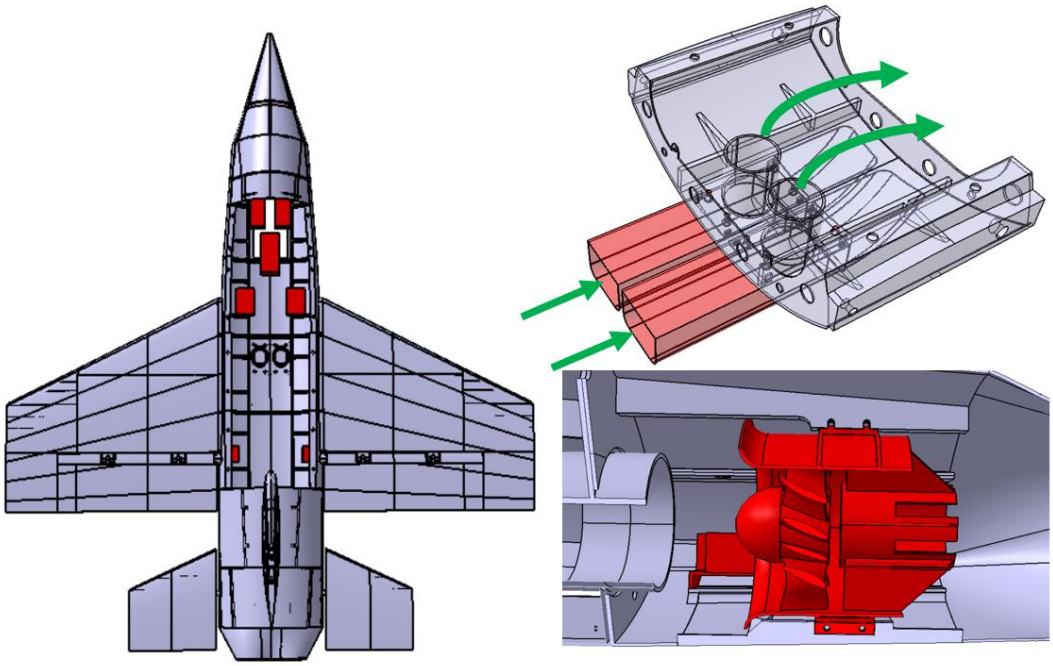

Figure 3.2 Internal Geometry and Air Intake Location of ANOYA

The aircraft's wingspan measures 1500 mm, with a length of 1200 mm and an approximate wing area of 0.3 m². These dimensions are selected to ensure stable flight dynamics and sufficient lift generation for the desired mission profile. Weight distribution is managed to provide aerodynamic balance. The battery is installed symmetrically the longitudinal line to minimize pitch and yaw movement instability. Optionally, removable landing gear is integrated for ground-based testing. The UAV is designed to fly for approximately 15 minutes under normal conditions, using a high-capacity lithium-polymer (LiPo) battery.

Finally, conceptual model provides the baseline geometry and parameters for structural analysis, CFD simulations and experimental setup in the following chapters. Design cases between manufacturability, weight, performance, and structural durability and maintainability are considered during to process. This conceptual design section

creates the base-line using all structural, aerodynamic analysis, and experimental data.

3.2. Structural Analysis

The structural behavior of the UAV was evaluated with three different analyses: static, modal, and explicit dynamic analyses. These analyses were investigated using ANSYS Workbench, and all models were designed and optimized via CAD program which called as CATIA. PLA material was used for UAV structural design, which manufactured via FDM. To ensure simulation accuracy, material properties were not assumed theoretically but were derived from experimental tensile tests. Mechanical properties of PLA material were taken from the study which directly obtain with tests which 20 different specimens were tested under varying 3D printing parameters (Fernandes et al., 2018). The data of test results include ultimate tensile strength, strain at fracture, elastic modulus, yield strength, and toughness, as shown in Table 3.1. These values were directly used in the analysis creating a library in ANSYS.

Table 3.1 Mechanical Properties of PLA (Fernandes et al, 2018)

Experiment #	UTS [MPa]	f [%]	E [GPa]	Yld [MPa]	T [J/cm³]
1	20.71	3.33	1.04	17.27	0.46
2	19.09	3.36	0.94	15.71	0.53
3	20.2	4.16	0.93	15.32	0.69
4	17.67	4.4	0.72	10.96	0.74
5	22.63	3.59	1.01	16.49	0.4
6	19.79	3.69	0.93	14.14	0.47
7	21.36	4.33	0.89	12.78	0.58
8	18.2	4.4	0.78	12.73	0.61
9	24.18	4.08	0.95	14.49	0.59
10	22.35	4.61	0.97	14.97	0.67
11	19.91	4.65	1.01	16.74	0.78
12	22.24	4.49	0.91	15.18	0.89
13	24.97	3.51	1.13	19.09	0.49
14	26.14	3.59	1.19	20.07	0.53
15	25.31	4.56	1.06	17.76	0.65
16	24.32	4.46	0.96	15.94	0.74
17	26.23	4.28	1.22	19.05	0.76
18	26.55	5.01	1.23	20.61	0.81
19	29.43	4.87	1.25	21.07	0.95
20	25.22	5.51	1.0	15.99	1.19

In the static structural analysis, 70 N force was applied to the UAV fuselage considering thrust direction to observe the reaction behavior of UAV. The purpose was to investigate global deformations and stress concentration zones in structural analysis.

Displacement boundary conditions were applied to simulate fixed supports at structural mounting points in analysis program. The finite element results provided from directional deformation and von Mises stress values across the fuselage structure. These results were used to validate or not that the design remains within the elastic range of PLA in flight conditions. In the modal analysis, the frequency characteristics of the wing were studied basically. Frequencies were verified to remain outside of the operational range, confirming structural safety against resonance. The explicit dynamic analysis of UAV focused on impact scenarios. Two conditions were analyzed; firstly, the aircraft hitting a rigid surface, and secondly, a small object colliding with the wing structure. These explicit analyses show localized strain concentrations, deformation behavior and plastic zone development.

All simulations include the same PLA material dataset and meshing strategy to ensure comparability. Directional deformation, maximum principal stress, and equivalent elastic strain were the primary evaluation parameters, which guided performance assessment and structural optimization investigated in this analysis.

3.2.1. Static Structural Analysis of Fuselage

According to the required methodology presented in Section 3.2, this subsection investigates into the specific concerns applied during the static structural analysis which are directional deformation, elastic strain and maximum principal stress. The structural analysis of this study was investigated using ANSYS. In some locations the finite element mesh was created with second-order tetrahedral elements with increased curvature conditions on the other hand first order selected for some specific basic surface conditions. Selection applied according to the complexity and forming of surface. Mesh element sizes were gradually decreased in locally sensitive areas such as holes, fillets, intake connections and curvature zones to make sure sufficient resolution of stress and strain gradients provided. Rear fuselage meshing of CAD model shown in Figure 3.3.

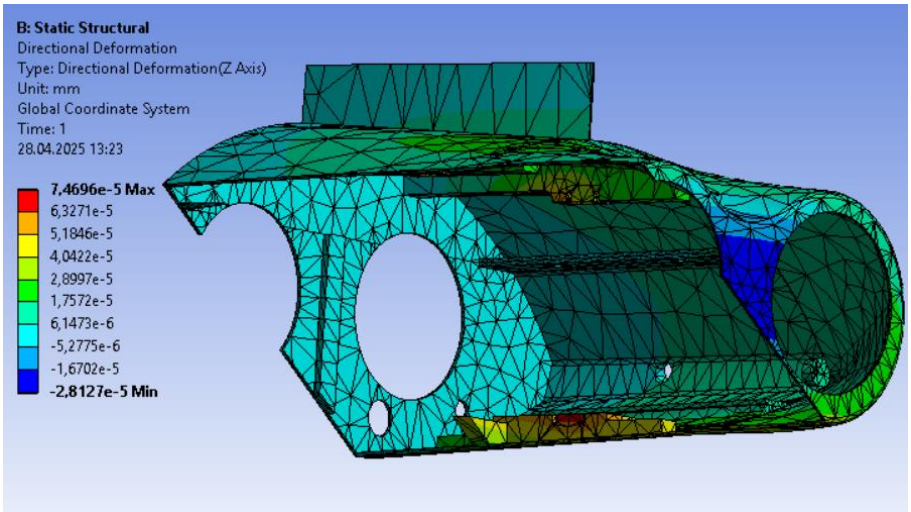

Figure 3.3 Rear Fuselage Meshing of ANOYA

$$[K]\{u\} = \{F\} \tag{3.1}$$

where [K] is the stiffness matrix, {u} is the displacement vector, and {F} is the external force vector. This formula calculates how an applied force at any node of a structure effect displacement. Actually, the stiffness matrix is essential in structural analysis. Because, it explains how a structure internally resists deformation under external loading and it mathematically describe the relationship between nodal forces and displacements. Following the solution of displacements, internal stresses were calculated based on Hooke's law for isotropic materials. PLA is theoretically behaved like orthotropic material because of the usage of FDM method. But in this study, material assumed as isotropic for calculations due to complexity and test requirement of orthotropic material conditions. Because of this, material assumed as isotropic in a lot of study. (Özsoy et al, 2019), (Rajkumar, 2022), (Ezeh and Susmel, 2020).

The von Mises stress was used to explain multiaxial stress condition and potential yielding area. The equivalent stress was computed using:

$$\sigma\_eq = \sqrt{[\ ((\sigma_1 - \sigma_2)^2 + (\sigma_2 - \sigma_3)^2 + (\sigma_3 - \sigma_1)^2) / 2\ ]} \tag{3.2}$$

This formula is used to predict the plastic deformation and yielding behavior of the design.

Boundary conditions and loading definitions were already explained in Section 3.2 and they were directly implemented into the analysis. Analysis output includes entire data on nodal displacements, stress and equivalent strain distributions on model. Output data of analyses are investigated in results sections.

3.2.2. Modal Analysis of Wing Structure

Modal analysis has important role for structural dynamics analysis of an UAV. Anlaysis used to explain natural frequencies and related mode of structure withouth external effect. Analysis evaluates the dynamic characteristics and define the resonance of wing structure for an UAV. In this study, a modal analysis was performed for the wing structure of the UAV using ANSYS.

In this analysis, second order meshing selection provide to obtain more accuracy and enhance stress gradients on curveted wing body surface according to usage of first order elements. In order to ensure realistic dynamic restrictions, wing root of UAV fixed to fuselage in analysis. According to this process, system behavior has been solved for undamped free vibration using eigenvalue equation.

$$[K - \omega^2 M]\{u\} = 0 \tag{3.3}$$

In this equation, [K] represents the global stiffness matrix, [M] is the global mass matrix, ω is the angular displacement, and {u} is the corresponding mode of eigenvector. This equation gives discrete natural frequencies and their deformation patterns which characterize the vibration behavior of structure.

As seen in Figure 3.4, six distinct vibration modes were identified. The lowest natural frequency was found to be 87.021 Hz. Mode shapes indicated a combination of translational and torsional movements, depending on the frequency level. The figure also includes a graph representing the mode number versus frequency relationship for the first six modes.

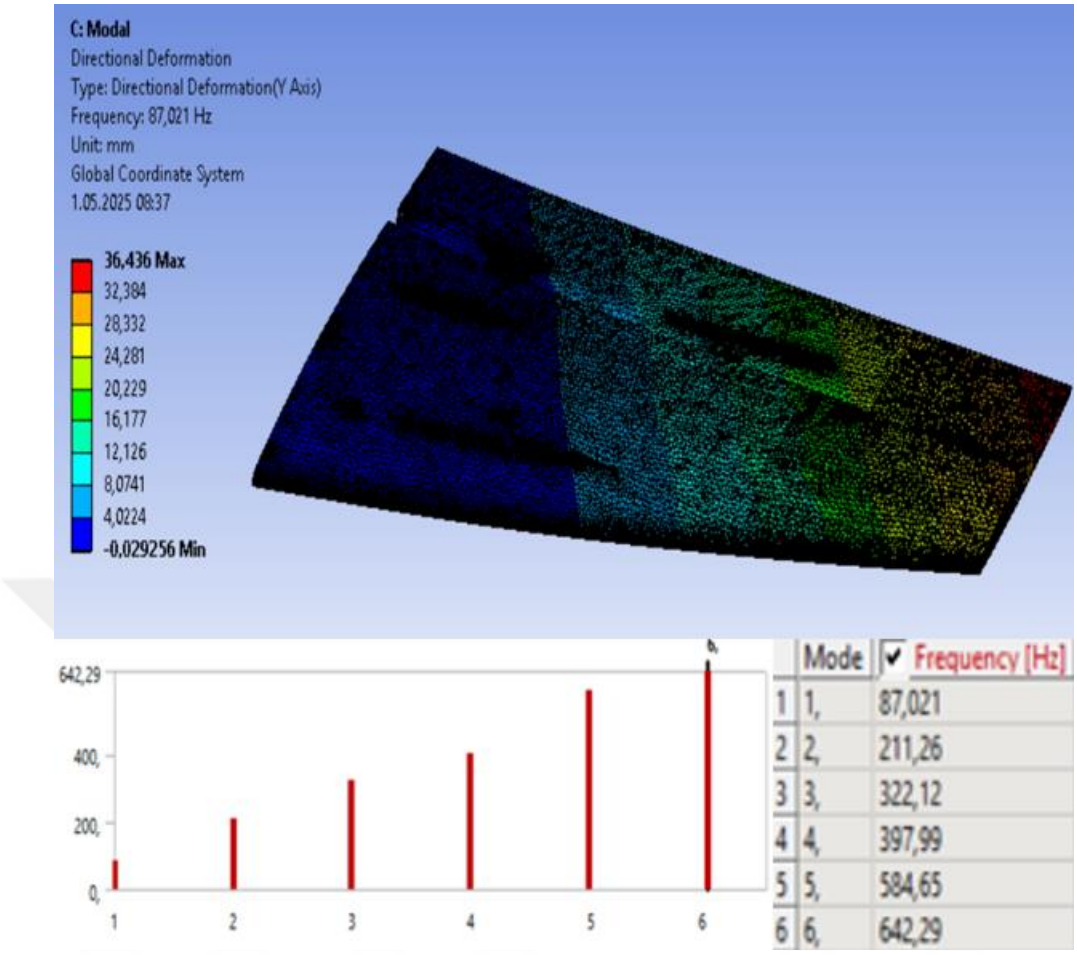

Figure 3.4 Modal Analysis of Wing Structure

3.2.3. Impact Based Explicit Dynamic Analysis

The structural dynamic response of the UAV to high-velocity impact was investigated in this section through an explicit dynamic analysis. The simulation scenario that follows is examined and presented: A hard wall is struck by a UAV traveling at 80 m/s. This condition was used to investigate the energy dissipation properties during the impact, the distribution of equivalent von Mises stress, and the direction of deformation behavior. Since an explicit dynamic solver works best when dealing with problems that are transient and have significant non-linearity, like impacts, it was used for the analysis.

High-order tetrahedral cells were specifically employed in the UAV's nose to improve stress wave resolution and increase accuracy when local deformations were present. The following formula was used to determine the von Mises equivalent stress:

$$\sigma_v = \sqrt{[\ (1/2) \times ((\sigma_1 - \sigma_2)^2 + (\sigma_2 - \sigma_3)^2 + (\sigma_3 - \sigma_1)^2)]} \quad (3.4)$$

The stress wave was generated near the nose and propagated inside the fuselage, where the greatest stress amplitudes and deformations were observed, mainly near the nose. Directional deformation analysis exhibited remarkable values of displacement are revealed to be located in the impact face. Such deformations offer an exploration of the structural edge and of breaking points under extreme conditions.

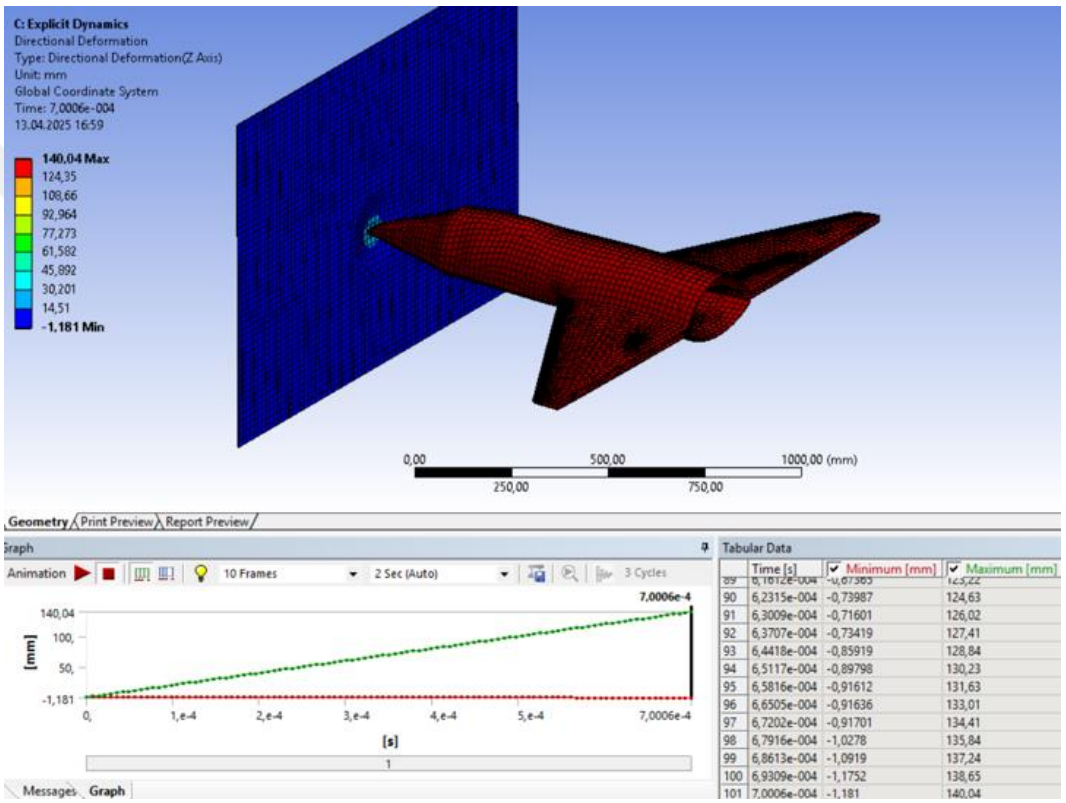

Figure 3.5 Equivalent Stress and Directional Deformation on Impact with a Wall

3.2.4. Aerodynamic Design and CFD Analysis

Aerodynamics is an essential factor in unmanned aerial vehicle (UAV) design, especially in optimization for stability, lift generation, and propulsion efficiency. Aerodynamics configuration has a big amount of influence on the flight performance or power efficiency, and mission operations. In the present work, Computational Fluid Dynamics (CFD) analysis was performed to study the external and internal flow field around the UAV. Then the external flow (3.3.1) was analyzed in order to study the

pressure distributions, the separated flow regions, and the turbulent properties around the fuselage and wings. Streamlines and velocity contours were developed in order to show a laminar flow over critical areas, such as the wing leading edge and the fuselage-wing junction.

Air intake geometry is critical for Electric Ducted Fan (EDF) propulsion performance. In order to minimize pressure, drop and turbulence, intakes were positioned and designed to provide sufficient and consisted airflow into the fan housing. According to geometry design, method of internal flow behavior investigated in section 3.3.2.

Lastly, lift performance was investigated under different velocities until required according to other studies. Using pressure data which obtained from CFD simulation, the lift force acting on the wing was estimated using the Bernoulli principle and Integrated Surface Pressure method. The lift coefficient was evaluated under different velocity scenarios. Calculated lift values were compared against the total mass of the UAV to ensure flight feasibility. (3.3.3) This complex aerodynamic design process enabled for structural and propulsion components to optimize UAV reliability. External Flow Analysis

Computational Fluid Dynamics (CFD) analysis were utilized in this work to investigate the characteristics of the external flow for the ANOYA fixed-wing UAV. The analysis were performed by ANSYS Fluent, with a pressure-based solver for steady-state and incompressible situations. The mesh domain was built around a complete aircraft to take a high enough resolution of the flow features, while the local refinements were applied in the wing, fuselage, and tail geometry. Boundary conditions were set to velocity, pressure far-field, and no-slip wall condition for the solid walls.The airflow domain was enlarged at least five times the chord length towards all regions to suppress the influences of the artificial boundaries' interaction.Turbulence was simulated by the realizable k-ε model and standard wall functions. External flow simulations performed ignoring gravity condition. Inlet velocity values were used of 80 m/s to investigate aerodynamic performance at the theoretical limit.

The nature of the flow was defined by the Reynolds number, calculated using these equations:

$$Re = (\rho * v * c) / \mu \quad (3.5)$$

where ρ is the density of air (1.225 kg/m³), v is the freestream velocity, c is the mean aerodynamic chord, and μ is the dynamic viscosity of air (1.81×10^{-5} Pa·s).

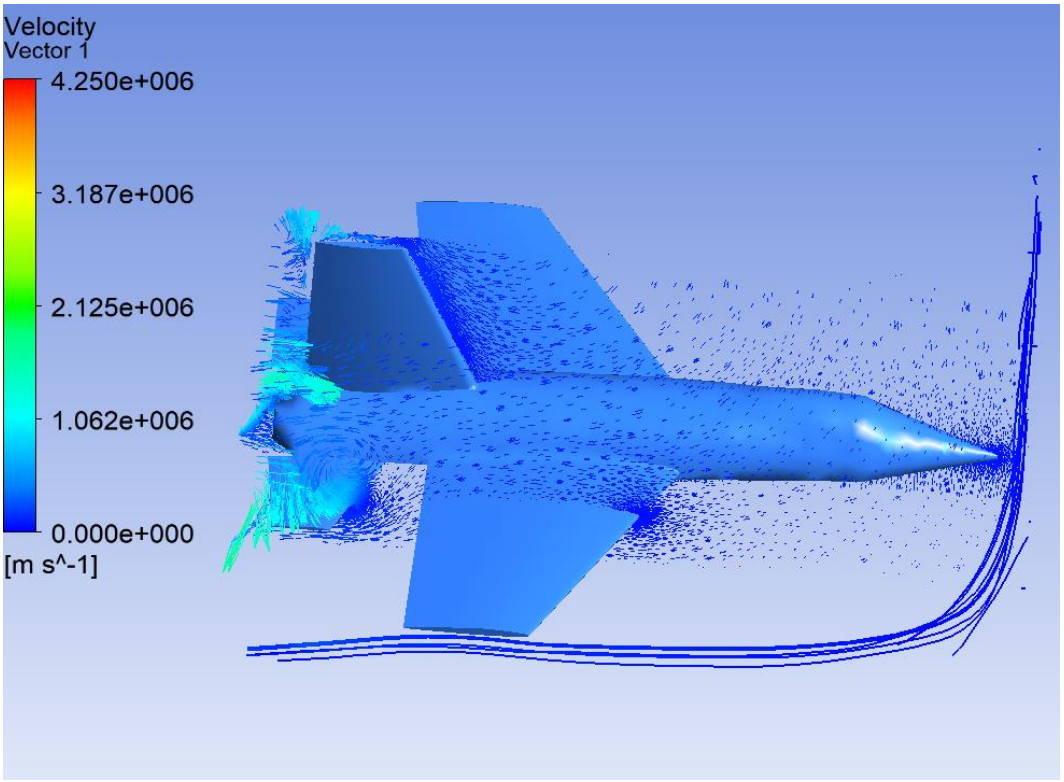

Figure 3.6 External CFD Analysis of ANOYA UAV at 30 m/s Velocity

3.2.5. Internal Flow Analysis of Air Intake

In this section, the internal aerodynamic performance of the air intake for the developed UAV is examined by Computational Fluid Dynamic analysis. The airintake flow feeding the twin EDF motors also has a significant effect on pressure loss recovery and aerodynamic issues. Design process focused on the improve flow linearity and and provide steady mass flow to the EDF motors. CAD model of the UAV with curved air-intake and ducts design was used to provide the internal airflow for UAV. Fig. 3.20 shows the air-intake's internal CFD domains for the fan interface, curved transition, and inlet regions. Vectors in figure, show the main direction of airflow. Geometry features a smooth and same size from the output of air-intake to the fan section to accelerate the flow as required. In this case, pressure loss will be eliminated for velocity change. Two

fundamental fluid dynamic laws serve as the foundation for the analysis.

The first is the continuity equation, which is represented as follows and ensures mass conservation throughout the duct:

$$A_1 v_1 = A_2 v_2 \tag{3.6}$$

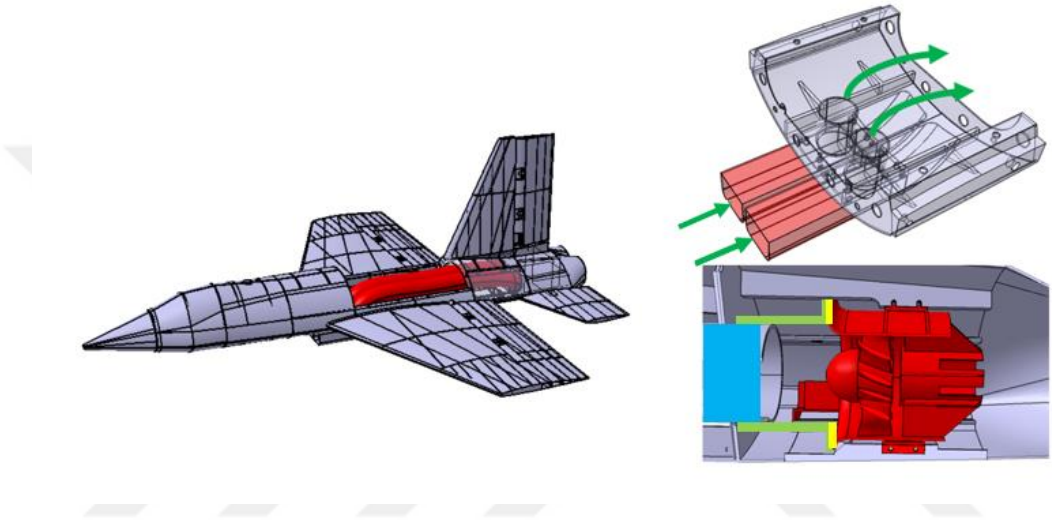

Figure 3.7 Air Intake Location and Interfaces on UAV

This formula represents the cross-sectional area of the duct and the velocity of the flow. As the area decreases in the converging part of the duct, the velocity increases according to change. This is confirmed by the CFD results which is shown in Figure 3.21, where the internal flow experiences an increase in velocity as it moves through the intake section.

The second principle is Bernoulli's Equation, applied in the subsonic incompressible flow assumption:

$$P + \tfrac{1}{2}\rho v^2 = \text{Constant} \tag{3.7}$$

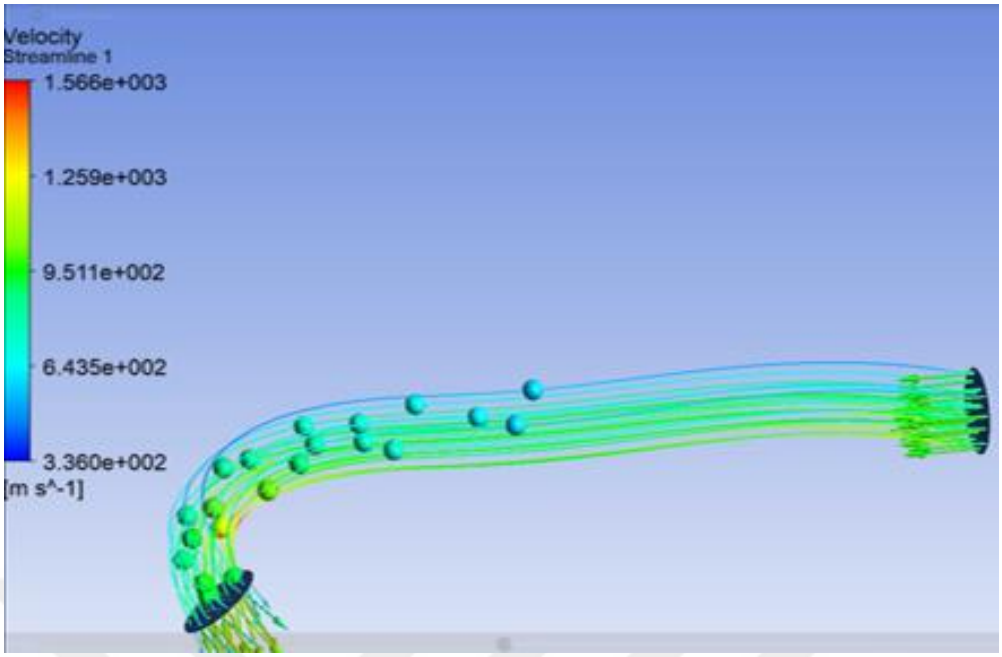

Figure 3.8 Velocity Behavior of Air Intake Design

This relation highlight the dependency of the increase in velocity corresponds in case of the pressure loss at local locations which aligning with pressure distribution in analysis. Because of this, analysis validate the duct design in minimizing pressure loss and avoiding flow seperation. To simplify explanation, the streamline distribution and pressure variation along the duct wall are examined. These data help to verify airflow remains which attached to the duct surface minimizing vortex formation and pressure losses. The curvature of air-intake was designed to comply with empirical guidelines for low Reynolds number duct flow, ensuring the system operates within laminar-to-transitional regimes under loading conditions. Additionally, the boundary conditions for the simulation were set using enviromental atmospheric pressure at the inlet and mass flow outlet conditions at the EDF interface.

Generally, the internal flow analysis confirms the aerodynamic compatibility of the duct with the EDF, which validating its design in terms of flow delivery, pressure uniformity and drag minimization . The CFD results will be used to validating structural airflow loads applied in downstream simulations considering performance assessments of the EDF motors

3.2.6. Lift Estimation at Variable Velocities

This section used CFD analysis to estimate the lift forces generated on the UAV wing for different velocities. The airspeeds of the simulations are 30 m/s, 50 m/s, 70 m/s

and 80 m/s, which represent the low, moderate, and high flight situations, respectively. The objective was to determine how lift force varies with speed and whether the wing design provided the minimum amount of lift necessary to support the entire mass of the UAV.

The lift force was calculated using a relation, where it is the pressure distribution over the upper and lower surfaces of the wing:

$$L = 0.5 \times \rho \times v^2 \times S \times Cl \tag{3.8}$$

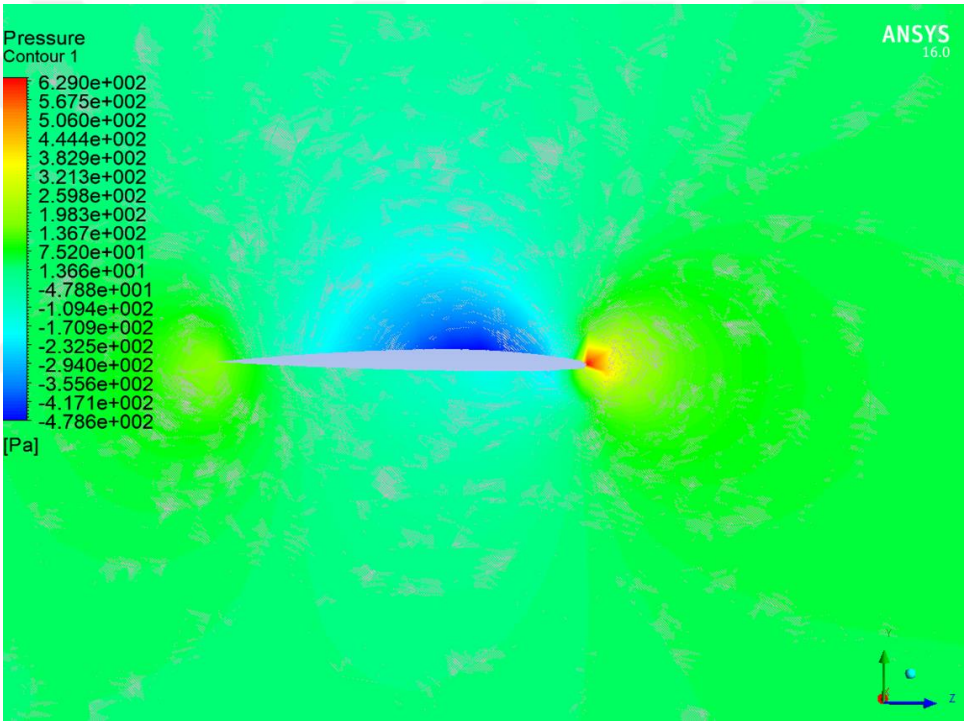

Figure 3.9 Lift Estimation for Left Wing at 50 m/s Velocity

3.7. Manufacturing and Assembling of UAV

In this section, the production and assembly of the designed UAV's structure is described with images. Special attention was paid to the application of additive manufacturing processes for structural components. The CREALITY K1 MAX 3D printer was used to manufacture all strcutural parts with some specifications. The printing settings, support structures, and infill density were optimized to achieve a high strength-to-weight ratio and ideal dimensional tolerance. After manufacturing,

the sub-assemblies were assembled to check the fitting of the parts and ease of integration into the next step.

3.7.1. Additive Manufacturing of UAV

The UAV's structural components were manufactured using fused deposition modeling through the Creality K1 MAX printer. All slicing processes were performed using appropriate G-code generation software of Creality, and parts were printed with PLA material. The layer height was fixed at 0.2 mm for consistent wall precision. Infill patterns such as grid and monotonic were utilized depending on structural needs. Support structures were enabled with a 30° threshold angle to minimize overhang-related deformations. Figures 3.10–3.12 illustrate the slicing previews and printer configurations for several major components.

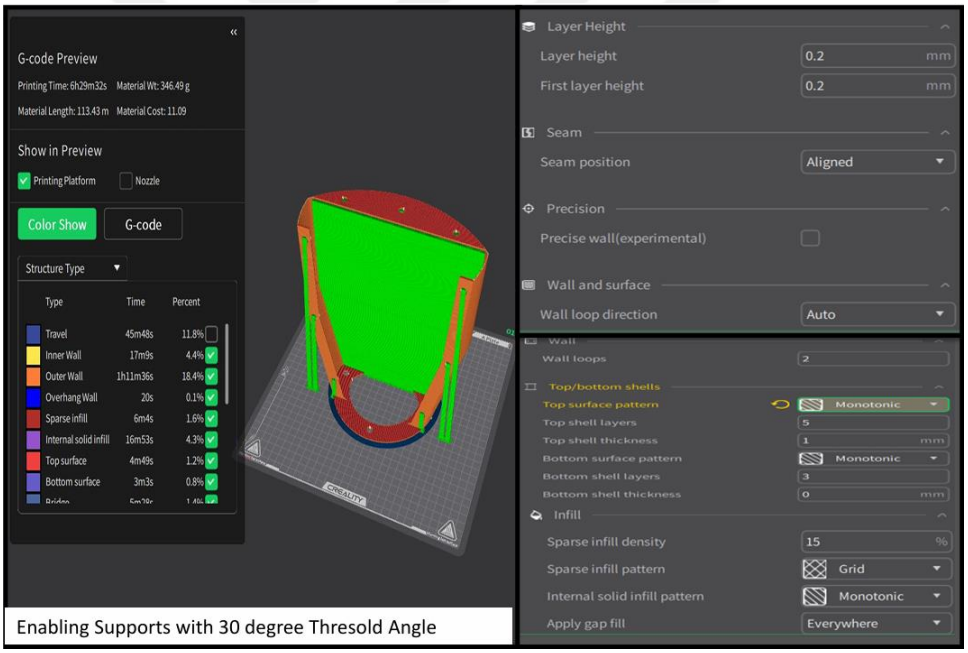

Figure 3.10 G-code preview and slicing settings for Front Fuselage Part-3

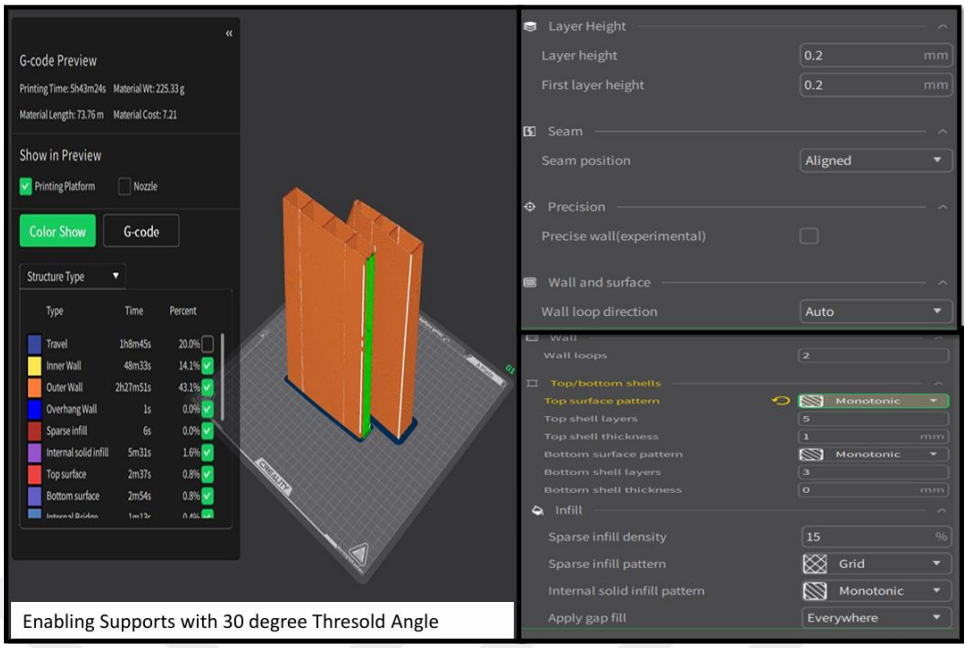

Figure 3.11 G-code preview and slicing settings for Left Wing Part-1 and Part-2

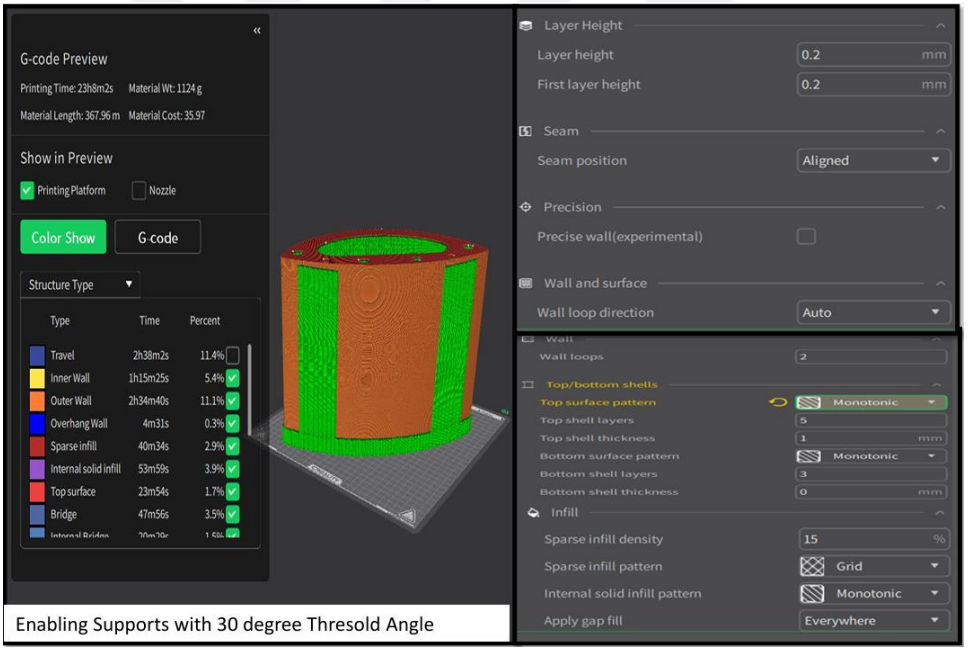

Figure 3.12 G-code preview and slicing settings for Rear Fuselage Part-1

3.7.2. Assembling of Structural Parts and Equipments

According to manufacturing with settings which specified in previous section; all structural parts were successfully printed, they were assembled at the sub-assembly level. This step involved manually assembling the fuselage sections and control surfaces to check for geometric conformity. Slot and alignment features within the 3D

printed models facilitated rapid and accurate joining of sections. The images below show the manufacture and assembled sections for aircraft.

Figure 3.13 Installation of Front and Center Fuselage View-1

Figure 3.14 Installation of Entire Fuselage View-1

Figure 3.15. Manufactured Wing Profile of ANOYA

3.8. Health Monitoring Implementation

In this study, health monitoring is not physically implemented on the UAV prototype. However, a fundamental theoretical framework is presented regarding the required steps and system architecture. Health monitoring systems in UAVs primarily aim to observe structural and operational integrity in real-time using embedded sensors, data processing units, and predictive algorithms. The effective integration of health monitoring can significantly reduce maintenance costs and improve mission reliability

for UAV missions. This section presents the necessary methodologies for placing the sensors, acquiring data and managing signal processing for UAV health monitoring.

3.8.1. Sensor Placement and Data Acquisition

Structural Health Monitoring in aerospace structures relies on precise sensor placement for accurate data acquisition. Due to this, selection of sensor types and their integration locations were determined based on stress and strain distribution results which obtained from finite element analysis. Critical loading regions were chosen as primary installation locations for measurement sensors to monitor damage progression considering maximum principal stress and equivalent strain values.The fuselage of the UAV was divided into three sections where are front fuselage, center fuselage, and rear fuselage for targeted sensor implementation. In subsequent studies, much more zone will be investigated for sensor implementation.Each section show different stress behaviors due to structural features and load distribution. In the front fuselage, high principal stress values were observed near the curvatures and frame. Thus, strain gauges were strategically placed across those regions. In order to record distributed strain data, Fiber Bragg Grating (FBG) sensors—which provide multiplexing and immunity to electromagnetic interference—were incorporated along the internal stiffeners' longer, linear sections. The analysis of the center fuselage showed areas of relatively high strain close to the mounting holes and compartment junction lines. In this study, strain gauges and FBG sensors were used to observe local deformation and strain values for structural parts with aircraft structural integrity behaviors. For this investigation FBG sensors cover large areas for more comprehensive evaluation for principal stress behavior. In the other hand, strain gauges measure strain values of structural part for high gradient regions.

The pressure levels at the rear fuselage were lower than in other areas, even though it had essential connections that require continuous inspection. Hence, FBG sensors were installed at the rear arc and curvatures, whereas strain gauges were implemented on flat regions around bolted joints.

The strain at a certain point was derived from the engineering strain as described by:

$$\varepsilon = \Delta L / L_0 \quad (3.9)$$

In which ε is the engineering strain.

The principal stresses under these loading conditions. To access the internal stress distribution, particularly the principal stresses generated during structural loading, the following equation is used:

$$\sigma_{1,2} = (\sigma x + \sigma y)/2 \pm \sqrt{[\,((\sigma x - \sigma y)/2)^2 + \tau xy^2\,]} \quad (3.10)$$

Here, σ_1 and σ_2 are the principal stresses, respectively, σx and σy are normal stresses in the x and y directions, as well as τxy is the induced shear stress in the xy-plane.

Using these formulations, the collected data from the sensors can be compared against theoretical predictions and simulation outputs to validate the structural integrity of the UAV throughout its operation.

3.9. Predictive Maintenance Planning Strategy

In this study, a predictive maintenance strategy has been investigated theoretically which based on the structural and aerodynamic analyses of the ANOYA UAV. Although health monitoring based sensor data could not be obtained during the related step of the research; Von Missess stress, plastic deformation and CFD based evaluations performed using different analysis methods which have been used to propose a predictive maintenance perspective. This approach built on the prediction for subsequent sensor integration studies which guided by the specified locations in previous sections considering finite element analysis. This FEA analysis will enable a health monitoring and predictive maintenance approach for subsequent studies.

The methodology begins with defining a maintenance philosophy which is restricted with UAV operational conditions and physical limitations. In the section, the operational boundaries, such as flight velocity ranges, material strength limits, and other mechanical behaviors have been conceptually investigated using simulation outputs. Failure Mode and Effects Analysis (FMEA) has been investigated on structurally sensitive components which are determined by static and dynamic analysis to assess possible degradation mechanisms. Although sensor responses are unavailable,

theoretical failure scenarios and stress distributions provide a base for component risk ranking.

In other subsection Model-Based reasoning strategy has been proposed for the estimation of Remaining Useful Life (RUL), investigating degradation results which are obtained from modal analysis and structural stress distributions via finite element simulations. Although no direct fatigue analysis or experimental sensor data has been studied, the estimations are theoretically grounded in the observed behavior of structural components under repeated stress conditions which also reported in relevant studies. (Sikorska et al, 2011). In subsequent studies, Long Short-Term Memory (LSTM) networks and regression-based Weibull distributions may be integrated to refine RUL predictions for more dynamic and adaptive manner considering sensor data which will be obtained from health monitoring results.

Furthermore, maintenance scheduling and cost optimization methods are investigated within this study. The optimization is currently explained through theoretical maintenance intervals which aiming to minimize UAV downtime and service cost.

3.9.1. Maintenance Philosophy and Operational Boundaries

The maintenance philosophy for the UAV has been developed in this study for the concepts of maintainability, cost-efficiency, and operational availability of ANOYA UAV. Although real-time sensor data is not obtained in this phase, the strategy relies heavily on simulation-based investigations which derived from finite element structural analysis and operational load scenarios. This approach is commonly referred to as a hybrid predictive maintenance perspective which combining theoretical degradation behavior with scenario-based operational profiles. Similiar investigation has been performed by Jardine et al in 2006.

In here, adopted maintenance philosophy approve a Condition Based Maintenance (CBM) structure. CBM strategies are built upon the assumption that degradation occurs gradually and that its detection allows preventive interventions before failure. In this perspective, failure-prone regions were previously identified through static structural analysis and maximum principal stress evaluations. Stress points on the wing-fuselage interconnections, EDF Motor mount regions and Landing Gear supports have been specified and dedicated for further observation in future prototyping phases. Although

direct damage accumulation measurements are not computed here due to the absence of fatigue or life-cycle data , these locations are has been considered primary high-maintenance zones.

Operational boundaries were defined according to the expected flight envelope of the UAV, which includes maximum working speeds up to 80 m/s and estimated load factors under common maneuvers. For the definition of operational boundaries, assumptions on velocity, altitude range and mission duration have been estimated based on typical tactical operation profiles. These parameters create the expected stress spectra on the structural frame.

Mathematically, the maintenance intervals can be considered in relation to the critical stress ratio:

$$\eta = \sigma\_max / \sigma\_yield \quad (3.11)$$

Formula show the normalized stress index, is the simulated maximum von Mises stress in the component, and is the yield strength of the PLA material used. Maintenance inspection intervals are assumed to be shorter due to higher sensivity to mechanical and fatigue behavior , particularly in loaded regions. Additionally, boundary diagrams were proposed to correlate mission profile severity to required inspection frequency. For instance, high-speed operations near the maximum velocity conditions require inspection after every 10 cycles, while low-speed surveillance missions allow intervals up to 30 cycles.

A conceptual function for maintenance interval estimation is given as:

$$MI = \alpha \cdot e^{(-\beta \cdot \eta)} \quad (3.12)$$

Where MI is the maintenance interval in cycles, and α, β are tunable coefficients to be defined after operational data becomes available.

Based on the finite element analyses which related with the rear fuselage's EDF Motor section of the UAV, stress ratio (η) values were calculated to estimate potential

maintenance intervals for critical structural fault regions. The stress ratio is defined as η = σ_max / σ_yield, where σ_max is the maximum von Mises or principal stress obtained from analysis, and σ_yield is the yield strength of the PLA material which approved in previous sections. In this study, the yield strength of PLA was taken as 60 MPa considering approved test data in previous study of Fernandes et al in 2018. The results of three key stress concentration zones are presented below. In regions where η exceeds 0.6, early inspection and shortened maintenance intervals are recommended due to increased risk of fatigue or strength induced damage. The table below summarizes the calculated stress ratios and their implications on EDF connection area.

Table 3.2 Stress Ratio Based Maintenance Inspection for EDF Motor Zone

Location	Max Stress (MPa)	Stress Ratio (η)	Maintenance Inspection
EDF Mount Interfaces	3.23	0.054	Moderate – Periodic check every 30 cycles
Lower Inner Flange	2.79	0.046	Low – Check every 40+ cycles
Edge Hole Vicinity	2.36	0.039	Low – Regular inspection during routine checks

As seen in the table 3.2, the stress ratios are well below the critical threshold of 0.6 which calculated using equiation 3.11. According to given data for structural integrity of components, it can be maintianed under loading scenerios.Nevertheless, due to the proximity to load transfer joints and interface hole; these areas are spotted for monitoring in future sensor-augmented test flights. These estimates will form the baseline until strain gauge feedback or fatigue testing data become available.

3.9.2. Failure Modes Effect Analysis and Critical Component Assessment

In predictive maintenance investigation for UAV systems, Failure Modes and Effects Analysis (FMEA) show important role for potential failure mechanisms within critical components. Declearing Risk Priority Numbers (RPN) for individual zones of the UAV structure, engineers can rank subsystems for maintenance, or redesign operations. Important factors in calculating of RPN existing Severity (S), Occurrence (O), and Detection (D). which formula is:

$$RPN = S \times O \times D. \quad (3.13)$$

This method provides an important result to guide predictive maintenance operations and optimize operational safety. In this study, five critical UAV regions were examined for structure: Wing Root, EDF Mounting Zone, Air Intake Zone, Front Fuselage Nose Structure, and Main Landing Gear Zone. Each of these components was evaluated using engineering judgement and analysis results to assign numerical values between 1 and 10 for severity, occurrence, and detection of failure. For example, the Wing Root showed the highest severity due to structural stress concentrations and low inspectability owing to its internal layout. Wing Root RPN calculated as 189 score which was showing it as most critical zone of ANOYA UAV. Reversely, the Front Fuselage Structure received to moderate score for severity leading to relatively lower RPN of 108. These results help to rank inspection frequencies and improve sensor placement strategies. A high RPN typically show the fault, which is both likely to occur and severe in consequence. But difficulty to detect fault early, precautions must be taken for predictive maintenance operations. In addition to RPN calculations, a fault ranking line chart was created to visualize the comparative criticality across the UAV's zones and structures. This graphical perspective helps maintenance planners to determine which zones demand critical attention. This type of visualization tools are especially beneficial during design reviews and mission preparations. This methodology does not replace of physical testing or real-time monitoring, but improve the design process by specifing structural behaviors during the pre-deployment phase. As similtanious operational data becomes available, the FMEA matrix and RPN values can be continuously refined for better accuracy.

In summary, FMEA provides a important baseline for decision-making in UAV predictive maintenance operations. It ensures that critical failures are not only foreseen but also reduce through targeted inspection strategies. Combined with other tools such as Fault Tree Analysis or sensor-based diagnostics, it forms the backbone of a risk-informed maintenance architecture.

Table 3.3 Risk Priority Number for UAV Zones and Structures

Component Zone	Severity (S)	Occurrence (O)	Detection (D) and RPN
Wing Root	9	7	3 (RPN=189)
EDF Mounting Zone	8	6	4 (RPN=192)
Landing Gear Zone	7	6	4 (RPN=168)
Air-Intake Zone	6	5	5 (RPN=150)
Front Fuselage Nose Structure	6	6	3 (RPN=108)

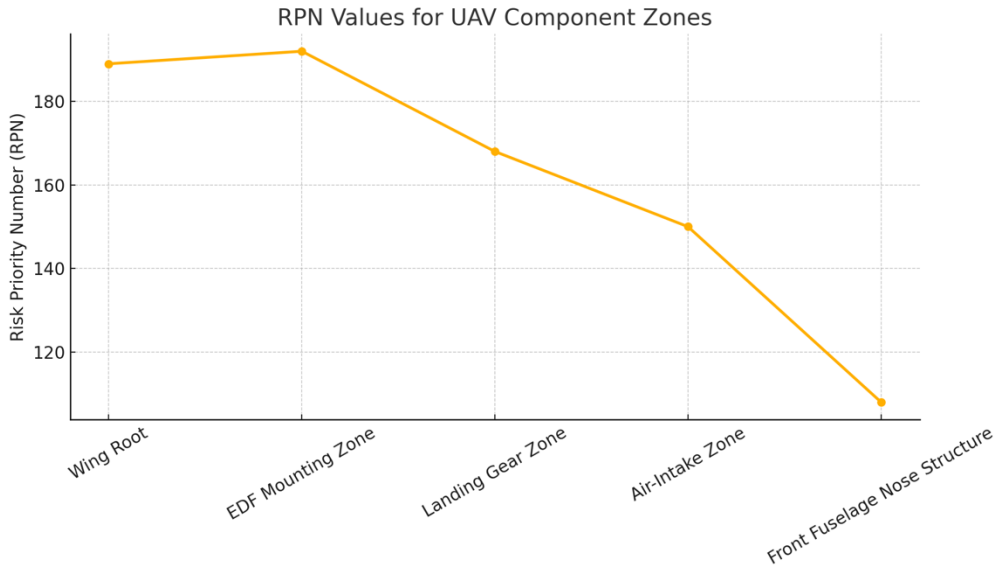

Figure 3.16 FMEA RPN Values for UAV Component Zones

3.9.3. Remaining Useful Life (RUL) Estimation Models

In this section, Remaining Useful Life (RUL) estimation was investigated through a model-based solution perspective. This approach combine the results which obtained from structural analysis such as static stress distribution, modal frequencies, and explicit dynamic analysis.It helps to define regions with higher damage potential using this method. Although sensor-based degradation was not investigated due to the absence of

experimental or in-flight data, the available analysis offer a strong baseline for theoretical RUL estimations. The normalized stress index (η), calculated as the ratio between the maximum von Mises stress and the yield strength of PLA material. It observe an important role for identifying high-risk zones. Zones with η values which greater than 0.6 were pointed as potential early failure zones. RUL is conceptually estimated using the inverse of damage accumulation principles in this UAV.

However, due to the lack of fatigue test sensor data or real-time strain measurements; Miner's Rule could not be applied for RUL estimation.

Specified function used for RUL prediction is given by:

$$RUL = R_0 \times e^{(-\beta \times \eta)} \quad (3.14)$$

Where R_0 is the initial reference life, β is a degradation constant derived from material behavior, and η is the normalized stress index. Although this function remains theoretical at this stage, it will show as a baseline for subsequent studies in future once sensor-based condition monitoring is enabled. Zones such as the EDF Mountings, Wing Root, and Landing Gear were investigated to control and visualize this approach.

The chart which specified below presents a notional RUL degradation profile for different UAV components. This graph is constructed using simulated η values and projected degradation rates. Ultimately, this RUL perspective orient with condition-based maintenance philosophy which introduced in Section 3.6.1 and complements the criticality assessment from Section 3.6.2. Once empirical sensor data available, machine learning models like LSTM or Gaussian process regression can be integrated to refine and adapt these predictions. Because of this, it offers a foundational strategy for sensor based predictive maintenance UAV operations in subsequent studies.

Table 3.4 RUL Estimation for Structural Components

Component Zone	Normalized Stress Index (η)	Estimated RUL (cycles)
Wing Root	0.65	180
EDF Mounting Zone	0.68	165
Landing Gear Zone	0.55	240
Air-Intake Zone	0.48	270
Front Fuselage	0.42	300

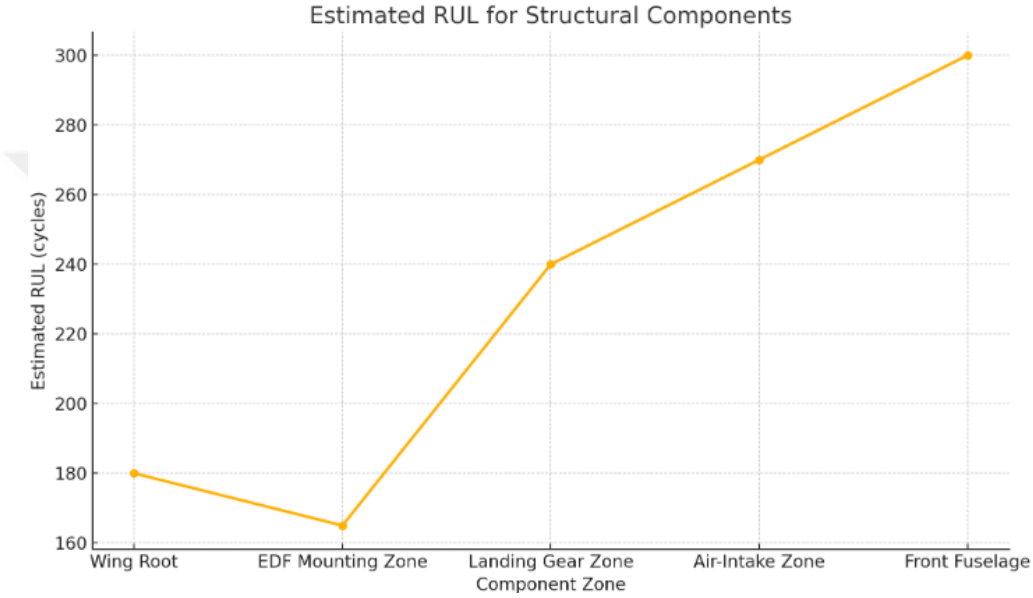

Figure 3.17 Line Chart for RUL Estimation of Structural Components

3.9.4. Maintenance Scheduling and Cost Optimization

In this section, cost and interval-based optimization of maintenance scheduling for UAV components is discussed. In case of the usage of predictive maintenance application, structural manufacturing intervals and cost will be depends on the health monitoring datas without dependency of preventive flight hours. For this study, PLA material usage, unit cost (650 ₺/kg), and auxiliary production expenses (e.g., electricity, labor) at a flat rate of 25 ₺/hour were used as the basis for cost calculations. For each structural zone, the estimated maintenance cost per task was derived by combining material cost and time-based energy/labor consumption. The purpose of this study was to identify and removed the zones requiring frequent and high-cost maintenance tasks in order to preventive actions using health monitoring based predictive maintenance tasks. Total values may depending on exchange rate fluctuations and inflation. These figures are based merely on current data of operation.

Table 3.5 Estimated Corrective Maintenance Costs for Selected Structural Zones and Parts

Component	PLA Usage (kg)	Print Time (hr)	PLA Cost (৳)	Electricity & Labor (৳)	Total Cost (৳)	Maintenance Interval (Flights Hour)
Wing Section	0.78	8.0	507.0	200.0	707.0	20
EDF Housing	0.33	4.5	211.25	112.5	323.75	25
Landing Gear Zone	0.3	4.0	195.0	100.0	295.0	15
Sensor Mounts	0.1	1.5	65.0	37.5	102.5	30

4. RESULTS

This section shows the results which are obtained from the structural and aerodynamic analyses of the ANOYA UAV. The design's structural integrity and dynamic response were evaluated with finite element analysis which including static stress, modal deformation and explicit dynamic analysis. Aerodynamic characteristics of UAV were evaluated via external and internal CFD analysis to determine aerodynamic behavior under variable flow conditions and and air-intake efficiency about pressure distribution. Due to technical and logistical issues, sensor integration could not be installed on the physical UAV prototype. Because of this, predictive maintenance strategies and health monitoring evaluations were investigated with based on simulation data. These results provide a detailed explanation of the UAV's loads and aerodynamic forces responses which were used to determine approximate damage-critical zones and potential failure scenarios. According to obtained data, Failure Modes and Effects Analysis (FMEA) and Remaining Useful Life (RUL) estimations were investigated which derived from analysis results. These evaluations allowed for classification of structural components in terms of severity and expected maintenance requirements. Cost and maintenance interval predictions were based on modeled part replacement strategies according to analysis results rather than experimental degradation results which will be obtained in subsequent studies. This results chapter provides a data-driven foundation for predictive maintenance planning in UAVs, even in the absence of real-time sensor data. While this result gives certain assumptions, it allows for strategic predictive maintenance perspective based on simulated stress and strain behavior for performance on ANOYA UAV. The findings represent an important step for RAMS based design validation in UAV structures which are manufactured via additive methods.

4.1. UAV Structural Analysis Result

The structural integrity of the ANOYA UAV was evaluated through a sequence of simulation-based analyses, which are including static structural, modal, and explicit dynamic assessments. These analyses were performed on the CAD model using finite element methods (FEM) with boundary conditions and material definitions for PLA-

based components. The static structural analysis explain that maximum stress concentrations occurred around the EDF mounting zone and landing gear interfaces which aligning with areas previously identified as critical in the design phase. Directional deformation results indicated a maximum displacement of 0.0145 mm in the vertical (Z) axis, which remained within acceptable design tolerances. The equivalent elastic strain values remained below 1.7x10^-5, confirming that no plastic deformation was expected under nominal loading conditions. Principal stress results highlighted localized stress peak points of approximately 3.2 MPa which especially around bolt holes and curvature transitions on body structure.

On the other hand, modal analysis results identified natural frequencies and deformation modes with the first bending mode which occurring below 250 Hz. According to obtained data, bending mode range considered as safe for the expected UAV operational envelope.

Additionally, the explicit dynamic analysis simulated for a high-velocity impact scenario (80 m/s) to examine energy absorption and structural failure behavior of UAV against steel wall. This study revealed concentrated stress wave propagation near the nose structure and deformed zones which offering insights into potential areas for structural reinforcement in subsequent studies. Although no fatigue or lifecycle modeling was performed according to material selection; the analysis served as an important approach for identifying failure-effected zones.

In summary, the structural analysis results show that the UAV model is mechanically strong under the analyzed conditions, with stress, strain, and deformation values for required structural strength. These findings will help sensor placement and maintenance planning in subsequent studies where experimental validation and long-term monitoring are expected to be introduced.

4.1.1. Static Structural Analysis Results

In the result study, a number of finite-elements were examined for structural performance of the UAV and its components under 70 N force scenerio. The analytical results present information into the stress distributions, deformation results, and strain localizations of various components under static loading conditions.First, the distribution of maximum principal stress in the structure of the nose (Fig. 4.1) presented a peak value in the front of the fuselage of 2.519 MPa, which indicated a critical

location in load transfer from the nose. Also illustration show 2.2897 mm elastic strain and 88.341mm directional deformation at Z direction of aircraft.

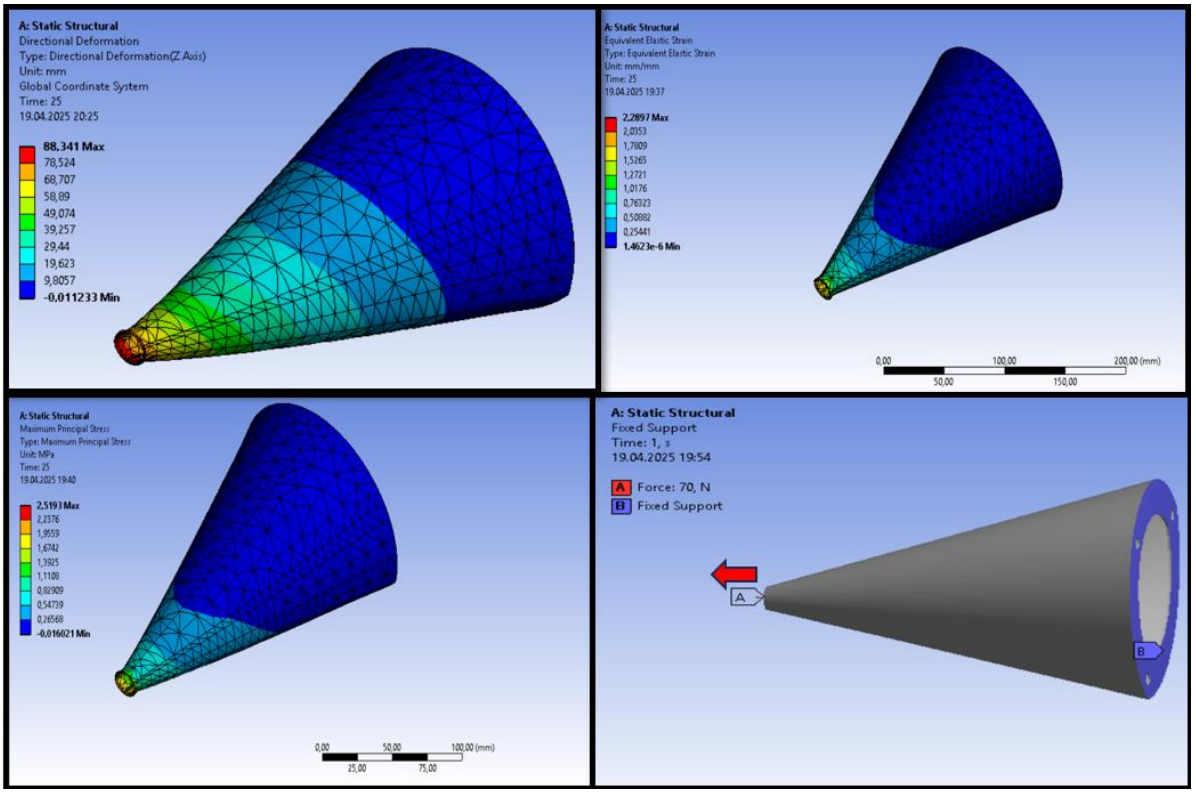

Figure 4.1 Stress & Strain Distribution at Front Fuselage Nose

Analysis in a structure casing (Fig. 4.2) indicates a maximum displacement at Z Directional Deformation of 13.178 mm, focused around frame cutout, caused as a result of the load applied boundary. A corresponding elastic strain of 10.97 mm/mm was found mainly at the curvature transition and the region around bolt holes and this zone could be possible regions of fatigue risk it should be investigated with sensor integration. For the same part, the peak principal stress was 12.385 MPa with higher stress concentration at the upper flange and hole interfaces. These results indicate selective design reinforcement in these regions. Fiberbrag sensors can be implemented in problematic areas of this zone.

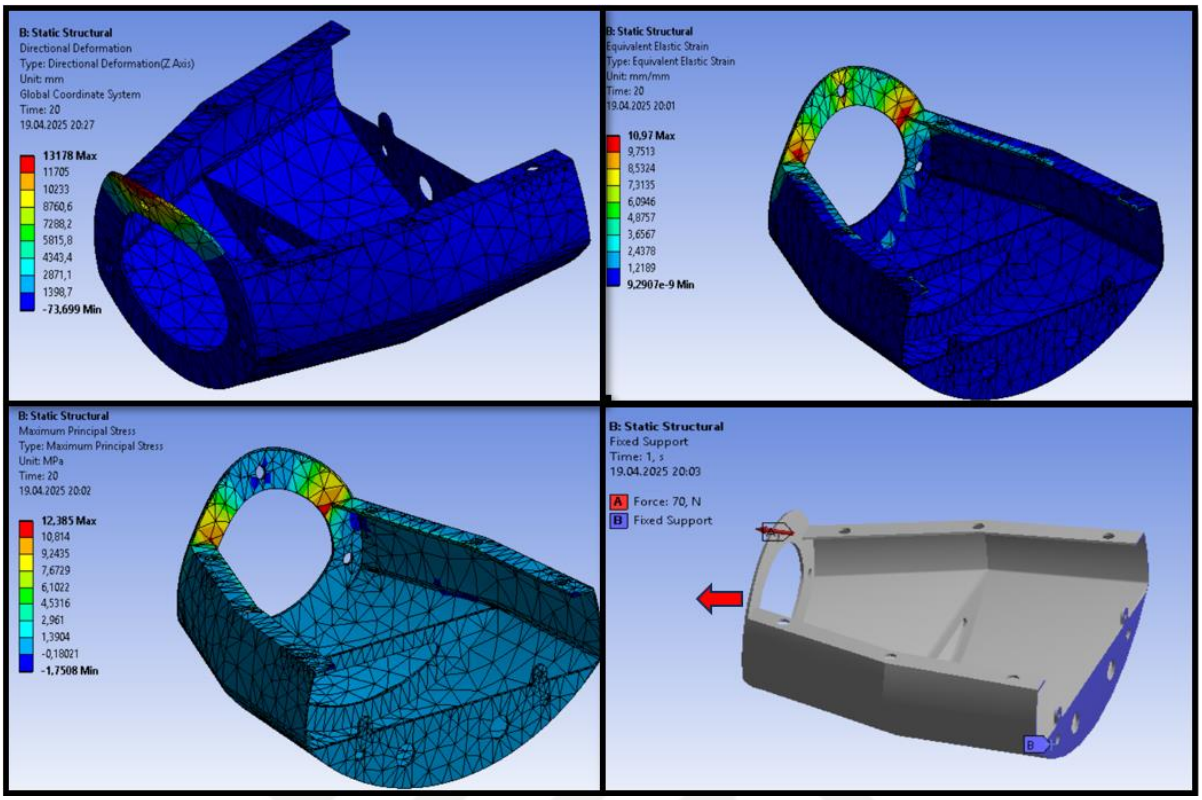

Figure 4.2 Stress & Strain Distribution at Front Fuselage AN531002 Part.

In the third setup (Figure 4.3), the directional deformation achieved 14.020 mm, significantly higher than previous ones; hence, refinement of material increasing strength value at trim operation of creality or revision of geometry may be required to provide better deformation results at this point. Sensors can be installed in specified area to observe deformation in subsequent studies.The corresponding elastic strain magnitude for this case was 12.754 mm/mm, which indicates a substantial local elastic strain, especially in the lower frame at NLG Zone. This was also confirmed by the stress analysis, where the highest principal stress attained 14.253 MPa, indicating there would be a potential risk of local yielding if not prevented.

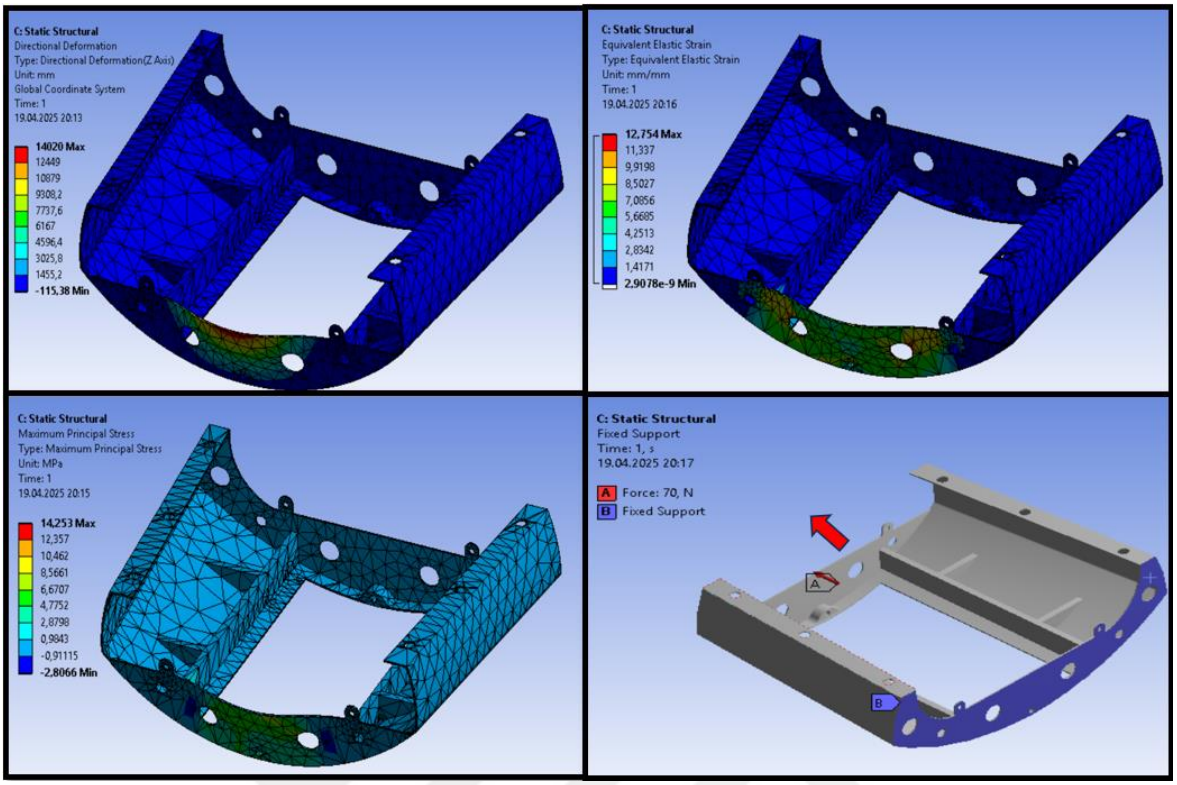

Figure 4.3 Stress & Strain Distribution at Front Fuselage AN531003 Part.

For a structural part AN531004 (Figure 4.4), directional deformation reduced significantly to 4.944 mm after it was 5.42 mm, and stiffness can be raised by geometry optimizing. it was also reduced to 7.112 mm/mm Elastic Strain behavior. Finally, the maximum principal stress was limited to 7.203 MPa, indicating a structurally safer profile in general. Due to this, sensor implementation can be ignored for this zone in subsequent studies.

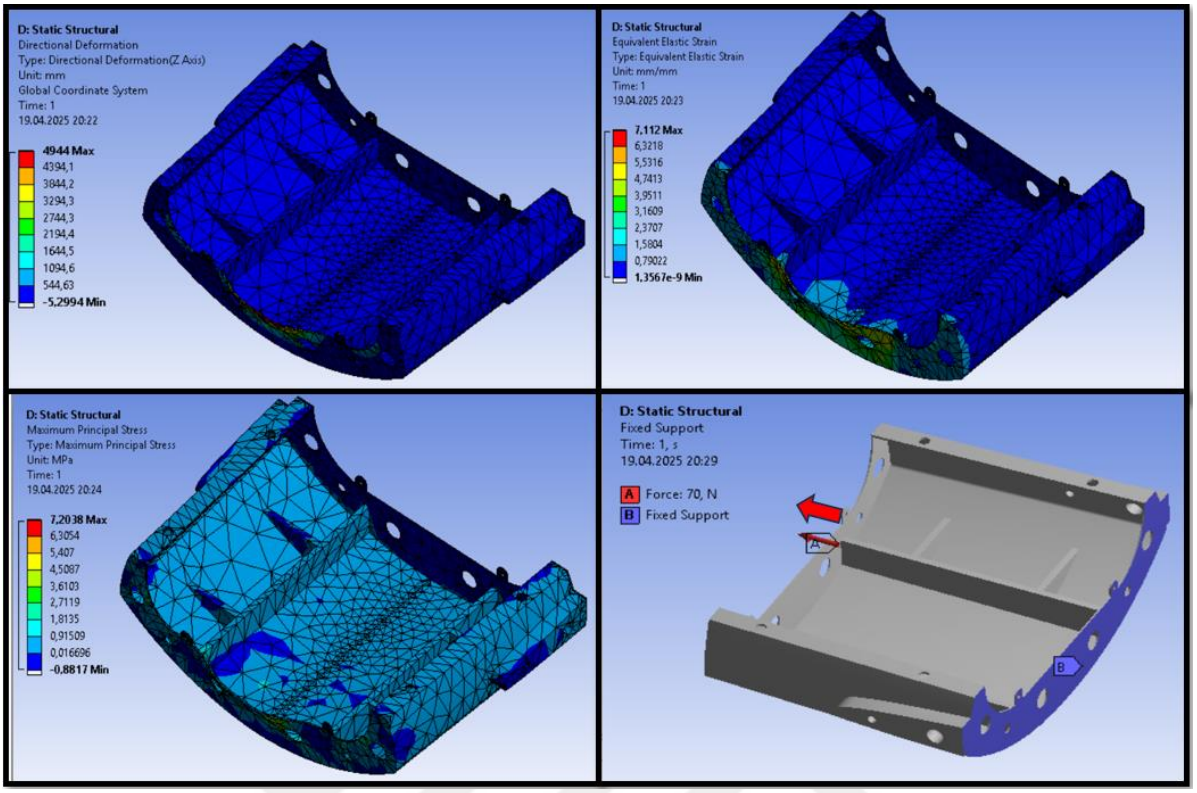

Figure 4.4 Stress & Strain Distribution at Center Fuselage AN531004 Part.

Analysis (Figure 4.5 and 4.6) show a much better shape with a slight deformation (0.029 mm) and significantly decreased strain and stress figures. During analysis, the maximum equivalent strain reached 3.059 x 10-5 mm, and the maximum principal stress was 5.9169 MPa. This data was consistent with the border of efficient load transfer and the enhanced integrity of the structure at EDF airintake zone. For streamwise deformation in this configuration, the maximum magnitude of directional deformation was limited to 4.996 mm and the associated strain and stress values were (5.4655 mm/mm) and (5.7084 MPa), respectively. Normally, these results indeed indicate satisfactory performance under the existing material and structural data. But considering airintake problems due to enviromental hazard, it must be controlled and changed regularly according to FMEA and RUL results.

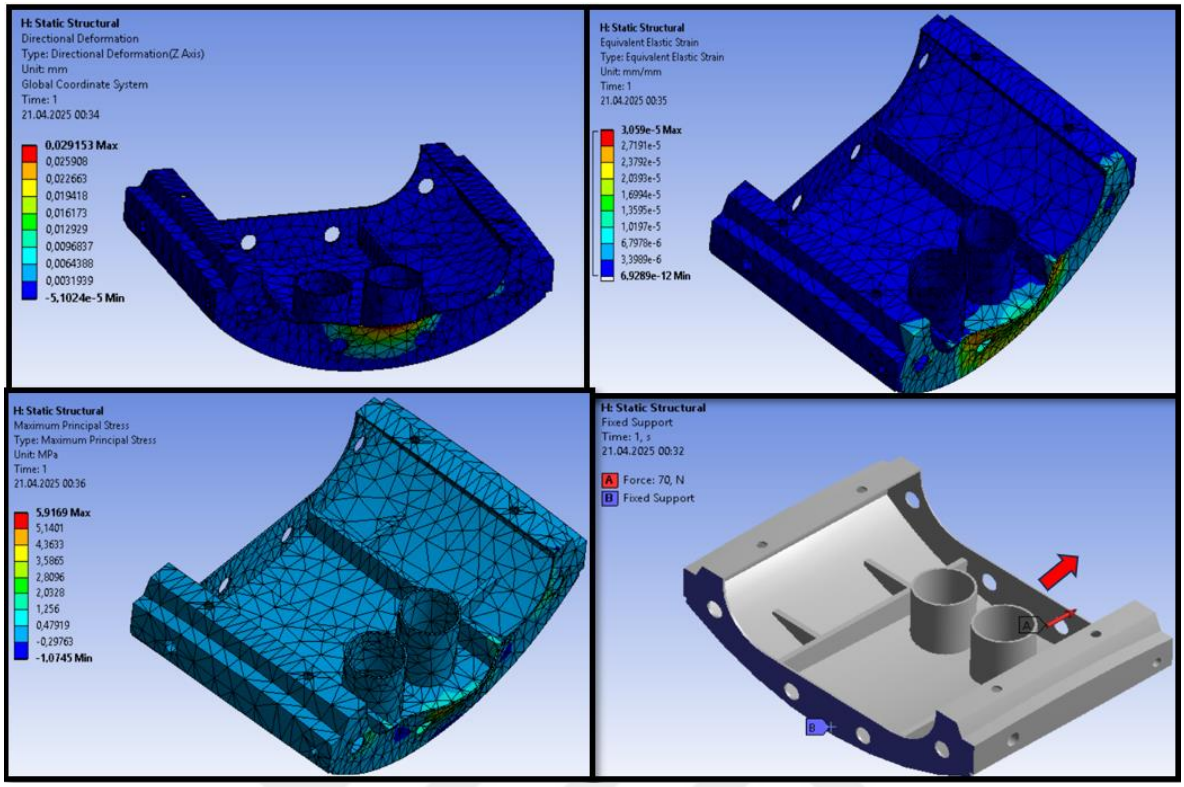

Figure 4.5 Stress & Strain Distribution at Center Fuselage AN531005 Part.

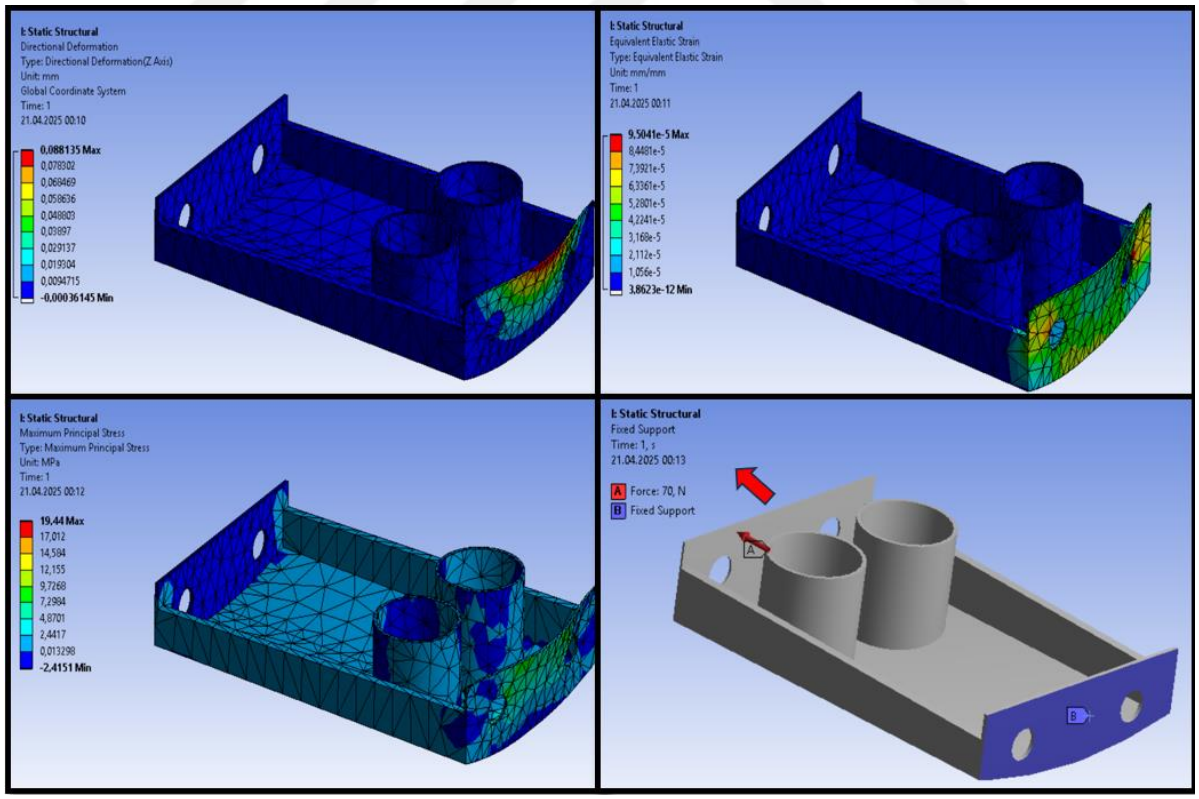

Figure 4.6 AN531005 Part Cross-Section Stress & Strain Distrubution

For a structural part AN531006 (Figure 4.7), directional deformation is 5.4655 mm and stiffness can be raised by geometry optimizing in next studies. it was also reduced to 5.7084 mm Elastic Strain value. Lastly, the maximum principal stress was 7.203 MPa, which showing a structurally safer profile. Due to this sensor implementation can be ignored for this zone in future.

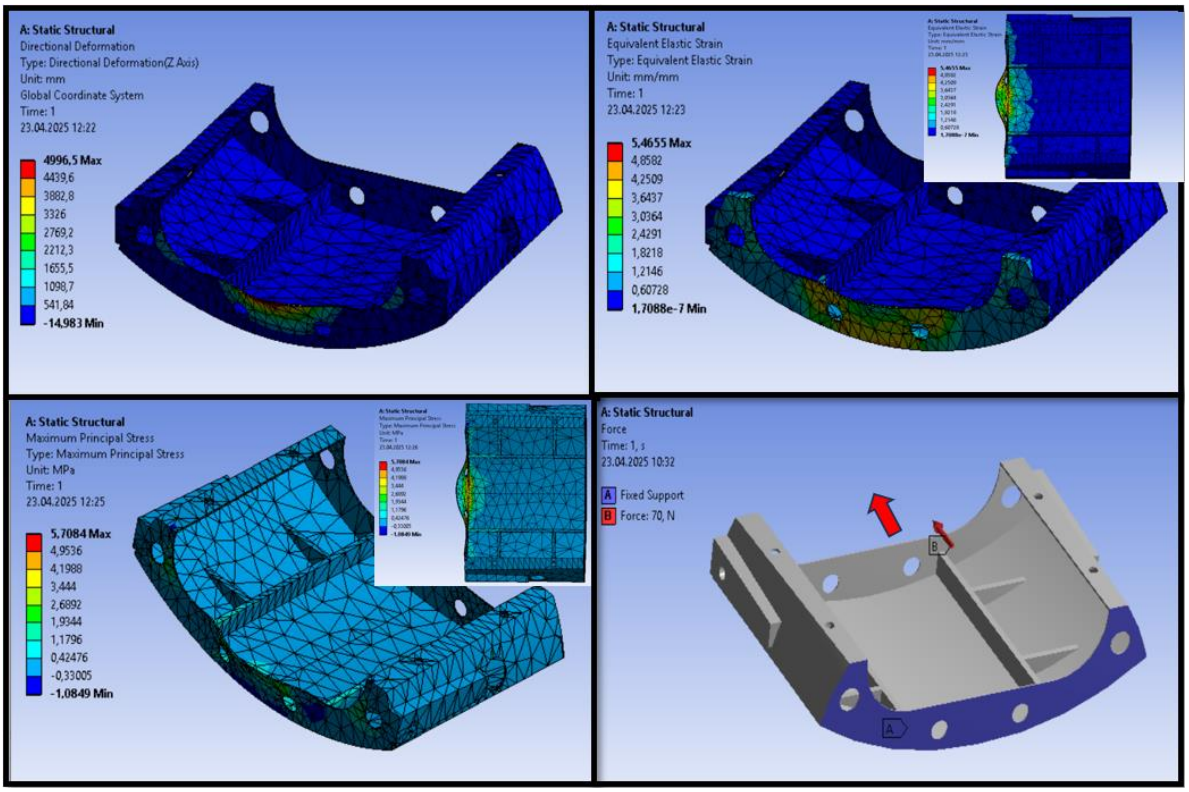

Figure 4.7 Stress & Strain Distribution at Rear Fuselage AN531006 Part.

Another part in Rear Fuselage (Fig. 4.8) showed static performance with deformation of 0.014 mm, true strain approximately lower than 1.669e-5 mm, and maximum principal stress around 3.2254 MPa. Also, cross-sectional stress map indicated for similiar loading of all the structure with no abrupt gradients of concentration unless front direction of frame. But , MLG Zone of aircraft must be implemented with sensors to obtain exact implicit behavior during to landing operation of aircraft. According to occurance of deformation in dangerous zone, structural part must be maintained with local operations or replacement of specified part.

Finally, EDF Mounting part (Figure 4.9) was investigated in last illustration, in which it was found that the direction deformed significantly, and the stresses

significantly increased. The maximum deformation was 7.469e-5 mm, strain was 3.455e-6 mm/mm, and maximum principal stress was below 0.751 MPa. Considering dynamic load distribution during to flight operation, specified zone must be inspected regularly.

These results confirmed the requirement for design modification and observation of structural behavior with sensors in subsequent studies.

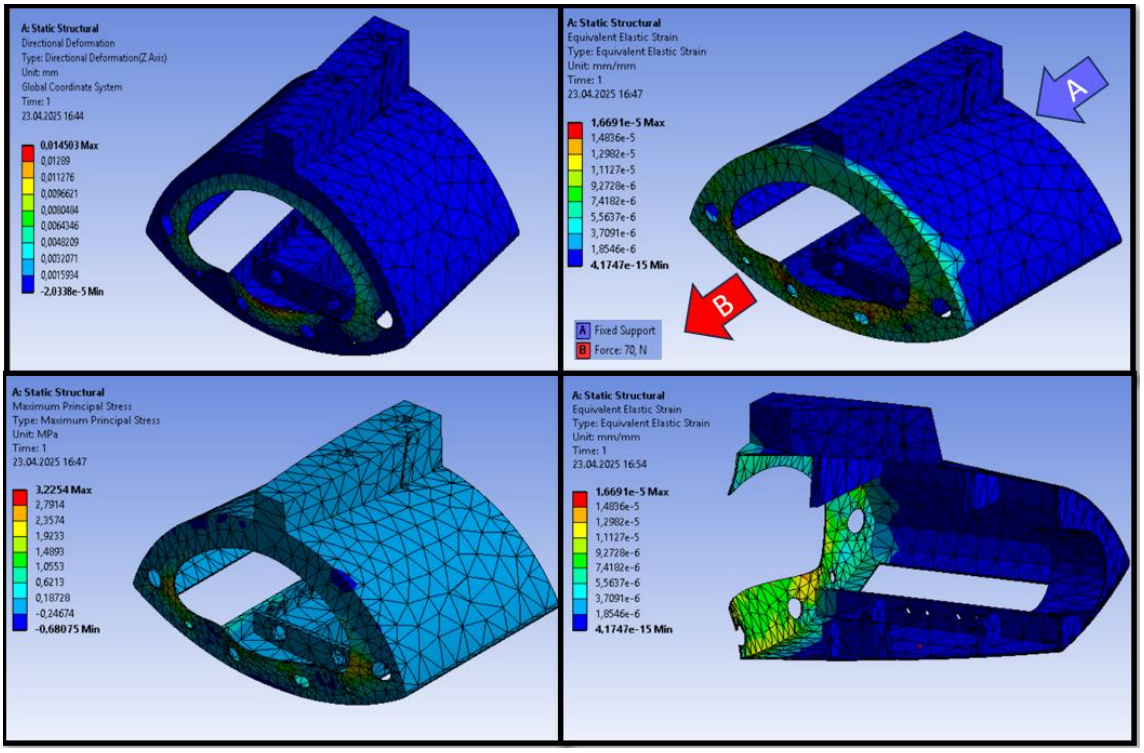

Figure 4.8 Stress & Strain Distribution at Rear Fuselage AN531007.

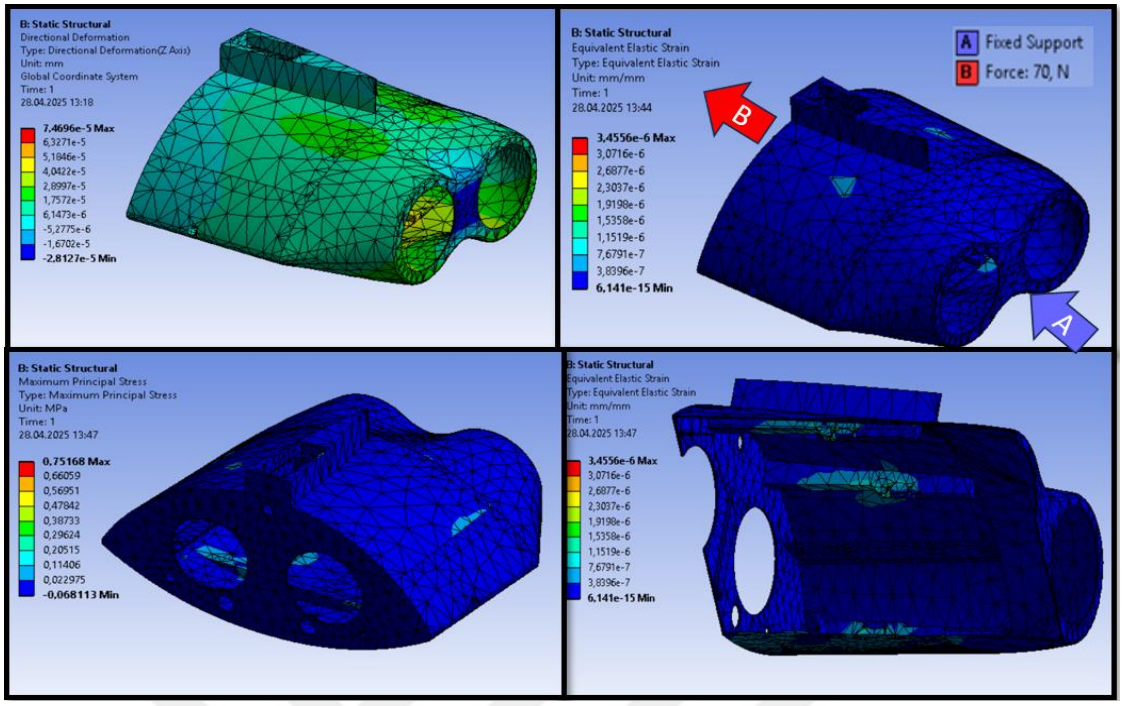

Figure 4.9 Stress & Strain Distribution at Rear Fuselage AN531008.

4.1.2. Modal Analysis of Wing

In this section, the modal analysis of the wing was investigated to determine its natural vibration frequencies and corresponding mode behaviors. Totally six modes were taken out from the simulation with the fundamental frequency observed at approximately 87.021 Hz in Mode-1. This initial mode represents the first bending motion of the wing, showing the structural modal response under vibrational effect. The highest mode identified during the analysis was found at 642.29 Hz, which is representing a more localized deformation behavior likely concentrated toward the leading and trailing edges which identified as Mode-6. The visual inspection of the directional deformation results for each mode provides idea for vibrational behavior of UAV. For instance, while the first and second modes show global oscillations, higher modes exhibit more complex node distributions and localized curvatures in analysis. These modal analysis results show the importance of structural behavior distribution for the natural frequency behavior of the wing. According to taken data, modal behavior is critical for identifying potential resonance risks and validating the structural integrity under dynamic conditions in flight. Although physical test or sensor implementation was not applied, these results align with theoretical expectations and finite element models. Generally, the modal frequencies are sufficiently spaced to mitigate the risk of resonance-induced structural failure.

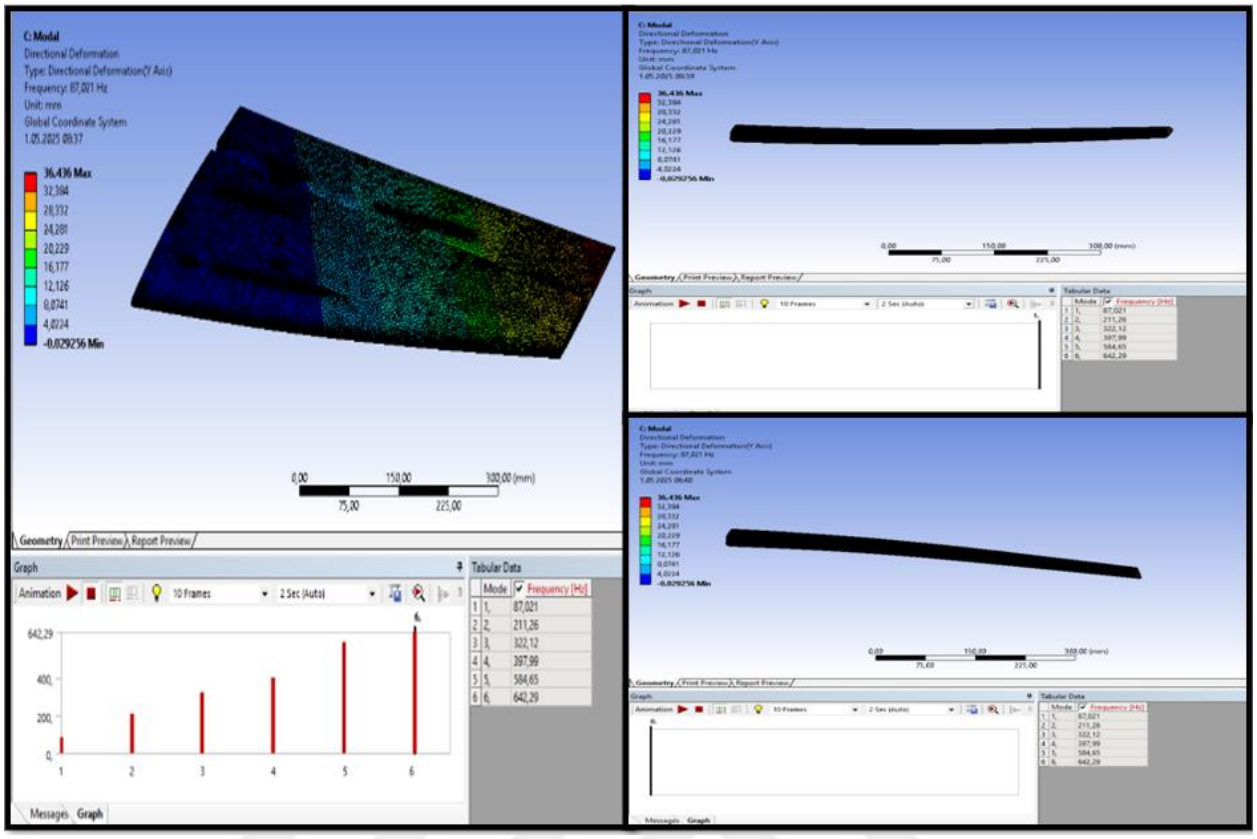

Figure 4.10 Modal Analysis Response of Wing Structure

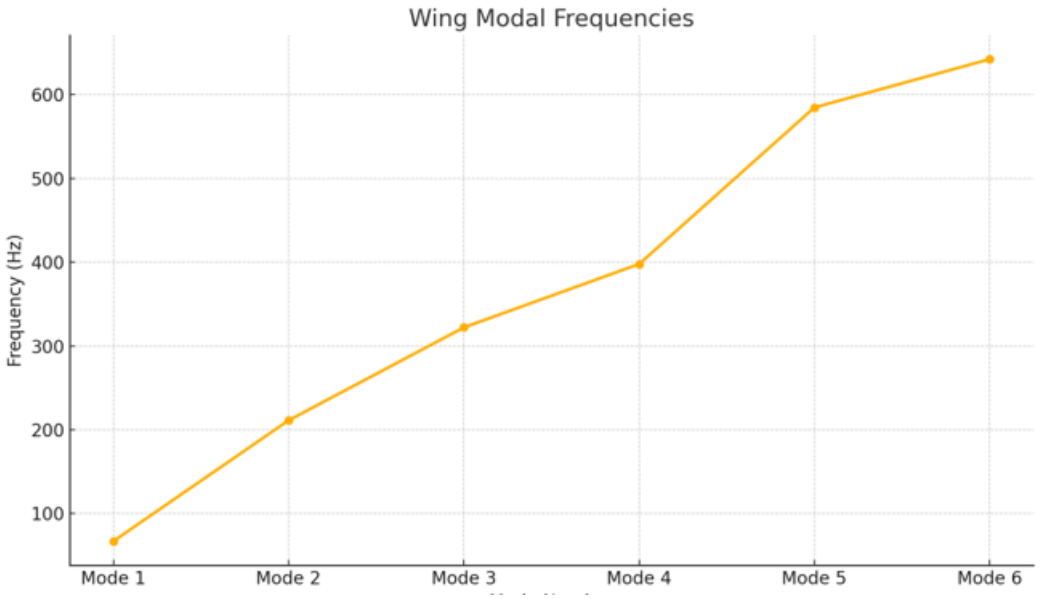

Figure 4.11 Frequency Response of Wing Under Different Modes

4.1.3. Explicit Dynamic Analysis Results

The explicit dynamic analysis was investigated to simulate the impact behavior of the UAV under high-velocity conditions. The UAV model was subjected to a collision with a rigid wall at a velocity of 80 m/s to observe equivalent (von-Mises) stress distribution and total deformation. High Resolution mesh design was used in the especially nose section to observe localized stress wave effect. Figure 4.12 shows the deformation of the UAV at the impact moment. The highest deformation was observed as 140.4 mm, which mainly localized at the nose section due to the concentrated load transfer. Similarly, maximum stress value 14653 MPa specified in Figure 4.13 which illustrates the von-Mises equivalent stress distribution.

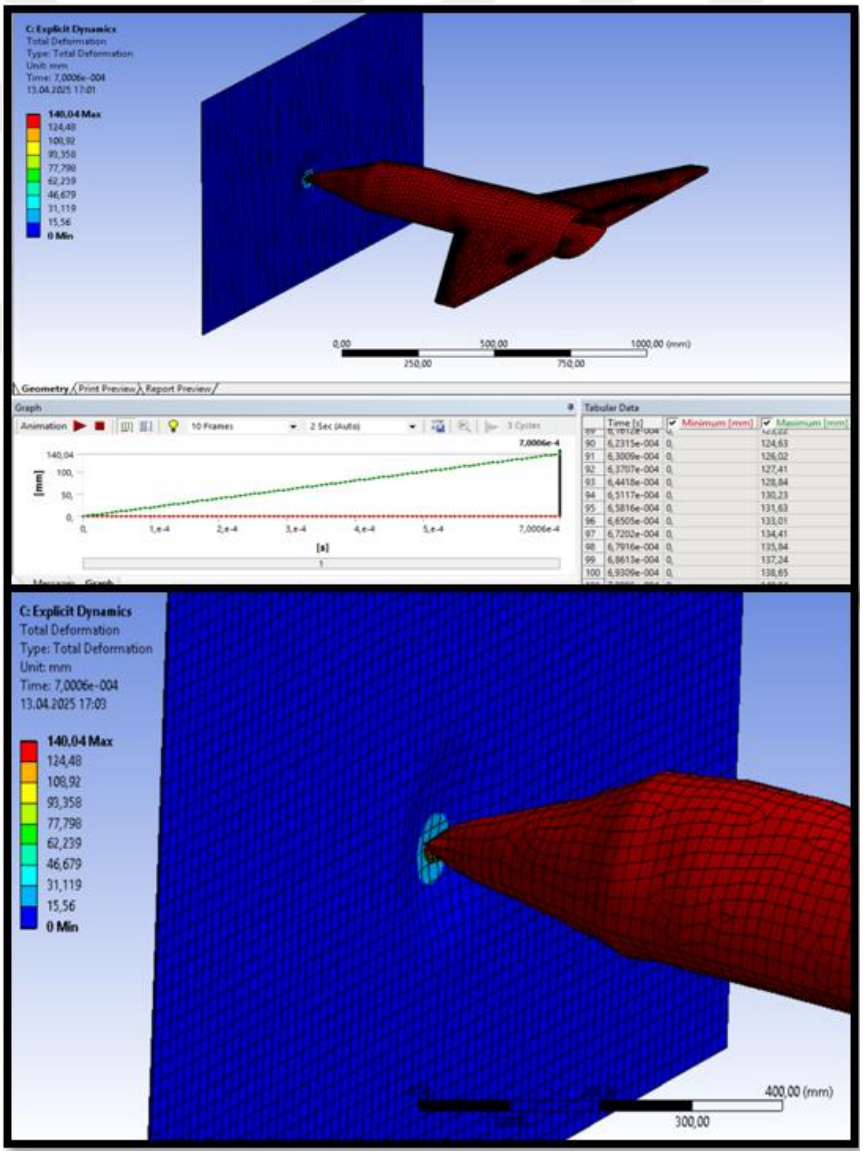

Figure 4.12 Deformation at Impact Condition of UAV

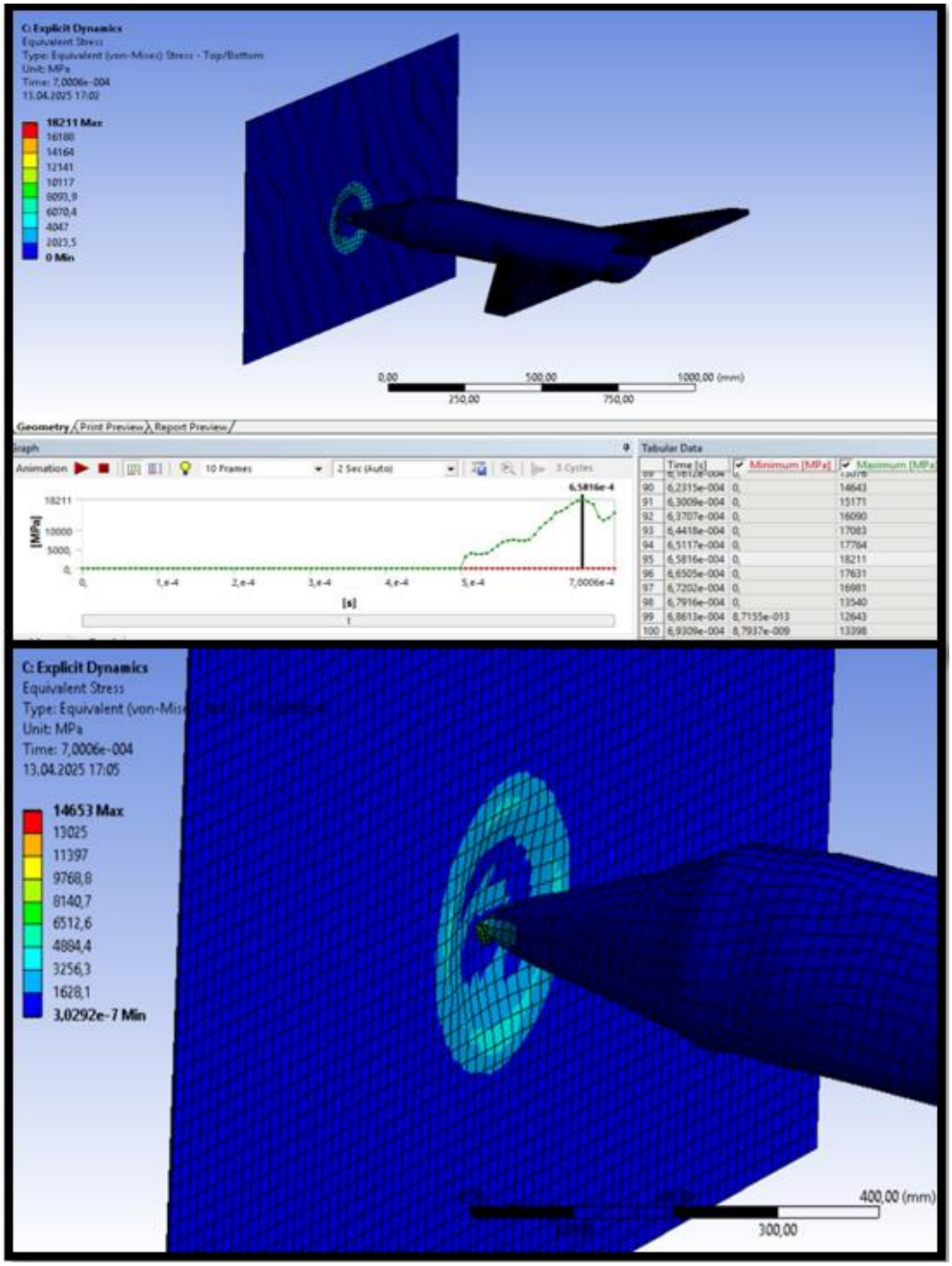

Figure 4.13 Von Misses Equivalent Stress at Impact Condition of UAV

These maximum values show critical failure regions which align with the zones previously identified through static structural analysis results. The following line charts were created based on the obtained analysis data:

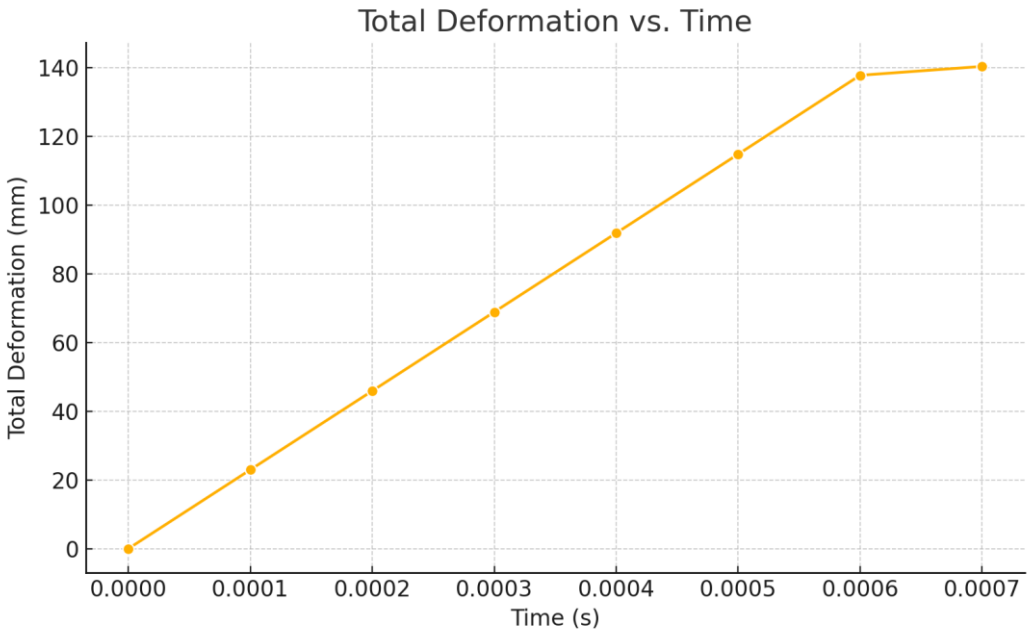

Figure 4.14 Line Chart of Total Deformation in Impact Scenario

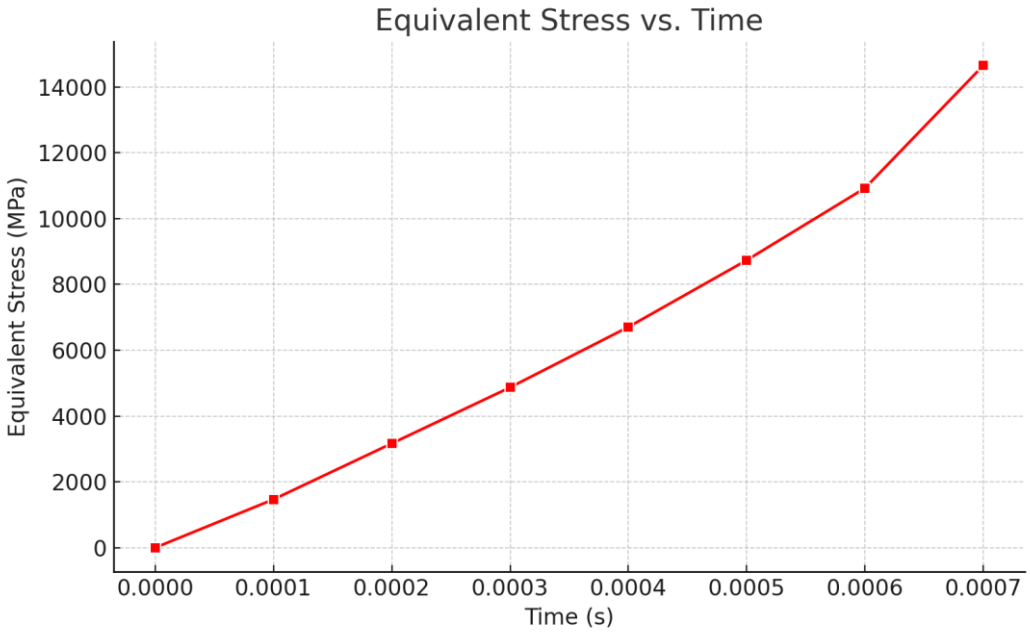

Figure 4.15 Line Chart of Von Misses Stress in Impact Scenario

From the total deformation graph (Figure 4.14), it is show that deformation increases linearly up until approximately 0.0006 seconds. Then, it slightly decreases,

this behavior shows the plastic deformation onset. On the other analysis result (Figure 4.15), the equivalent stress graph shows a continuous increase with time. Especially step after 0.0005 seconds, show a growing stress field and onset of structural failure in graph.

4.2. Aerodynamic Performance Results

This section presents the aerodynamic performance evaluation of the unmanned aerial vehicle based on computational fluid dynamics analysis results. In the first part (4.2.1), an external flow analysis was conducted to observe the airflow distribution around the UAV's master geometry including velocity, pressure contours and potential turbulence regions of UAV. This analysis is essential to predict drag characteristics and evaluate the flight stability of the UAV. In the second subsection (4.2.2), the internal flow behavior through the air-intake duct was examined. Parameters such as velocity, pressure gradients, inlet efficiency, and possible backflow regions were analyzed to ensure effective airflow which delivery to the EDF Motor. Finally, the estimated lift behavior at different velocities was investigated under section 4.2.3. It shows how changes in flight speed effect the lift generation of the UAVs wing profile. This study provides to understanding flight envelope characteristics and identifying critical performance intervals.

Generally, the CFD analysis conducted under these three subsections which provides a complete view of the UAV's aerodynamic characteristics. The results assist to validate the master geometry and informed subsequent studies for UAV performance. These findings are valuable in the absence of wind tunnel prior to physical prototyping.

4.2.1. External Flow Analysis Overcomes

In this section, external aerodynamic behavior of the UAV is evaluated under different AOA values, which including -15°, 0°, and +15° AOA configurations. The CFD analysis results were explained using velocity streamline plots which are providing critical seperation into flow separation and overall aerodynamic efficiency.

At 0° AOA, the streamline pattern indicates a symmetric flow with stable velocity distribution around the body and wings. As seen in Figure 4.16, the maximum velocity reaches approximately 90.4 m/s which suggesting good aerodynamic balance during flight.

When the UAV is loss altitude using pitch down as 15° which illustrated in Figure 4.17, the streamlines become more dense over the upper surface of the aircraft. This compression increased velocity up to 129.3 m/s.This high velocity flow nearby of the nose and upper wing surface, suggest a pitch-down scenario which potentially contributing to a nose-diving moment.

Reversely, the ANOYA UAV exhibits a significant increase in flow separation towards the aft of the wing and fuselage at +15° AOA (Figure 4.18). The maximum velocity reaches 138.2 m/s on the lower surface, which indicating enhanced lift generation due to the suction effect on the upper surface.

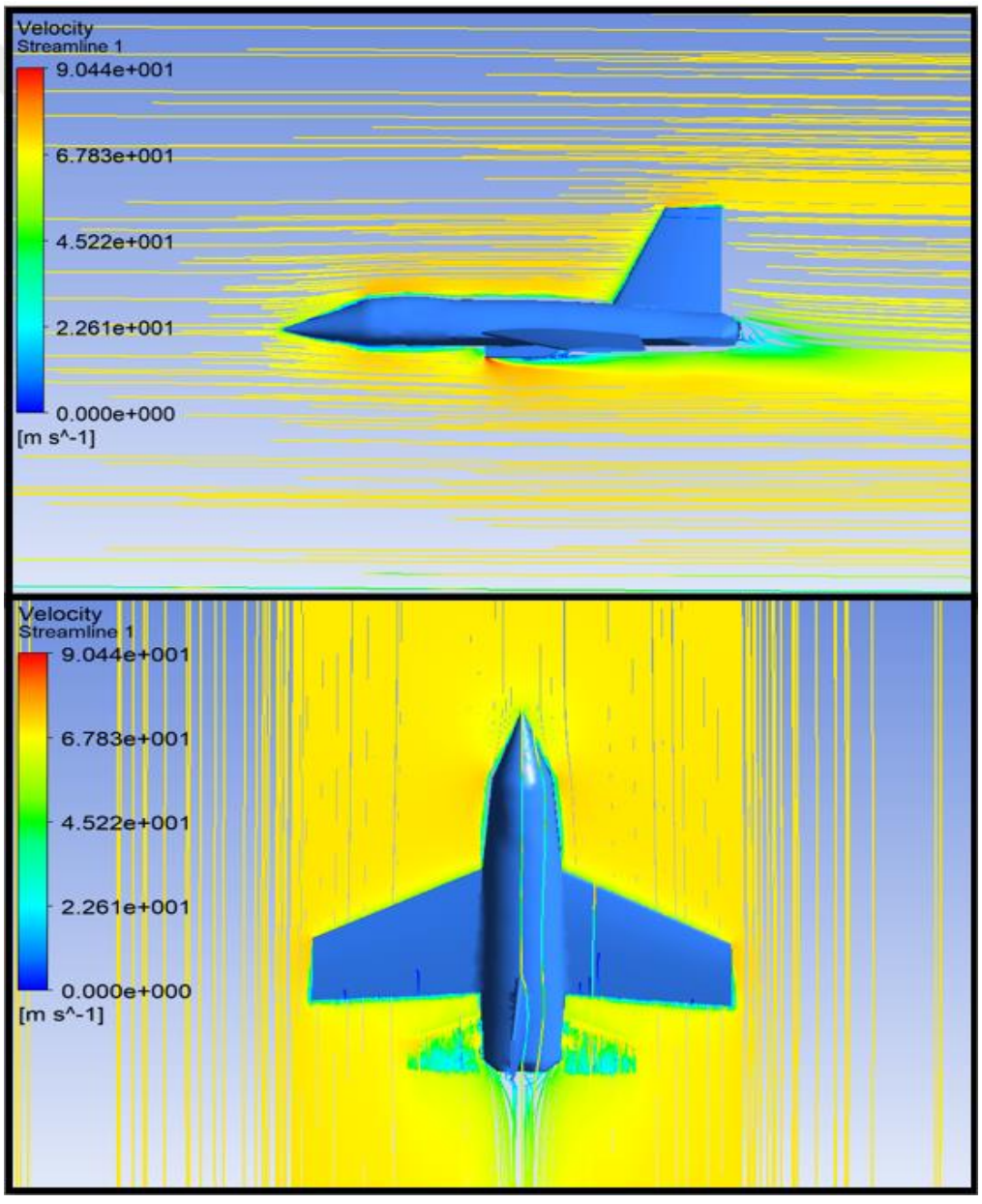

Figure 4.16 Velocity streamlines of 0° Angle of Attack at 70 m/s Velocity.

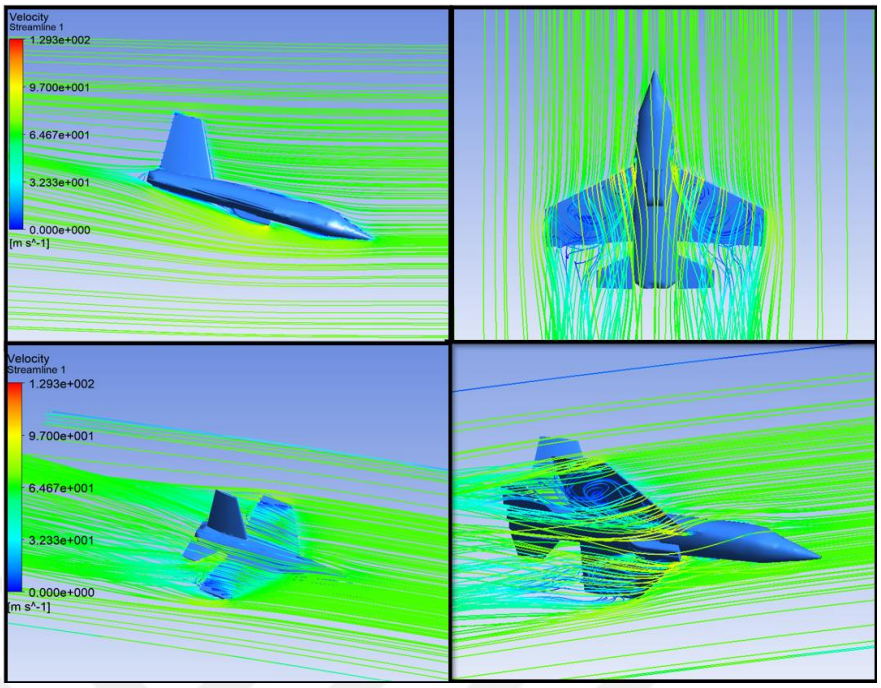

Figure 4.17 Velocity streamlines of -15° Angle of Attack at 70 m/s Velocity.

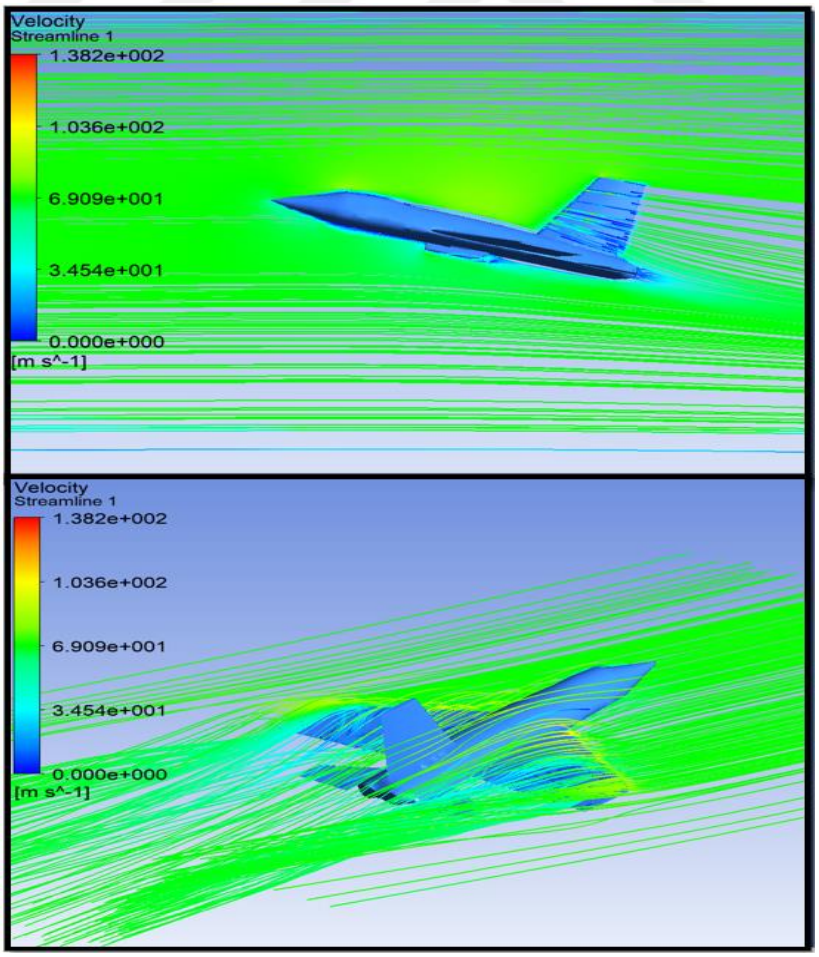

Figure 4.18 Velocity streamlines of +15° Angle of Attack at 70 m/s Velocity.

These results show that pitch-induced changes in AOA have a direct effect on flow behavior of the ANOYA UAV. The sensitivity of the external flow to AOA shows the importance of attitude control, especially during aggressive maneuvers. Additionally, the information which specified above provides a base for predicting lift and drag performance under dynamic conditions.

In consequent studies, the addition of yaw and roll angles can further expand the aerodynamic characterization of the platform. On the other hand, the pitch direction focused CFD behavior for AOA values were investigated to observe airflow behavior of UAV in this study.

4.2.2. Internal Flow (Air-Intake) Analysis Overcomes

In order to provide required airflow to the EDF Motor; an air intake was integrated into the UAV's fuselage. The air intake begins below the fuselage and continue through a curved duct before reaching the fan inlet as illustrated in Figure 4.19. Internal CFD analysis was studied to evaluate the aerodynamic performance of this air-intake and ducts. It focus on pressure distribution, velocity magnitude and streamline behavior in the study. As analysed in Figure 4.20, the pressure within the duct decreases regularly until reaching a minimum value near the curved section. The contour graph in Figure 4.21 shows a significant velocity increase along the duct, then peaking at approximately 242.4 m/s near the fan inlet. This behavior is further supported by the streamline illustrations which presented in Figures 4.22 and 4.23. In this location, flow directionality remains consistent despite the curvature of the duct.

Additionally, the analysis show that minimal flow separation occurred along the duct walls which suggesting a well-optimized internal geometry. The bar chart in Figure 4.24 specify the velocity changes through three main duct sections. At the entrance, the velocity starts at 24.24 m/s and rises to 145.4 m/s in the middle section. It reaches the maximum value as 242.4 m/s at the fan inlet location of UAV. The progressive increase illustrates a successful duct acceleration profile.

These results approve the efficiency of the duct design in consistent and increasing airflow, which is critical for engine performance.

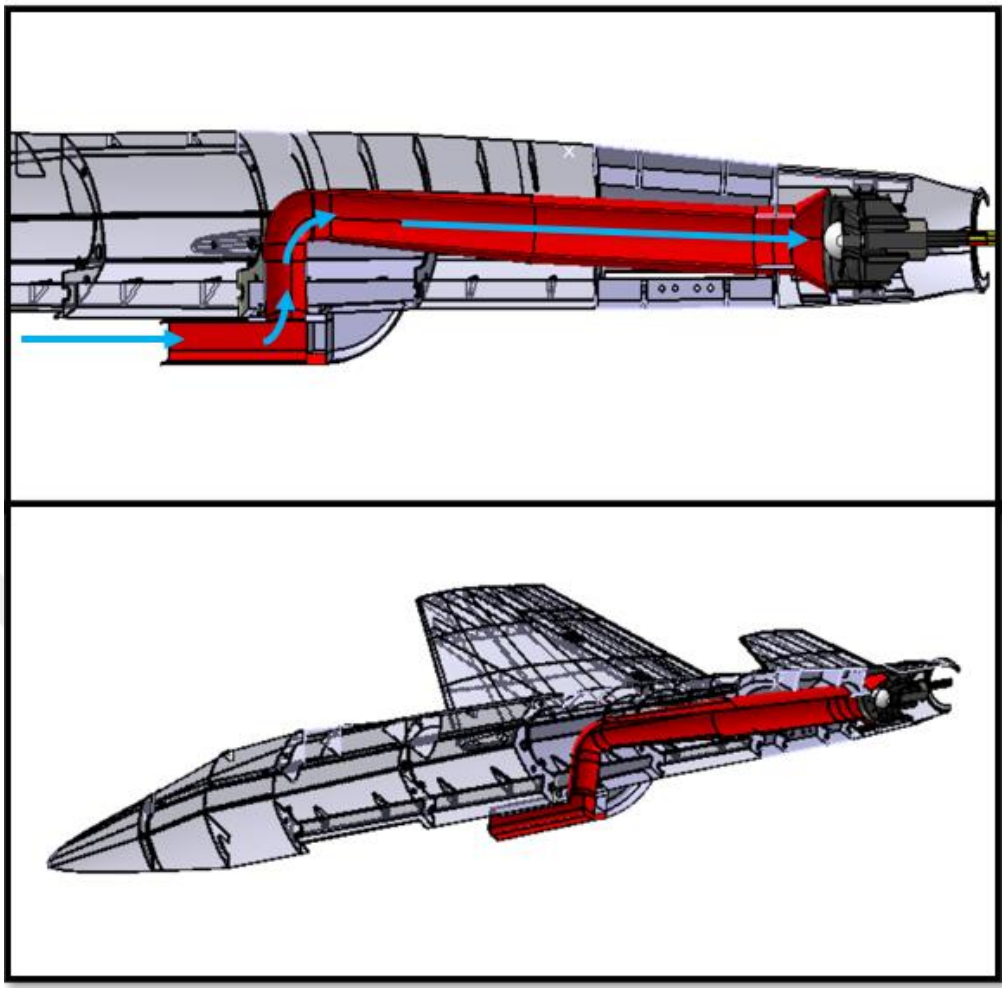

Figure 4.19: Air-intake layout of the UAV.

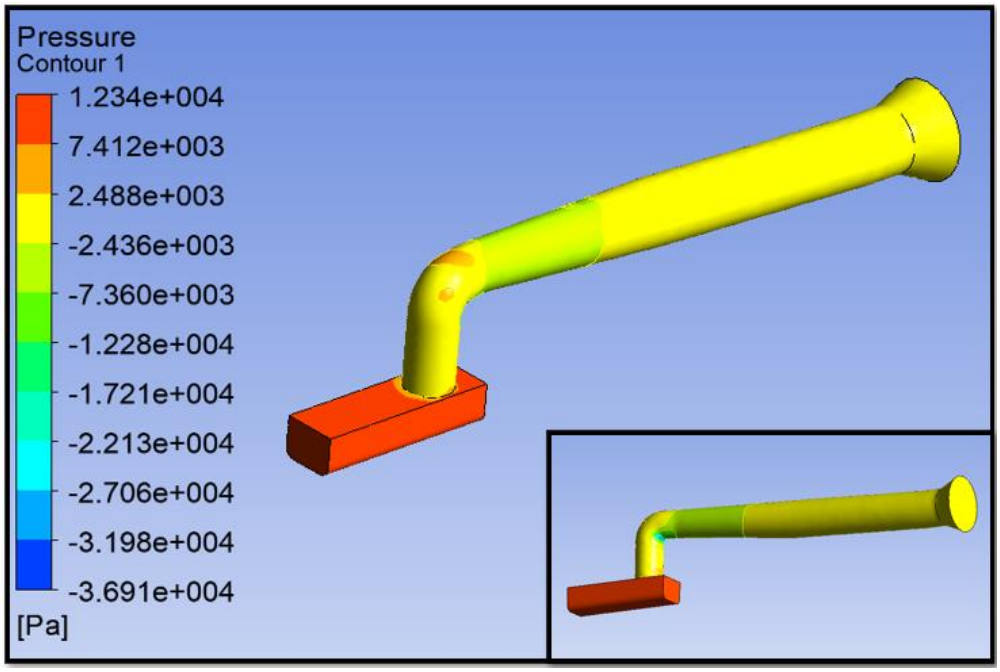

Figure 4.20: Pressure distribution in the air-intake duct.

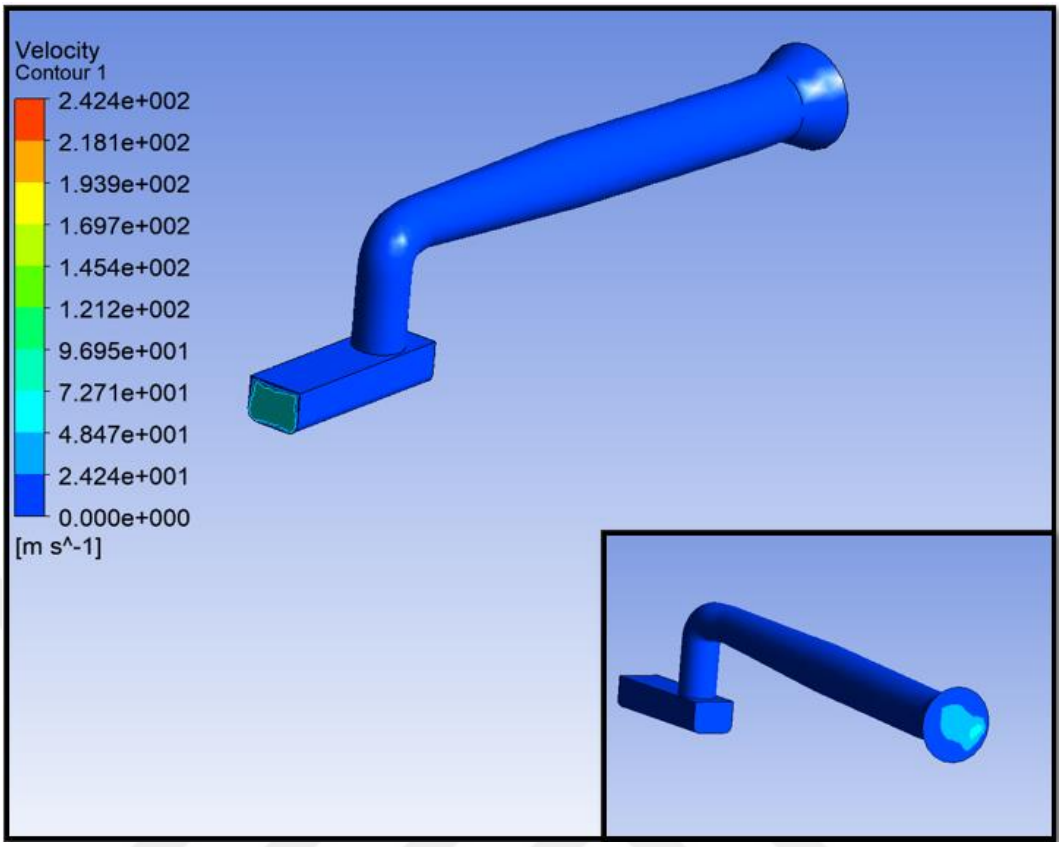

Figure 4.21: Velocity behavior in air-intake geometry.

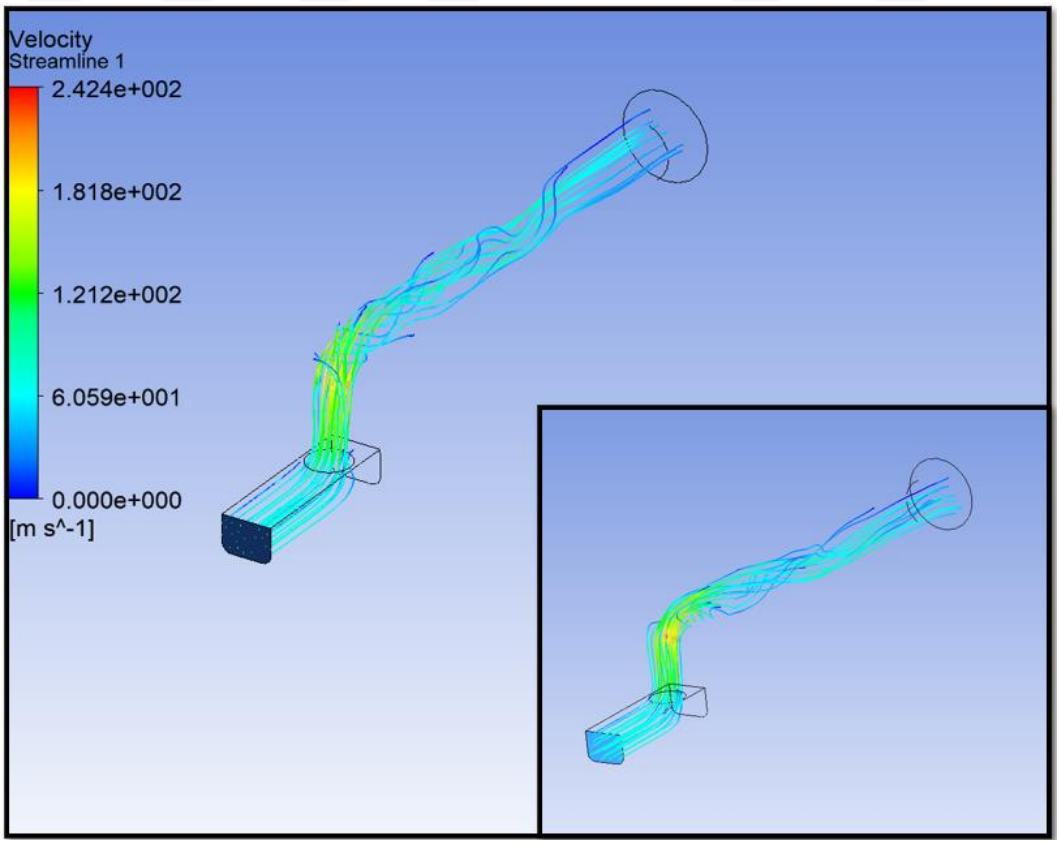

Figure 4.22: Velocity Stream Lines for air-intake CFD analysis

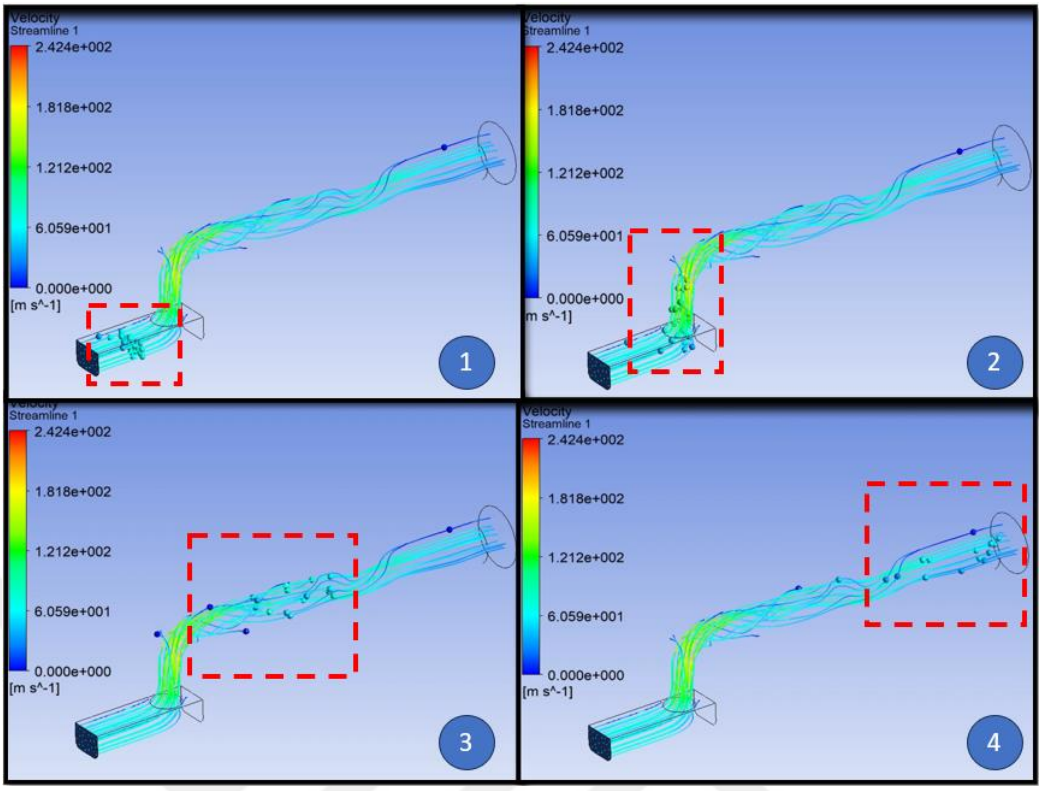

Figure 4.23: Velocity Stream Lines at at different nodes

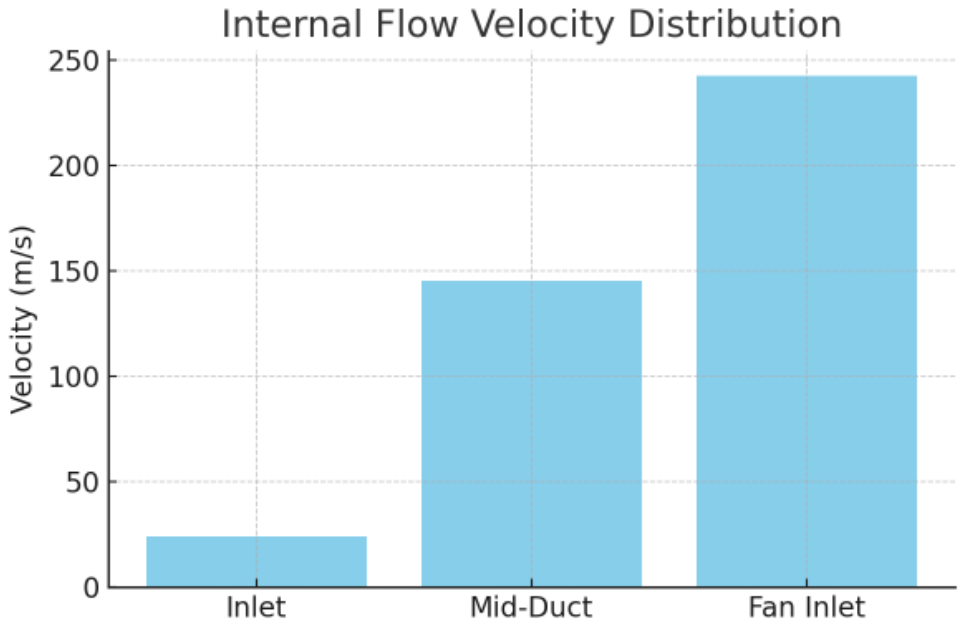

Figure 4.24: Internal flow velocity distribution chart.

4.2.3. Lift Behavior at Different Velocities

In this section, the lift generation capability of the UAV's wing was investigated under different velocities. As the UAV design aims to operate safely up to 70 m/s maximum velocity and in extreme conditions up to 80 m/s; CFD analysis for lift estimation were investigated at 30, 50, 70, and 80 m/s velocity conditions. The aerodynamic lift was obtained based on the pressure contour plots and integrated force values. Figure 4.25, 4.26 4.27 and 4.28 illustrates the pressure distribution over the airfoil surface for each velocity scenario.

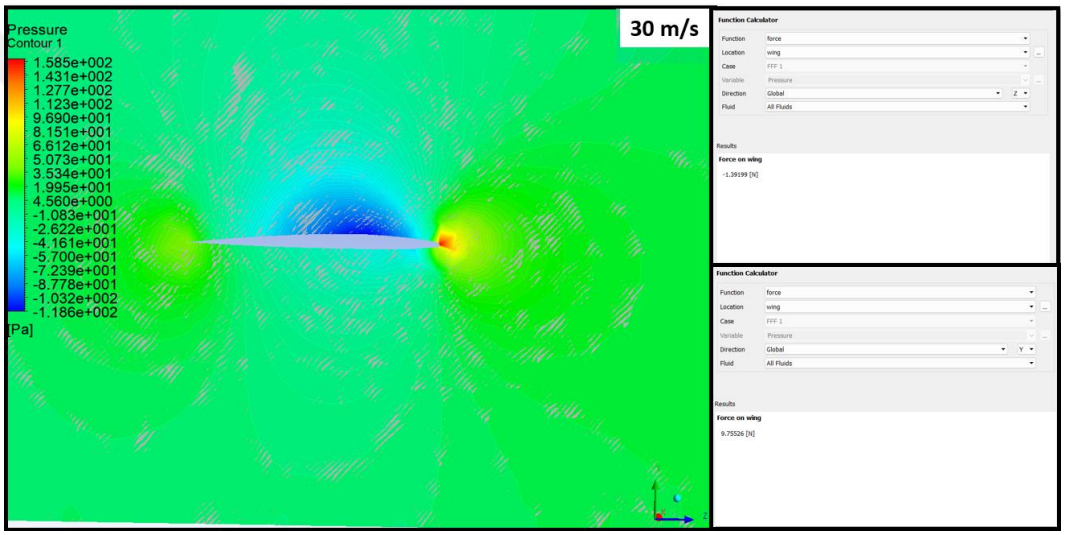

Figure 4.25: Pressure contour plots and lift forces at 30 m/s velocity.

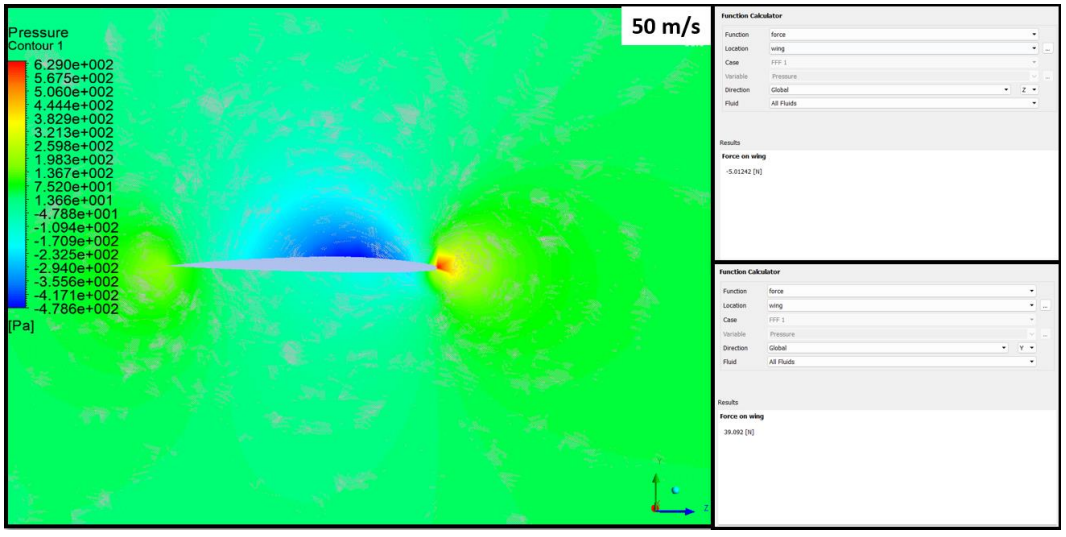

Figure 4.26: Pressure contour plots and lift forces at 50 m/s velocity.

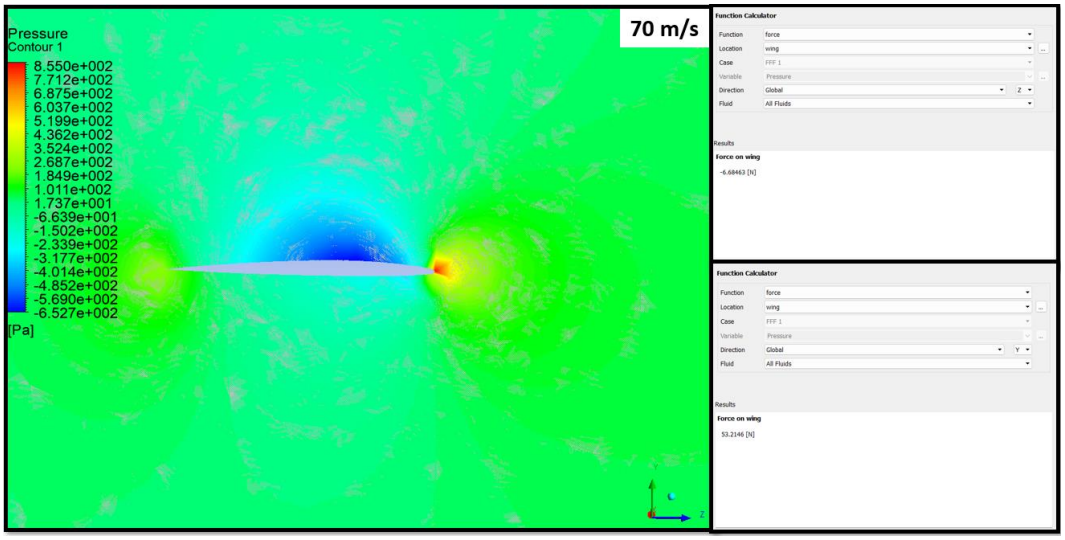

Figure 4.27: Pressure contour plots and lift forces at 70 m/s velocity.

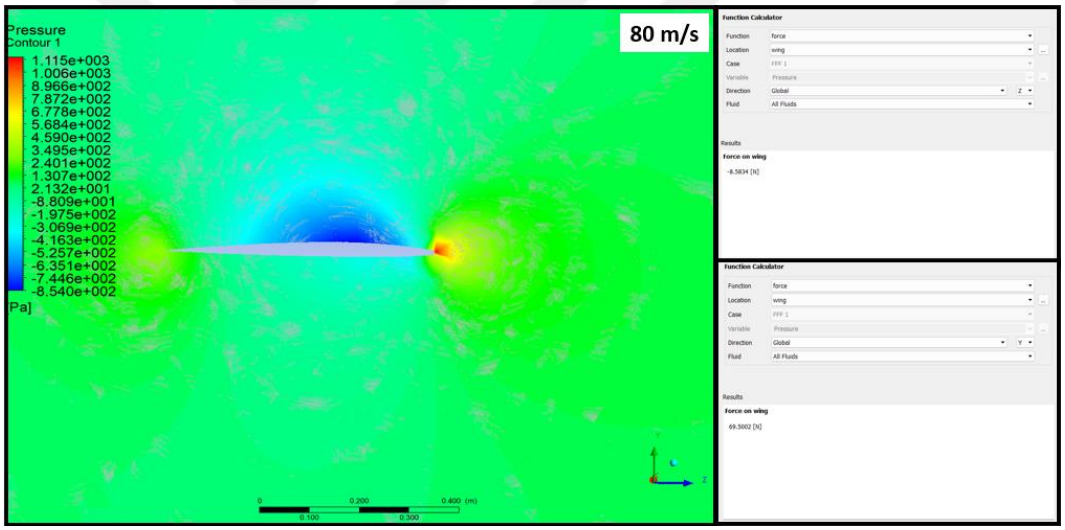

Figure 4.28: Pressure contour plots and lift forces at 80 m/s velocity.

According to observed data which obtained from the CFD analysis results, the lift force increased with increasing of velocity as expected from aerodynamic theory. This is results appropriate with Bernoulli's principle and dynamic pressure correlation, where the higher velocities give higher pressure differences across the wing surfaces. According to analysis results, the calculated lift forces were 9.75 N at 30 m/s, 39.09 N at 50 m/s, 53.21 N at 70 m/s, and 69.50 N at 80 m/s. Lift force vs velocity line graph conducted in Figure 4.29.

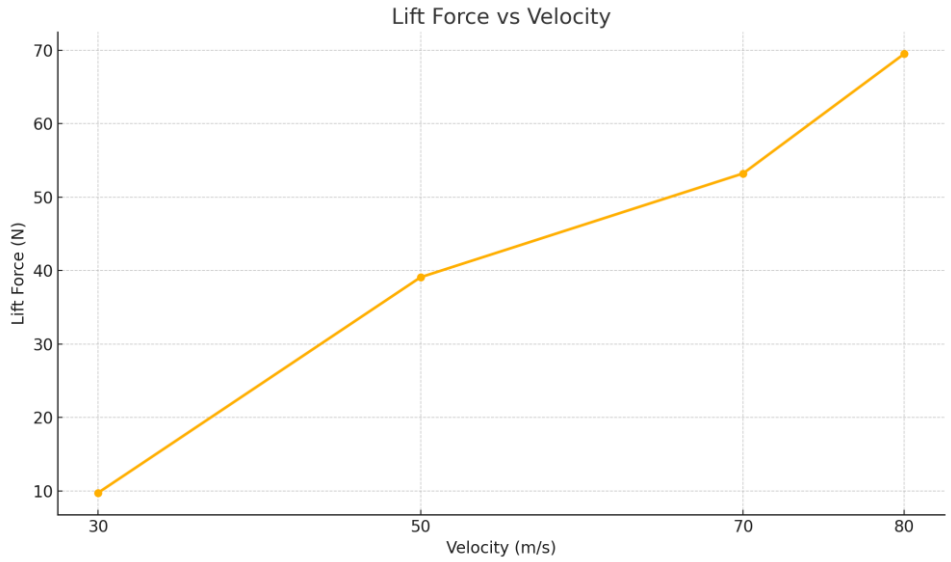

Figure 4.29: Lift forces for varying flight velocities.

It is important to note that the wing geometry and dimensions was explained based on the related UAV configuration which is shown in Figure 4.30. The wingspan of 1.5 m and chord length of 0.28 m give a reference wing area for lift calculations. Even though the coefficient of lift (Cl) slowly decreased at high velocities due to flow separation and turbulence effects, the generated aerodynamic lift approved as adequate for safe operation.

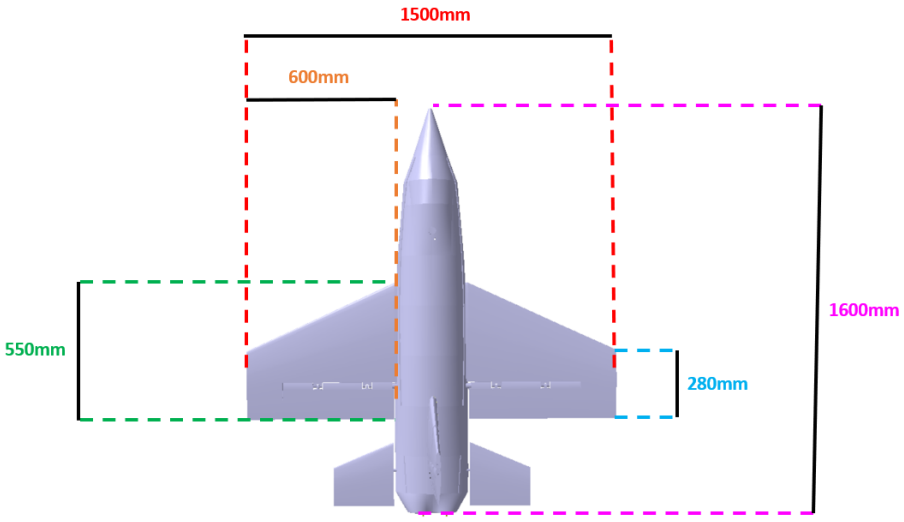

Figure 4.30: ANOYA UAV Geometry and Dimensions

According to obtained data from CFD analysis, the lift force reached over 53 N at 70 m/s, which satisfies the weight requirement when considering additional lift from the fuselage.

4.3. Manufactured UAV Layout

Considering all manufacturing process, so many iterations of component layout and structural design were carried out during the UAV manufacturing and assembly operations. Inconsistencies were observed especially in larger components, due to the layered structure of PLA filament which used with FDM 3D printing. Due to this, some parts re-designed considering manufacturing requirements. Also infill density of product was adjusted to improve the structural strength of the parts, particularly in load-bearing sections.

In the servo mounting regions, dimensional improvements applied the use of sealant support to ensure secure attachment, considering replacement of servo motor without disturbing understructure. This case highlighted the need for detailed dimensional control during production. Flaperon servo actuator and rudder servo actuator's assembly details for manufactured UAV shown in figure 4.31 and 4.32.

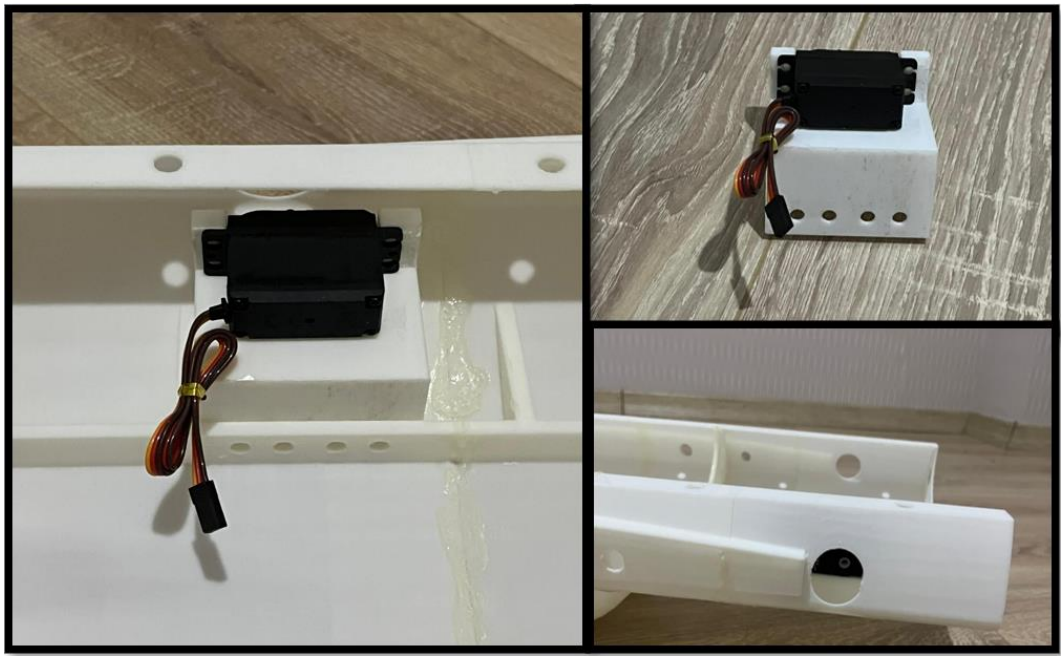

Figure 4.31: Flaperon Servo Actuator Assembly

Figure 4.32: Rudder Servo Actuator Assembly

Internal installation design layout shown effectively, providing large space for batteries, ESCs, and EDF motors and changement. Dedicated cable routing channels were created into the design to ensure effective internal wiring. Preliminary assembly of structural and system installation parts show the compatibility of structural integrity of the design.

EDF motor mountings were designed with vibration-damping regions, which will serve as reference points for subsequent vibration tests. Assembling of this parts shown in figure 4.33.

Figure 4.33: EDF Motor Assembly

On the other hand, guide holes on frame surfaces were helpfull in aligning parts during assembly phase which significantly reducing overall assembly time. Interfaces between fuselage and aerodynamic surfaces were optimized for rigidity of UAV. Additionally, fastening holes were re-designed for assembling of mechanical joints. All illustrations for UAV installation shown in figures 4.34 to 4.44.

Figure 4.34: Front and Center Fuselage Sub-Assembly

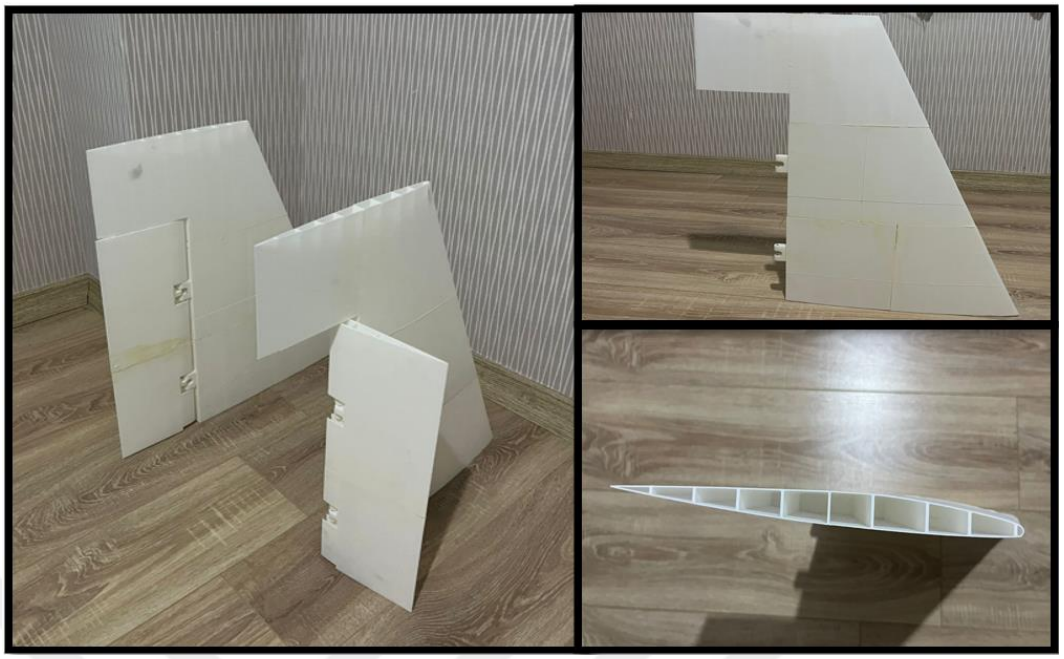

Figure 4.35: Manufactured Wing-Box with Flaperon Control Surface

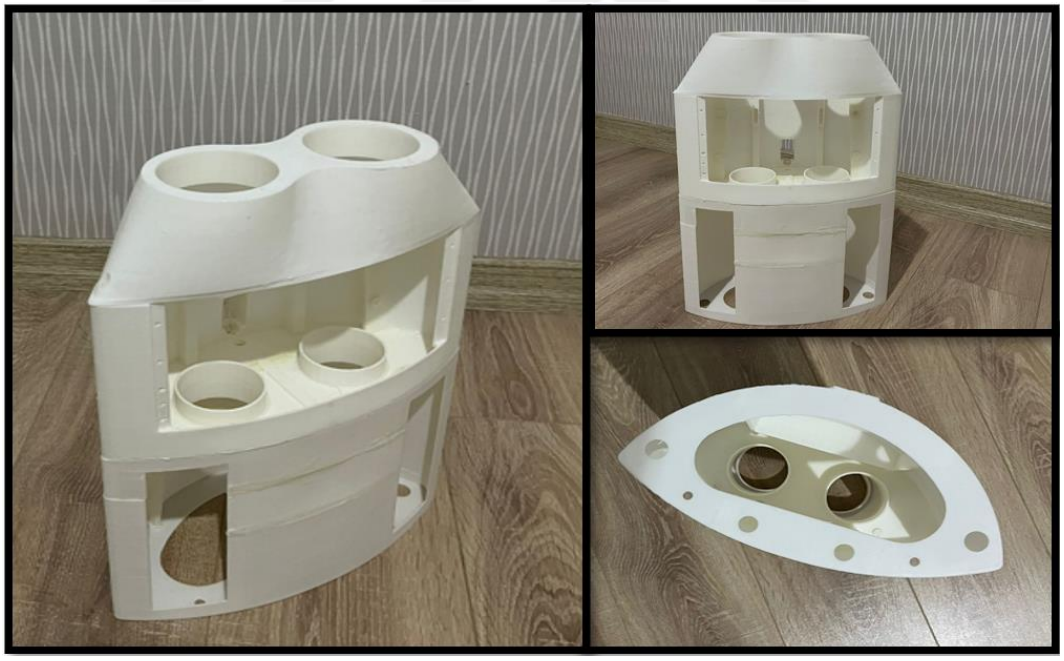

Figure 4.36: Manufactured Rear Fuselage of UAV

Figure 4.37: Manufactured Access Panel of UAV

Figure 4.38: Fuselage of UAV

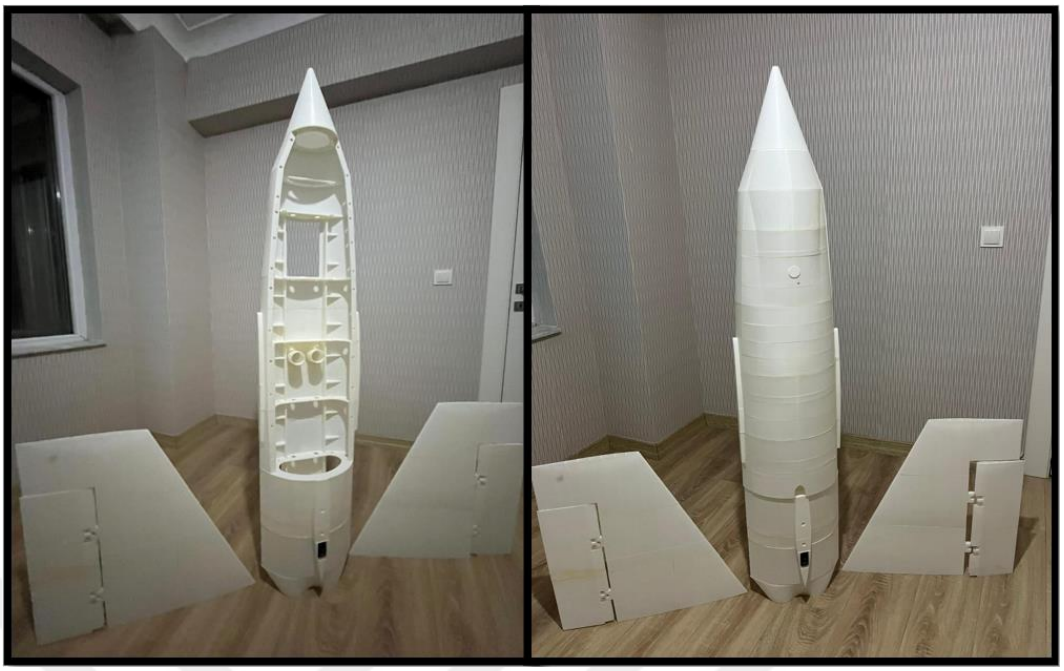

Figure 4.39: Manufactured Fuselage with Wing Assembly

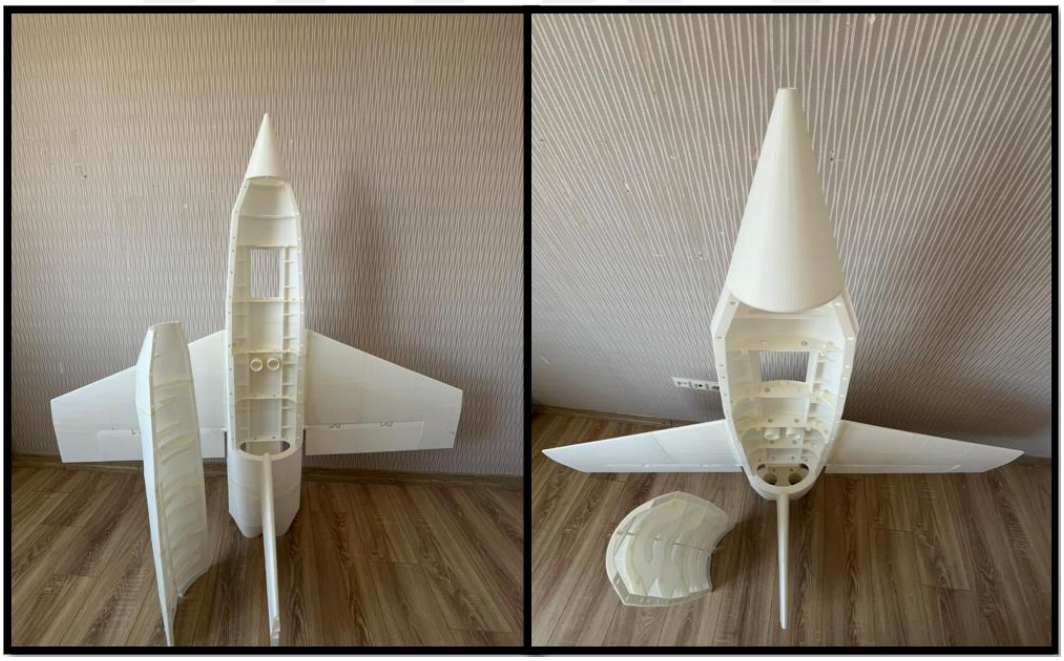

Figure 4.40: Sub-Assembled Fuselage View-1

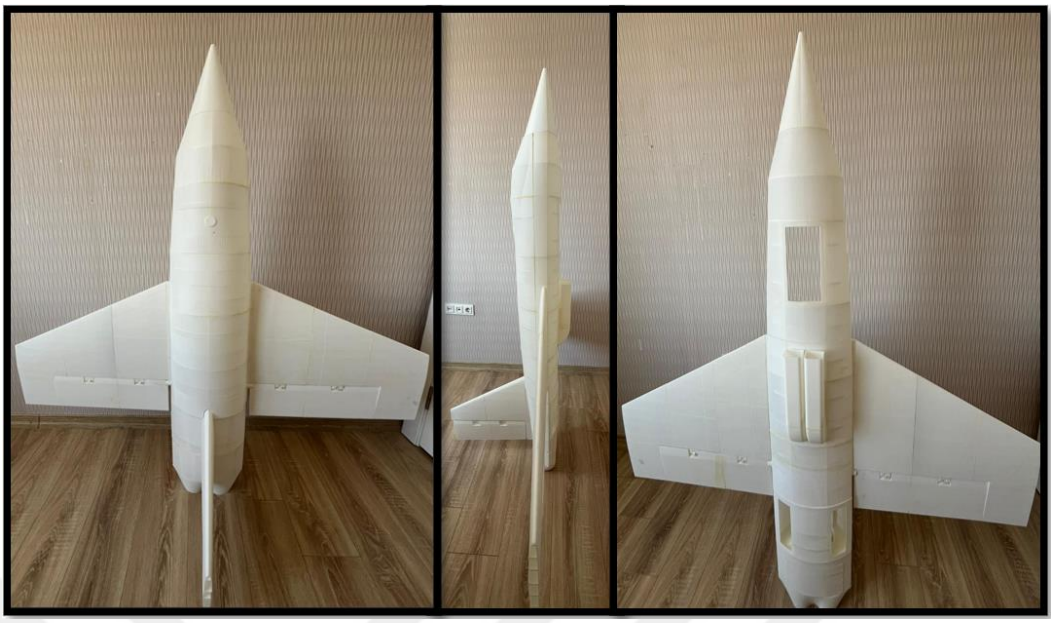

Figure 4.41: Sub-Assembled Fuselage View-2

Figure 4.42: ANOYA UAV Internal View

Figure 4.43: ANOYA UAV View-1

Figure 4.44: ANOYA UAV View-2

In summary, the physical structure not only provide visual and mechanic expectations, but also give satisfactory mechanical performance which is making it ready for functional integration and subsequent flight tests.

4.4. Health Monitoring and Predictive Maintenance Evaluation

In this section, a preliminary investigation is conducted for predictive maintenance task which is based on the structural stress and strain distributions where observed in critical fuselage regions. Hybrid sensor network design is conceptually implemented to expect potential structural failures and proactive maintenance strategies. The design includes both strain gauges and Fiber Bragg Grating (FBG) sensors, which

are known for their precision and accuracy.

According to data which obtained from in Figure 4.42, the front fuselage region shows to moderate equivalent elastic strain levels under nominal load conditions. The red dashed area indicates the suggested positions for strain gauge sensors, while the green dashed box outlines the intended locations for FBG sensors. This configuration shows the simultaneous monitoring of both elastic deformation and thermal stress behaviors. The maximum equivalent elastic strain in this region is approximately 1.09×10^{-2} mm/mm, as shown in the related analysis.

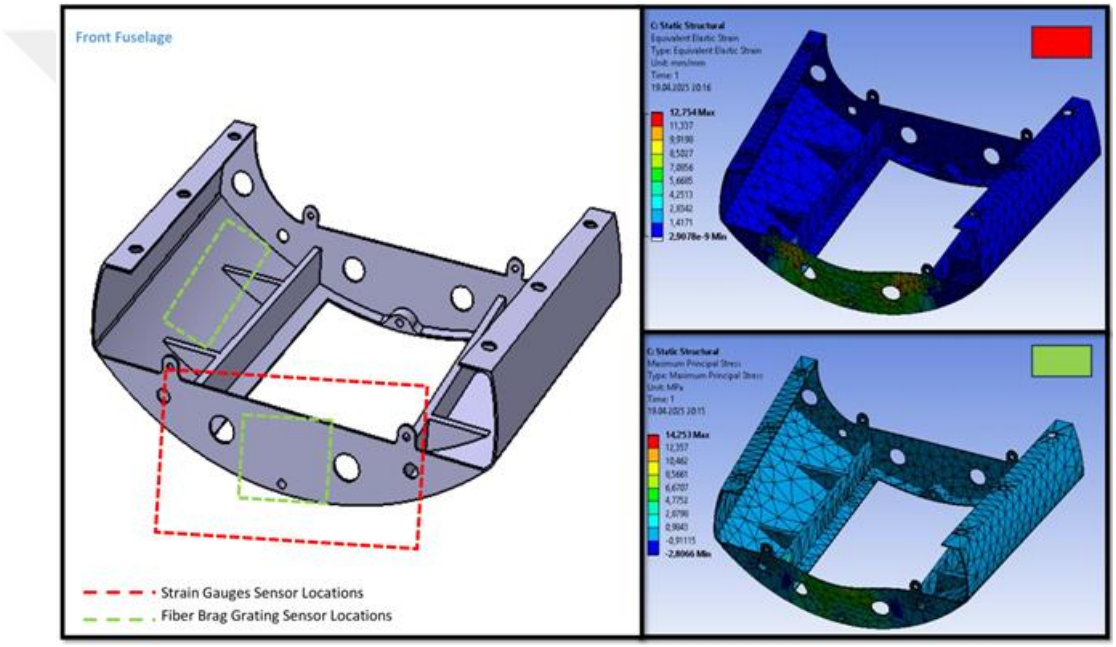

Figure 4.45: Sensor placement on Front Fuselage AN531003 Part

Highest principal stress values are localized near the inner connection frame which corresponds to the central fuselage section as shown in figure 4.43. This result suggests the requirement for dense sensor placement in these regions to take high-gradient stress transitions. The predicted maximum principal stress is approximately 4.17 MPa in this part. Sensor positions show the combination of strain gauge and FBG deployments to optimize predictive maintenance operations.

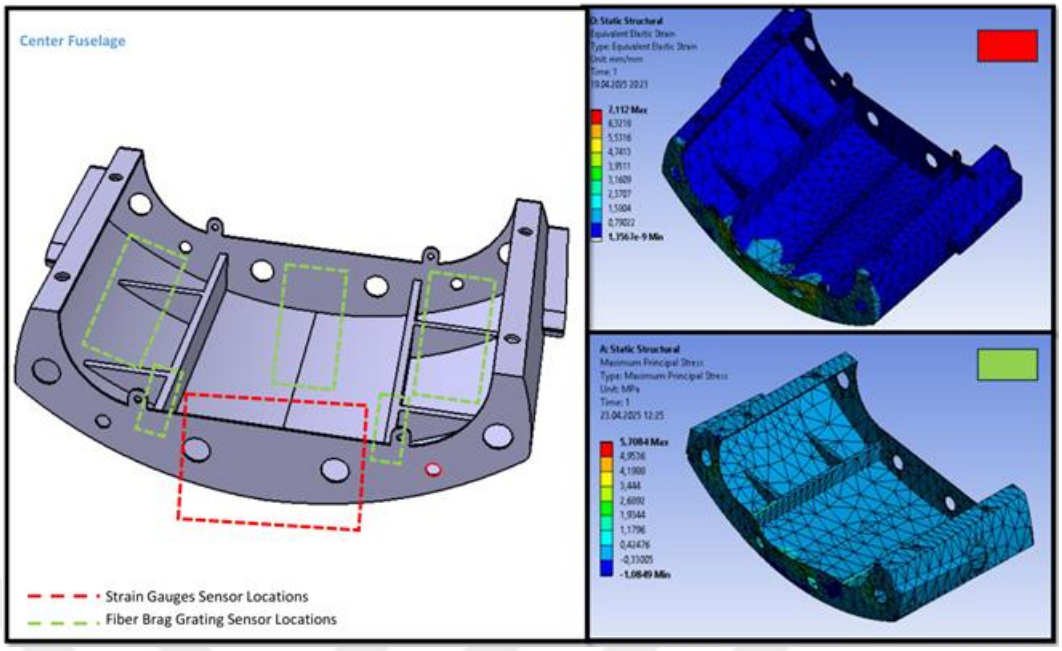

Figure 4.46: Sensor placement on Center Fuselage AN531004 Part

The rear fuselage study is illustrated in Figure 4.44. This region is unsafe for vibrational fatigue due to its location where nearby to the EDF Motor. Both structural analysis and principal stress behavior indicate critical loading near the circular joint interfaces where connect duct to air inlet line. Because of this, a sensor distribution has been defined to take axial and torsional strains simultaneously from UAV. The maximum equivalent strain in this section reaches 1.61×10^{-2} mm/mm, which show the necessity for high-frequency sampling and robust sensor bonding.

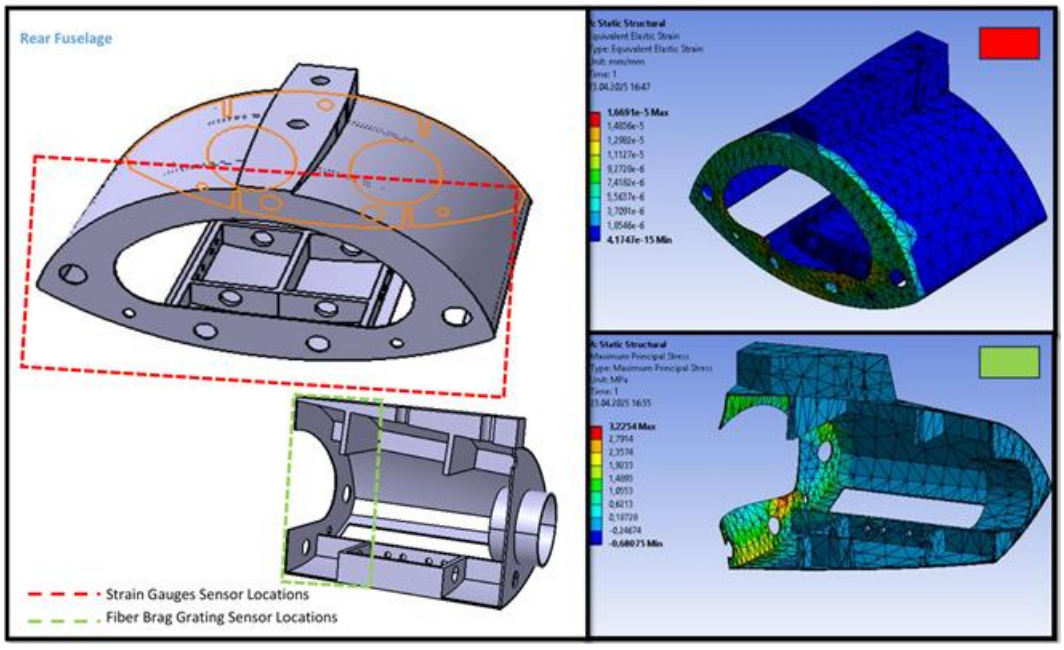

Figure 4.47: Sensor placement on Rear Fuselage AN531007 Part

In case of the usage of this integrated sensor framework; long-term health monitoring data can be collected to create a baseline for Remaining Useful Life (RUL) estimation to observe anomaly detection and real time health behavior. Although the integration and data acquisition were not performed within the scope of this thesis; the preliminary work given in this section is expected to provide baseline for subsequent experimental studies and software integration in future research.

5. DISCUSSION

A structural design and analysis of the fixed-wing UAV, ANOYA, has enabled obtaining valuable new information about the mechanical and modal behavior of lightweight airborne platforms made of thermoplastic materials. The sensor arrangement was determined by the recognition of significant load-carrying areas and high-stress zones during the finite-element analysis activities. Although it was not feasible in the course of this study to obtain real-time sensor data, theoretical groundwork for the selection and placement of the sensors for future health monitoring has been laid. Results indicate that the rear stabilizer mount, EDF motor housing, and fuselage-wing juncture bear the highest mechanical stress and deformities. These results induced a proposal to use piezoelectric or Fiber Bragg Grating (FBG) sensors because of the high strain sensitivity and an excellent fit with a composite. They offer a lightweight and efficient solution for UAVs by means of early detection of structural anomalies in terms of strain gradients or modal behavior changes. Integration of data from simulation modeling with the predictive maintenance aspects in this study is an important novel contribution point. It further allowed the construction of event-response pairs such as abnormal thermal expansion near EDF mounts indicating likely delamination or deviation from wing natural frequency suggesting that crack initiation has occurred, despite sensor-output data not being collected. It is on the basis of these relationships that the proposed predictive maintenance model was structured. Moreover, although impact and heat limits apply to the material, the choice of PLA through fused deposition modeling was justifiable at the design phase. The study focusses on the trade-off between produce and long-term reliability in high-temperature and/or high-speed operations. Therefore, it is beneficial to explain the importance of sensor technologies and material behavior in UAV life-cycle planning. The study has also shown how critical to take sensor installation into account during the design stage, especially for embedded or built-in systems, in order to prevent insufficient weight gain or aerodynamic loss. Despite the lack of actual sensor readings in the experiment, the logical and spatial consistency of the sensor integration supports an experimental extension of this work or even a practical application in subsequent study.

6. CONCLUSION AND RECOMMENDATIONS

This study presented a sensor-based predictive maintenance policy developed for composite materials of the UAV structures and also addressed the structural performance of the fixed-wing UAV through deep finite element analyses. Simulation-based results played a unique role in locating areas that were prone to structural damage, for which real-time sensor readings were not available. This data formed the basis for the proposed surveillance and maintenance system. Primitive damages like modal shift, excessive thermal expansion, or strain localization are potential triggers in a predictive system, as demonstrated in the fusion of simulation-driven know-how with maintenance solutions. The structure of the architecture and the logical relations between the structural behaviors and sensor outputs are designed as the basis of a powerful predictive maintenance model despite the fact that real-time health monitoring was not realizable. Subsequent studies should focus on the experimental verifications of this model by real-time data acquisition. Piezoelectric and FBG sensors should be installed in priority, particularly in the previously identified critical locations. Calibration of detection thresholds should be performed on the basis of modal analysis results from preliminary qualification tests for better reliability of the system. There are some mechanical and thermal limitations of PLA, which should also be considered. For better durability in harsh operating conditions, advanced composite materials such as CFRP may be addressed. Real-time telemetry integrated with health monitoring systems would increase the mission reliability of UAV platforms and would enable more autonomous decisions still. The approach reported in this paper aims to transition UAV maintenance from reactive to proactive. Applications in the military as well as in the civilian field may benefit from the scalability of the proposed framework and its ability to fit a variety of UAV configurations. In the long term, the design of UAV systems will be significantly simplified, and the operating costs further reduced, and the availability of the platform ensured for a wide range of mission types due to the integrated health monitoring.

REFERENCES

Altınörs, A., Yol, F. and Yaman, O. (2021). A sound based method for fault detection with statistical feature extraction in UAV motors. *Applied Acoustics, 183,* 108325. https://doi.org/10.1016/j.apacoust.2021.108325

Bogrekci, İ., Demircioğlu, P, Karatas, S. T. (2025). Integrated maintainability in the structural and system design of fixed wing UAVs. *International Journal for Multidisciplinary Research (IJFMR), 7(4),* 1–6. https://doi.org/10.36948/ijfmr.2025.v07i04.51018

Brandon, J. A., Whitfield, C. A., Trussa, C. W. and McCrink, M. (2021). *Performance analysis of a serpentine inlet design for an unmanned aerial vehicle*. AIAA Aviation Forum, 2021–2488. https://doi.org/10.2514/6.2021-2488

Fernandes, J., Deus, A. M., Reis, L., Vaz, M. F. and Leite, M. (2018). Study of the influence of 3D printing parameters on the mechanical properties of PLA. *Proceedings of the International Conference on Progress in Additive Manufacturing (Pro AM 2018),* 547–552. https://doi.org/10.25341/D4988C

Graba, M. and Grycz, A. (2023). Assessment of the mechanical properties of selected PLA filaments used in the UAV project. *Materials, 16(3),* 1194. https://doi.org/10.3390/ma16031194

Jardine, A. K. S., Lin, D. and Banjevic, D. (2006). A review on machinery diagnostics and prognostics implementing condition-based maintenance. *Mechanical Systems and Signal Processing, 20(7),* 1483–1510. https://doi.org/10.1016/j.ymssp.2005.09.012

Javadi, H. and Larsson, T. (2022). Fault detection methods for unmanned aerial vehicles: A comprehensive review. *Drones, 6(11),* 330. https://doi.org/10.3390/drones6110330

Kanesan, G., Mansor, S. and Abdul-Latif, A. (2014). Validation of UAV wing structural model for finite element analysis. *Jurnal Teknologi (Sciences & Engineering), 71(2),* 1–5. https://doi.org/10.11113/jt.v71.3710

Kulkarni, C. S., Corbetta, M. and Robinson, E. (2020). Enhancing fault isolation for health monitoring of electric aircraft propulsion by embedding Failure Mode and Effect Analysis into Bayesian networks. *Annual Conference of the PHM Society, 12(1),* 12. https://doi.org/10.36001/phmconf.2020.v12i1.1297

Lim, S., Choi, W. and Park, H. (2022). A study on design of S-duct structures and air intake for small aircraft applied to high-strength carbon–epoxy composite materials. *Materials, 15(9),* 3001. https://doi.org/10.3390/ma15093001

Raymer, D. (2018). *Aircraft Design: A Conceptual Approach, Sixth Edition*. American Institute of Aeronautics and Astronautics, Inc., Washington, DC (2018). https://doi.org/10.2514/4.104909.

Saif, A., Alsamhi, S. H. and Curry, E. (2023). Climate-resilient UAVs: Enhancing energy-efficient B5G communication in harsh environments. *arXiv*. https://doi.org/10.48550/arXiv.2309.09387

Sikorska, J. Z., Hodkiewicz, M. and Ma, L. (2011). Prognostic modelling options for remaining useful life estimation by industry. *Mechanical Systems and Signal Processing, 25(5),* 1803–1836. https://doi.org/10.1016/j.ymssp.2010.11.018.

Sun, J.-J., Yeh, T.-M. and Pai, F.-Y. (2022). Application of Monte Carlo simulation to study the probability of confidence level under the PFMEA's action priority. *Mathematics, 10(15),* 2596. https://doi.org/10.3390/math10152596

CURRICULUM VITAE

Surname, Name : KARATAŞ, Saim Taha

Foreign Languages : English, Russian, Azerbaijani

Education

Degree	Institute	Graduation Date
MSc	Aydin Adnan Menderes University, Graduate School of Natural and Applied Sciences, Mechanical Engineering	Cont.
BSc	Aydın Adnan Menderes University, Faculty of Engineering, Mechanical Engineering.	2020

WORK EXPERIENCE

Year	Company	Title
2018	Aselsan	Mechanical Design Intern
2019	Turkish Aerospace Industry	Weapon System Engineering Intern
2021-	Turkish Aerospace Industry	Maintainability Engineer

Bogrekci, I., Demircioglu, P., & Karatas, S. T., "Integrated Maintainability in the Structural and System Design of Fixed-Wing UAVs", *International Journal for Multidisciplinary Research (IJFMR),* 7(4), pp. 1–6, E-ISSN: 2582-2160, 2025. https://doi.org/10.36948/ijfmr.2025.v07i04.51018.